LBL-24788
UC-210

Lawrence Berkeley Laboratory
UNIVERSITY OF CALIFORNIA

APPLIED SCIENCE DIVISION

Electrocatalysts for Oxygen Electrodes: Final Report

E. Yeager

January 1988

APPLIED SCIENCE DIVISION

Prepared for the U.S. Department of Energy under Contract DE-AC03-76SF00098

DISCLAIMER

LBL-24788

ELECTROCATALYSTS FOR OXYGEN ELECTRODES

Final Report

January 1988

by

E. Yeager

Case Center for Electrochemical Sciences
Case Western Reserve University
Cleveland, Ohio 44106

for

Technology Base Research Project
Applied Science Division
Lawrence Berkeley Laboratory
University of California
Berkeley, California 94720

This work was supported by the Assistant Secretary for Conservation and Renewable Energy, Office of Energy Storage and Distribution of the U.S. Department of Energy under Contract No. DE-AC03-76SF00098, Subcontract No. 4527210 with the Lawrence Berkeley Laboratory.

PREFACE

This report only summarizes the results. For details the reader is referred to the corresponding references. The following personnel have been involved in the research on a full or part time basis:

W. Aldred	Research Assistant
I. Bae	Graduate Student
R. Carbonio	Research Associate
C. Fierro	Graduate Student/Research Associate
B. Simic-Glavaski	Senior Research Associate
S. L. Gupta†	Senior Research Associate
M. Hossain	Graduate Student/Research Associate
A. Tanaka	Graduate Student
D. Tryk	Senior Research Associate
E. Yeager	Project Director

† Report prepared by S. L. Gupta.

TABLE OF CONTENTS

I. SUMMARY

The overall objective of this research has been the development of very effective electrocatalysts for O_2 reduction and generation, combining high catalytic activity with long-term stability in concentrated acid and alkaline electrolytes. Emphasis is on achieving a fundamental understanding of O_2 electrocatalysis and the relation of the kinetics to the electronic and morphological aspects of the surfaces.

The specific catalyst systems investigated under the LBL project have included:

1. macrocycle catalysts and related complexes;
2. heat-treated macrocycles and nitrogen-containing polymers;
3. transition metal oxide systems;
4. modified carbon and graphite surfaces.

The research has involved electrochemical, spectroscopic and theoretical approaches. A considerable effort has been devoted to the purification and spectroscopic characterization of the transition metal macrocycles, particularly porphyrins and phthalocyanines. Iron tetrasulfophthalocyanine (FeTsPc) and other iron phthalocyanines are of special interest since these complexes adsorbed on electrode surfaces catalyze the 4-electron direct pathway in alkaline electrolytes. Raman spectroscopy, including depolarization measurements on monolayers of (FeTsPc) adsorbed on silver single crystal surfaces without activation of the silver, provide evidence that these complexes are oriented with the plane of the macrocycle ligand perpendicular to the surface. However, this may not be true for other phthalocyanines in general. Mossbauer studies on bulk crystalline FeTsPc and FeTsPc adsorbed at monolayer coverages on Vulcan XC-72 carbon suggest a μ-oxo or peroxo FeTsPc complex for the adsorbed species. Laser Raman and electrochemical studies of the adsorbed FeTsPc indicate the structure of the adsorbed layers to be strongly influenced by the nature of the supporting electrolyte.

In-situ fluorescence emission measurements have been made with the metal-free H_2TsPc adsorbed on various substrates (Ag, Au, Fe, Ni and graphite) in

order to better understand the electronic interaction of the macrocycle ligands with the substrate material. Work has also continued on surface-enhanced Raman spectroscopy involving adsorbed monolayers of phthalocyanine molecules on silver electrodes and silver bromide substrates. The analysis of electronic energy levels in semi-conducting silver bromide and the adsorbed phthalocyanine molecules suggest a new mechanism for the high enhancement factor in surface-enhanced Raman scattering.

The research has continued on macrocycles which promote the 4-electron reduction of O_2 to OH^- or H_2O without producing solution-phase peroxide. Various types of iron phthalocyanines and iron tetrapyridino porphyrazines have now been shown at Case to catalyze the direct 4-electron process in alkaline solutions. Quantum mechanical calculations at Case using the atom superposition-electron delocalization (ASED) molecular orbital method provide evidence for dioxygen Fe-O-O-N bridging in the iron phthalocyanines where N is a bridge nitrogen. This represents an interesting alternative to the intermolecular dioxygen bridging (Fe-O-O-Fe) proposed to explain the 4-electron O_2 reduction with several iron phthalocyanines. In tests of O_2 reduction performance under fuel cell or metal-air battery conditions, i.e., concentrated alkaline solution at elevated temperatures, these catalysts have thus far not shown sufficient stability. Other types of milder electrolytes, such as the hydrate melts of the alkali metal carbonates, are under investigation. These may stabilize some of the more vulnerable macrocycles. It is also possible that polymeric electrolytes may enhance their stability.

Heat-treated transition metal macrocycles such as Fe- or Co- tetramethoxyphenyl porphyrin (TMPP) dispersed on high area carbon have high activity for O_2 reduction in alkaline and acid electrolytes with good stability in concentrated alkaline solutions. The metal-free porphyrin H_2TMPP has been found at Case to be <u>not</u> active for O_2 reduction in either acid or alkaline electrolytes even after heat treatment on carbon blacks not containing signifi-

cant transition metal impurities. This is in contrast to findings reported in the literature in which carbons were used which contained iron compounds. It has also been found that H_2TMPP adsorbed on carbon can interact with intentionally added iron compounds during the heat treatment to produce highly active catalysts. The Case group has also confirmed literature reports that H_2TMPP on carbon can interact with intentionally added cobalt compounds during heat treatment, again producing highly active catalysts. Finally it has been found that H_2TMPP/carbon which has been heat-treated without transition metal compounds can interact with such compounds and gain O_2 reduction catalytic activity after the heat treatment. This has been done by 1) heating the material with precipitated metal hydroxides; 2) refluxing the material in acetic acid solution, for example with cobalt acetate or 3) by precipitating cobalt hydroxide in the electrolyte in the presence of the gas-fed electrode. In some cases more than one transition metal hydroxide was heated with solid material (method 1), with additional gains in performance noted in KOH electrolyte. More than one metal hydroxide was also added in some cases to the metal-free macrocycle on carbon prior to the heat treatment. For example, both iron and cobalt hydroxides were added to H_2TMPP on XC-72 and then heat-treated to 450°C. The O_2 reduction performance is quite promising.

The combined use of Fourier transform infrared, transmission electron microscopy, Mossbauer, X-ray diffraction, magnetic susceptibility and pyrolysis-gas chromatograph-mass spectroscopy has provided new insight into the effects of the heat treatment. The macrocycles partially decompose while retaining the pyrrole nitrogens. The pyrrole nitrogens then provide binding sites for adsorbed transiton metals such as Co and Fe, with the catalytic activity due mostly to the transition metal in an atomic state of dispersion. Guided by this concept, the Case group has identified some nitrogen-containing polymers such as polypyrrole black and polyacrylonitrile heat-treated with cobalt salts and high area carbon as very active O_2 reduction catalysts both in

acid and alkaline electrolytes. The activity is comparable to highly dispersed platinum in alkaline electrolytes. These catalyst systems function through a peroxide mechanism, similar to that involved with heat-treated CoTMPP and have comparable activity but much lower cost. Because of the possibility that some of these polymeric materials may contain the transition metal within the bulk of the polymer, they may show enhanced stability as well as a form of three-dimensional catalysis.

It has been shown that one of the life-limiting processes for the heat-treated CoTMPP-based air cathodes in alkaline solution is the loss of the transition metal out of the catalyst. The use of ionically conductive polymer phases incorporated into active layers of porous gas-fed electrodes has been pursued at Case in order to help stabilize the transition metal macrocycle catalysts in both acid and alkaline electrolytes. If electrodes are fabricated using a soluble form of Nafion 117, they appear to be more stable and exhibit much better polarization behavior in short-term tests in acid electrolytes. Another approach is to cover the solution side of the active layer with an ionomeric membrane. This approach has been tried in alkaline solution using a caustic-resistant anion exchange membrane with an active layer made from heat-treated CoTMPP on steam-activated Shawinigan black. The polarization curves are essentially the same with and without the membrane up to ~200 mA cm^{-2} with IR correction for the resistance external to the active layer (including the membrane). Long-term stability remains to be checked but is expected to be improved. Furthermore, the polymer permits the gas-fed electrodes to withstand substantial overpressure on the gas-side without blowing bubbles into the electrolyte.

Research was initiated on O_2 reduction and generation as well as peroxide decomposition on perovskite catalysts. A number of perovskites were prepared of the general type $La_xSr_{(1-x)}MO_3$ in which M stands for a transition metal or combination of transition metals including Cr, Mn, Fe, Co, Ni and Ru. These

compounds were characterized using X-ray diffraction, BET surface area, elemental analysis and magnetic susceptibility. One focus of the ongoing research on perovskite electrocatalysts for O_2 reduction and generation has been the catalysis of peroxide decomposition. Various methods have been used for the determination of peroxide decomposition rate constants for particular catalysts in alkaline solutions. Two involve monitoring the peroxide concentration in a stirred catalyst suspension. Another involves electrochemically monitoring the peroxide concentration in a porous gas-fed O_2 reduction electrode after current interruption. All yield first order dependence of the rate upon peroxide concentration. The last, however, yields pseudo-second order behavior at lower currents or longer times due to the influence of the discharge of the capacitance of the electrode.

The research has continued to develop catalysts which are active for both O_2 reduction and generation in alkaline electrolytes. The catalysts receiving the most attention are those which consist of tetramethoxyphenyl porphyrin, either metal-free or containing cobalt, heat-treated on carbon and mixed with transition metal-containing perovskites.

The presence of the perovskite does not appreciably affect the O_2 reduction performance of heat-treated CoTMPP on carbon. Cobalt-containing perovskites, however, have been found to greatly increase the performance of heat-treated H_2TMPP on carbon, probably because small amounts of Co(II) can go into solution and readsorb at nitrogen-containing sites on the heat-treated macrocycle-carbon surface. Since the loss of Co from heat-treated CoTMPP-based catalysts may be an important failure mechanism in long-term operation, perovskites may provide a back-up source of the transition metal. Most of the perovskites examined have been found to undergo irreversible surface reduction, some even in the potential range where O_2 reduction takes place. This surface reduction can seriously affect the catalytic activity for O_2 generation.

The self-supported ruthenate pyrochlores such as lead ruthenate offer

considerable promise for bifunctional O_2 electrodes provided sufficient stability can be achieved. They have high catalytic activity for O_2 generation as well as reduction but have a slight solubility in the KOH electrolyte. The use of an ionic conducting polymer or gel as the electrolyte phase in the porous electrodes should greatly improve the stability and is a promising approach. The bicarbonate-carbonate electrolyte should also result in much depressed solubility. These catalysts and electrolyte systems will be investigated during the coming year.

As part of the supporting research on oxygen reduction on various carbon and graphite surfaces, the kinetics and mechanistic aspects of O_2 reduction with respect to the involvement of surface functional groups on glassy carbon have been examined in alkaline solutions using the rotating ring-disk electrode and differential pulse voltammetry techniques. Oxygen is quantitatively reduced to peroxide over the investigated potential range (from 0 to -1.1 V vs. Hg/HgO, OH^-). Based on the Tafel slope, the reaction orders, the stoichiometric number and the kinetic isotope effects, a possible reaction mechanism at low overpotentials has been proposed for both O_2 reduction and HO_2^- oxidation. Quinonoid surface functional groups play a catalytic role for O_2 reduction at low overpotentials whereas at high overpotentials a non-catalyzed type of reaction occurs.

Oxygen reduction has also been examined on adsorptively attached and chemically linked quinones in alkaline solutions. The reduction behavior is very similar to that observed on glassy carbon and ordinary pyrolytic graphite in alkaline solution. From a detailed study of differential pulse voltammetry and rotating disk electrode data for solutions of different pH, it has been demonstrated that the quinone radical anion is responsibile for O_2 reduction to peroxide. The possible mode of interaction of quinone species with O_2 has also been discusssed.

In order to gain further insight into O_2 reduction and the role played by the electrode material, a series of carbon and graphite electrodes was examined in acetonitrile, in which superoxide is the product. Gold was also examined. The electron transfer rate constants were determined and were found to decrease in the following order: glassy carbon > ordinary pyrolytic graphite ≈ gold > highly oriented pyrolytic graphite. The rate constants only varied over about 1-2 orders of magnitude, consistent with the outersphere nature of the process in non-aqueous solvents. Interestingly, a pyrolytic graphite electrode with an adsorbed layer of cobalt tetrasulfonated phthalocyanine was less active than the bare graphite, probably due to either blocking or double layer effects.

In order to examine the effect of water as a proton donor, O_2 reduction on these same surfaces was examined in acetonitrile with and without added water. With no water, the O_2 reduction on these surfaces proceeds to superoxide as noted above. In the presence of water, the reduction proceeds to HO_2^- on these surfaces, but the reduction of superoxide to peroxide is much more facile on Au than on carbons, providing evidence for a catalytic role of the electrode surface for the conversion to peroxide.

II. OBJECTIVES AND INTRODUCTION

A. Objective

The performance of low and moderate temperature fuel cells and rechargeable metal-air batteries is limited by the catalytic activity and life of the O_2 electrocatalysts. The overall objective of this research has been the development of much more effective electrocatalysts for O_2 reduction and generation, combining high catalytic activity with long-term stability in concentrated acid and alkaline electrolytes. Research emphasis is on achieving a fundamental understanding of O_2 electrocatalysis.

B. Introduction

Over the last two decades a large amount of research has been carried out in various laboratories for a wide range of catalysts for O_2 reduction in alkaline and acid electrolytes and to a lesser extent O_2 generation, principally in alkaline electrolytes. Much of this research has been semi-Edisonian, guided by scientific hunches rather than an adequate understanding of the relations of the electrocatalytic activity to the electronic and steric properties of the catalysts. Consequently the emphasis in the ongoing research on O_2 electrocatalysts at Case has been on achieving a new level of the understanding of electrocatalytic activity for both reduction and generation in relation to the basic properties of the catalyst-electrolyte interface. The emphasis over the past three years has been on the study of transition metal macrocycles and related complexes (both without and with heat treatment), nitrogen containing polymers (with heat treatment), oxides and carbon surfaces as O_2 reduction catalysts in acid and alkaline electrolytes and in some instances as bifunctional catalysts for O_2 generation and reduction in alkaline electrolytes.

The work has involved a number of electrochemical, spectroscopic and theoretical studies. A considerable effort has also been devoted to the preparation, purification and spectroscopic characterization of the transition metal macrocycles and the corresponding metal-free species, particularly porphyrins and phthalocyanines.

III. ACCOMPLISHMENTS

A. Basic Research on Macrocycles and Related Complexes (Non-heat-teated)

The research has continued on macrocycles which promote the 4-electron reduction of O_2 to OH^- or H_2O without producing solution phase peroxide. Various types of iron phthalocyanines (FePc) have now been shown to catalyze the 4-electron process at Case. These compounds were synthesized in the mono-

mer form and thus avoid the complicated procedures necessary to synthesize the bridged, pillared, clamshell and other types of dimers. A number of spectroscopic techniques have been employed to try to pin down exactly what the structures are, including Raman, infared, uv-visible and Mossbauer.

1. Raman Studies

Much attention at Case has been devoted to iron tetrasulfonated phthalocyanine (FeTsPc), which has been found to catalyze the 4-electron reduction of O_2 to OH^- or H_2O over a substantial potential range without the generation of solution-phase peroxide. Results with Raman spectroscopy including depolarization measurements on monolayers adsorbed on silver single crystals (low index planes 111, 110 and 100) without activation provide evidence that the TsPc's are oriented with the plane of the macrocycle ligand perpendicular to surface (1). This orientation, however, is probably not true in general of the phthalocyanines. Vapor-deposited monolayer films of FePc prepared on a graphite substrate (cleavage plane) indicate that the molecules lie flat on the substrate using penning-ionization-electron spectroscopy (2). The uv-visible absorption spectra for some of the transition-metal TsPc complexes adsorbed on Pt and the basal plane of graphite also provide evidence for the perpendicular orientation which probably involves -o-(μ-oxo) and/or, less likely, -o-o-(dioxygen) bridging in oxygen containing solutions (3).

Further studies have been conducted on the behavior of adsorbed FeTsPc on a polycrystalline silver electrode with various supporting electrolytes at constant pH. The data obtained with resonant surface enhanced Raman spectroscopy, SERS, and cyclic voltammetry provide some details of the interaction with the electrode surface for the adsorbed species and their orientation. The structure of the adsorbed layer on the electrode surface appears to be strongly influenced by the nature of the supporting electrolyte (4). The interaction of

underpotential deposited lead with the adsorbed monolayers of Me-TsPc's has also been studied. Lead can be underpotential deposited on Ag single crystal surfaces with preadsorbed layers of MeTsPc without displacing the adsorbed macrocycle. However, efforts to examine the adsorbed Fe-TsPc with LEED on single crystal silver have been unsuccessful and this provides evidence of a random layer, as would be expected for the edge-on adsorption of the μ-oxo$(FeTsPc)_2O$ dimer. In-situ fluorescence emission has also been studied with metal-free tetrasulfophthalocyanine (H_2TsPc) adsorbed on silver, gold, nickel and graphite electrodes (5). It is anticipated that these photo emissions can be used to gain further understanding of the interaction of the macrocycle with surfaces. The details are given in References 1, 3, 4 and 5.

Work has also been carried out on surface enhanced Raman spectroscopy (SERS) involving adsorbed monolayers of phthalocyanine molecules on silver electrodes and silver bromide substrates. The analysis of electronic energy levels in semi-conducting silver bromide and the adsorbed phthalocyanine molecules suggests a new mechanism for the high enhancement factor in surface enhanced Raman scattering. The details of this work are given in Reference 6.

The fundamental research on macrocycles has been aimed at understanding the role of the redox potentials of the ligand as well as metal (s), and general electronic and steric properties of the macrocycle in O_2 electrocatalysis. Of particular interest is the question of specific interactions of O_2 not only with the transition metal species but also the macrocycle ligand. Consequently macrocycles with other than transition metals in the N_4-center have been examined. Stacked-ring silicon phthalocyanines $R_3SiO(SiPc)_n$-SiR_3 which were synthesized by Prof. M. E. Kenney of Case in a controlled manner as monomers, dimers, trimers, and tetramers (Fig. 1) have been studied by cyclic voltammetry and combined resonant Raman and surface enhanced Raman spectroscopy

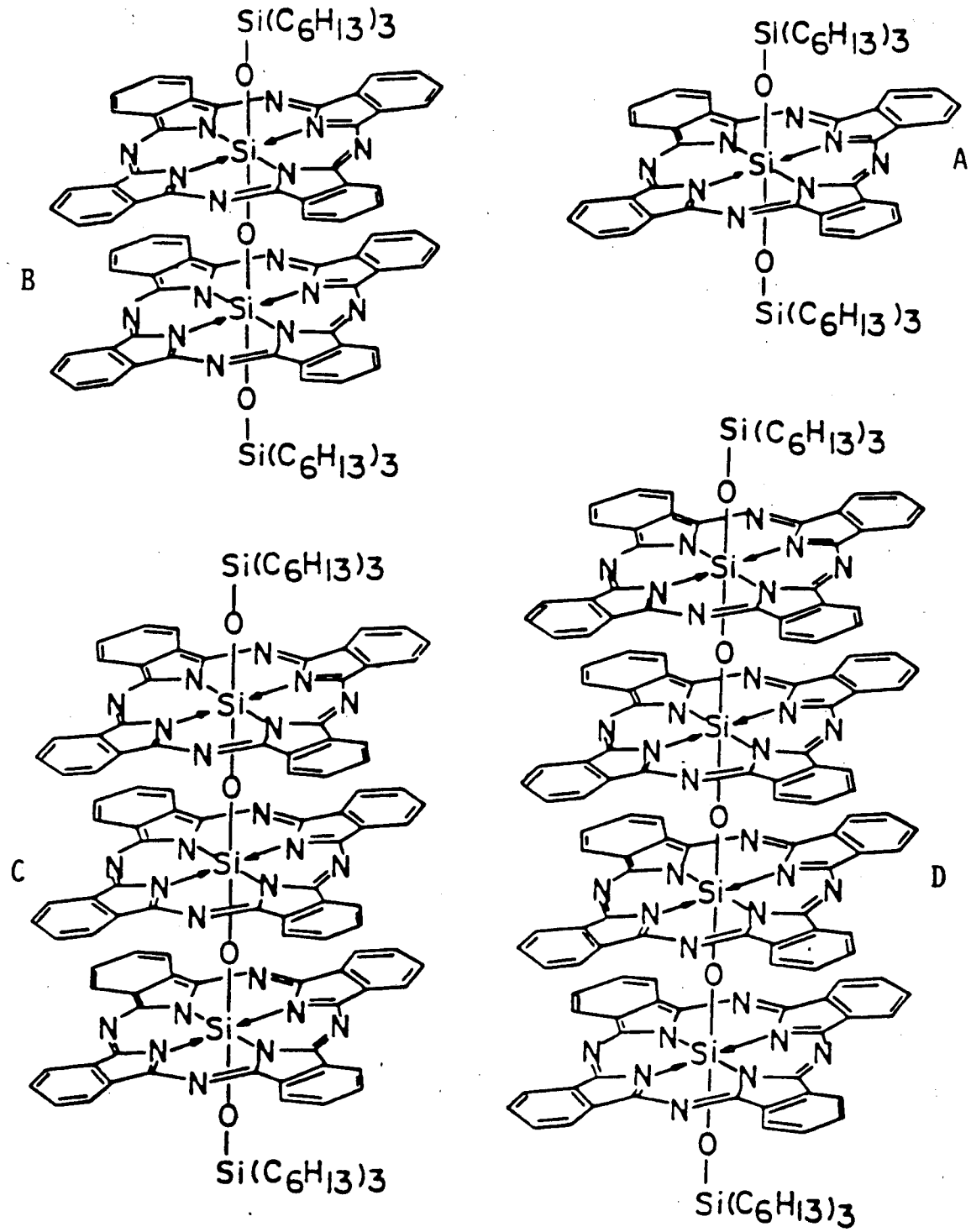

FIG. 1. STACKED CONFIGURATIONS OF POLYMERIC SILICON PHTHALOCYANINE. A - MONOMER; B - DIMER; C - TRIMER AND D - TETRAMER.

(RR/SERS). The Raman scattering signals obtained from the adsorbed monomeric, dimeric, trimeric and tetrameric species on the silver electrode in deaerated sulfate solutions are a function of the electrode potential and show essentially the same number of the vibrational bands as in the case of Fe-TsPc (7). The intensity changes both for fluorescence and Raman oxidation-reduction-cycles (ORC) for other adsorbed phthalocyanines. Raman (ORC) are related to the redox states of the adsorbed SiPc. The peaks associated with the solution phase ligand oxidation and reduction in voltammetry curves in methylene chloride show the splitting for the stacked polymers expected quantitatively on a quantum mechanical basis (8). Oxygen reduction polarization studies for the adsorbed species are in progress using rotating ring-disk electrode technique. The details are given in Reference 7.

2. Mossbauer Studies

In order to see how Fe-TsPc interacts with the carbon substrate, Mossbauer effect spectroscopy has been carried out on bulk crystalline FeTsPc and Fe TsPc adsorbed at monolayer coverages on high surface area carbon (Vulcan XC-72). One surprising observation is the negative isomer shift for the bulk Fe-TsPc as compared to the unsulfonated crystalline or adsorbed FePc (Table 1). This lower value of the isomer shift for the bulk FeTsPc probably indicates an increased charge density due to the 4 s-orbital at the metal center. The isomer shift, as well as quadrupole splitting, provide evidence that a group such as $-SO_3^-$ with a strong electron accepting characteristic interacts through an axial position with the d-orbitals of the metal. This may result in a radial contraction of the 4 s-orbital increasing the spherical charge density at the metal. Upon adsorption of FeTsPc on XC-72 carbon, however, the isomer shift returns to its usual value (Table 1) but with a small quadrupole splitting. These values are similar to μ-oxo-iron(III) tetramethoxyphenyl porphyrin

TABLE I

MOSSBAUER DATA FOR FEPC AND FE-TSPC (DRY)

Macrocycle	Isomer Shift, (mm/s) vs. α-Fe	Quadrupole Splitting, (mm/s)
Fe-Pc (bulk)	0.39	2.61
Fe-Pc (adsorbed)[+]	0.37	0.91
Fe-TsPc (bulk)	-0.03	1.37
Fe-TsPc (adsorbed)[+]	0.37	0.63

[+] Adsorbed on Vulcan XC-72 carbon.

$(FeTMPP)_2O$, suggesting a μ-oxo or peroxo FeTsPc upon adsorption on high area carbon.

Mossbauer spectroscopy has been one of the most useful tools in determining the state of the transition metal in macrocycles both in bulk and adsorbed on high area carbon with or without subsequent heat treatment. One interesting result is that iron phthalocyanine adsorbed on high area carbon black can decompose at temperatures as low as 300°C. The presence of trace O_2 in the heat treatment gas train may play a role. The presence of substantial amounts of an amorphous Fe(III) hydrated oxide at most positive potentials and on Fe(II) hydroxide at very negative potentials was observed with in-situ Mossbauer spectroscopy in alkaline solution. The details are given in Reference 9.

3. Voltammetry and O_2 Reduction Studies on Iron-Tetra-Pyridino-Porphyrazines

Most of the adsorbed transition metal macrocycles catalyze the O_2 reduction via the peroxide pathway, while a few [e.g., certain bimetal systems (10-12) and some monometal systems (13-15) catalyze the 4-electron reduction process but generally lack sufficient stability for fuel cell applications. All of these catalysts for the 4-electron overall process probably catalyze the O_2 reduction through the formation of a dioxygen bridge.

Recently, however, 4-electron reduction has been reported by Anson group (16) using cofacial porphyrins in which only one of the porphyrin rings is metallated. This raises some question with respect to importance of dioxygen bridging between two transition metal centers. On the other hand it would be difficult to obtain the face-to-face porphyrin with just the one metallated N_4 center without the dicobalt complex as a contaminant. It is also possible that bridge occurs between the cobalt of N_4 center and a nitrogen of the other N_4 center.

Over the past years work has been done on Fe(II)-tetrapyridino phorphyrazines (two isomers viz. 2,3- and 3,4-FeTPyPz) with the objective of establishing the relationship of the mechanism and kinetics of O_2 reduction to the redox properties of the complex. These compounds (Fig. 2) were synthesized and purified at Case according to the method reported by Smith et al. (17). The voltammetry of these compounds adsorptively attached to graphite has been found to be similar to that of FeTsPc (see Ref. 55) which catalyzes the 4-electron direct pathway in alkaline electrolytes. The influence of a change in the oxidation state of Fe(II) TPyPz adsorbed on ordinary pyrolytic graphite (OPG) disk on the reduction of O_2 has been investigated in 0.1 M NaOH. With the rotating-ring disk technique O_2 reduction polarization curves (Fig. 3) have indicated that the predominant mechanism is the 4-electron direct reduction of O_2 to OH^- at low polarizations but the peroxide generation becomes significant at high polarizations. At very large overpotentials, however, the peroxide formation again decreases to low values. It is suggested, that in addition to the dioxygen bridged adsorbed dimer, it may be possible that the macrocycle assisted reduction of O_2 involves the formation of a bridge of the form Fe-O-O-N, when N is one of the bridge nitrogens of the macrocycle (Fig. 4). The evidence for such is from quantum mechanical considerations at Case (15) using the atom superposition-electron delocalization (ASED) molecular orbital method developed by A. Anderson and R. Hoffman (18). The details are given in Reference 15.

4. Spectroscopic and Electrocatalytic Aspects of FePc and its μ-oxo Derivations

Considerable effort has been devoted by many research groups including the Case group toward gaining a deeper understanding of the nature of the FePc-O_2 interactions including the bonding geometry and energetics of the reaction pathway intermediates. Important information has been derived form in-situ

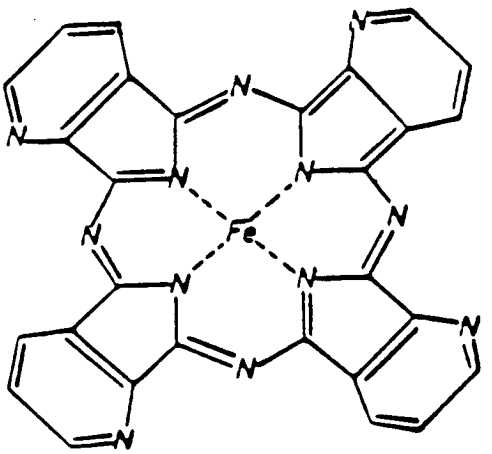

Structure of Iron Tetra-2,3-pyridinoporphyrazine

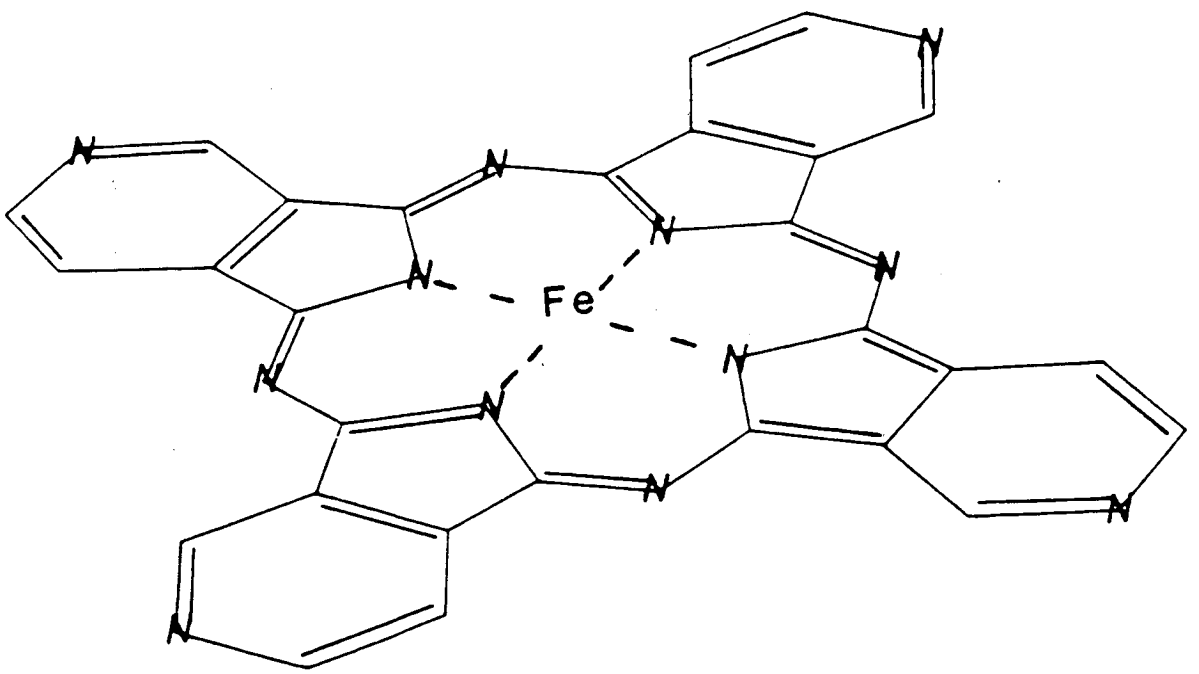

Fig. 2. Fe(II)Tetra-3,4-Pyridino Porphyrazine

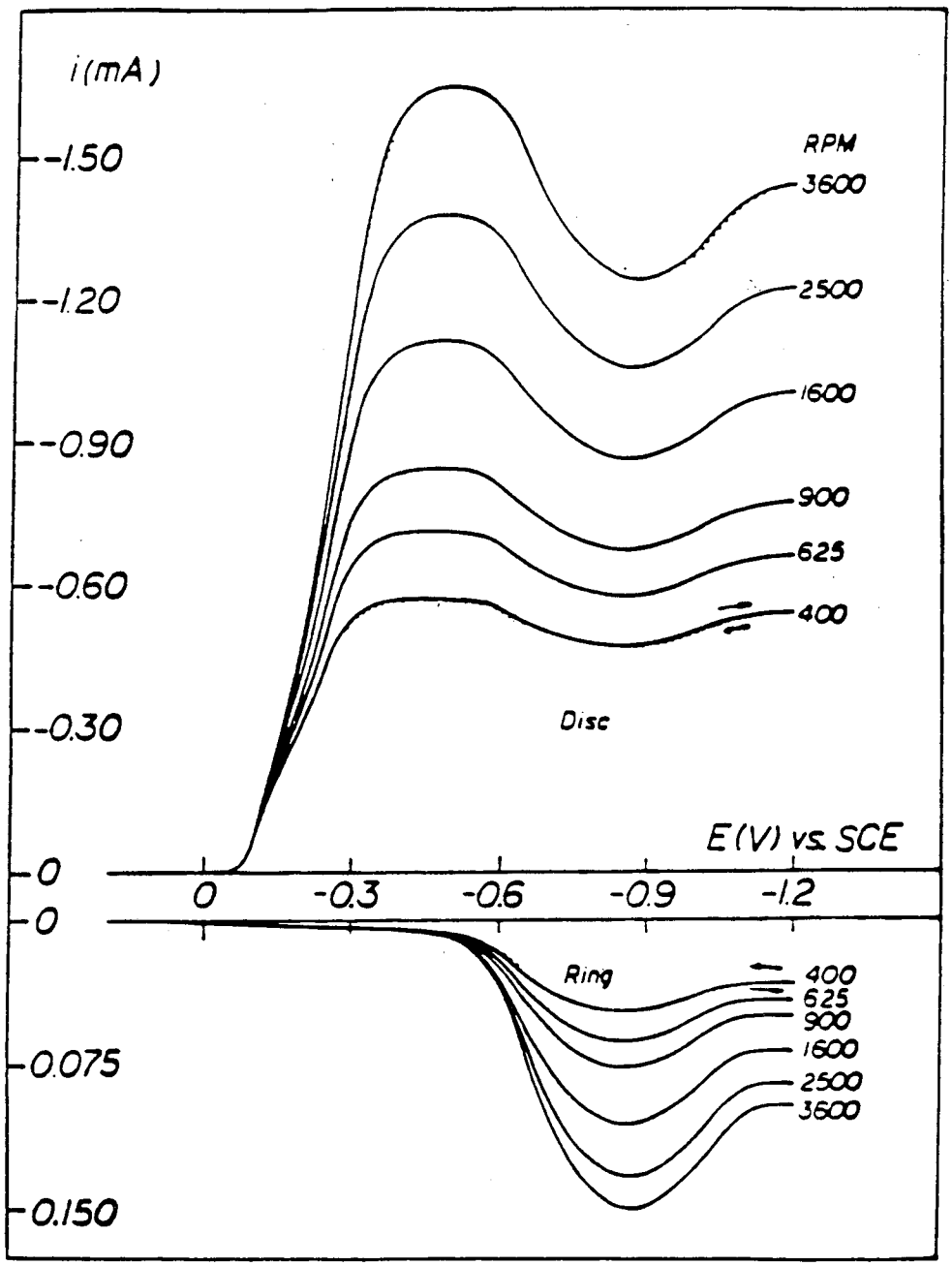

Figure 3. Ring-disk polarization curves at different rotation rates for O_2 reduction on FeTPyPz adsorbed on pyrolytic graphite disk in 0.1 M NaOH solution saturated with O_2. Electrode area = 0.196 cm^2, room temperature. Scan rate = 10 mV/s, Au ring (N=0.38) at +0.1 V vs. SCE.

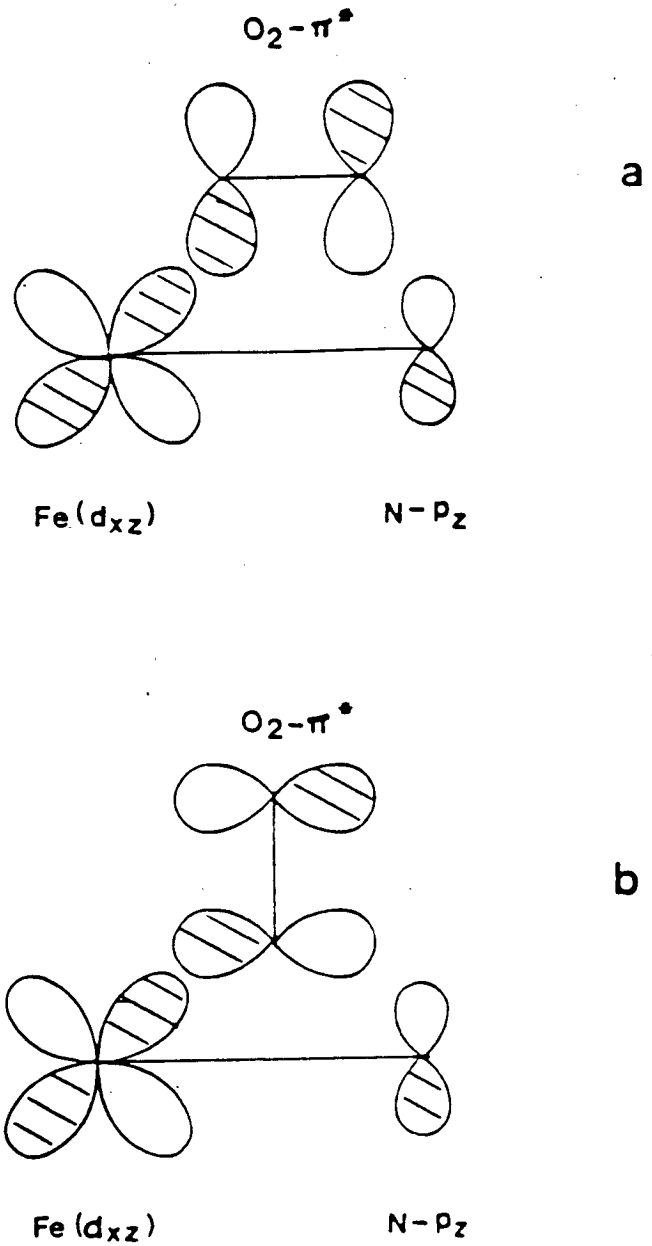

Figure 4. Possible bridge-interactions of O_2 with iron and one of the nitrogen in the ring

spectrochemical and electrochemical studies involving FePc and water soluble derivations including the tetrasulfonated phthalocyanines (FeTsPc) and pyridino porphyrazines (FePyPz) adsorbed on a variety of electrode materials. Nonetheless, the O_2 reduction on these adsorbed macrocycle layers is not fully understood and further research has been carried out during the past years to clarify the situation.

A thorough spectroscopic and electrochemical study of FePc and its μ-oxo derivations has recently been completed at Case which included FTIR and Mossbauer spectroscopy, scanning electron microscopy, voltammetry, rotating ring-disk electrode measurements and gas-fed electrode meaurements. There are two μ-oxo isomers: μ-oxo(1) is crystallized out of dimethyl-formamide solution, while the μ-oxo(2) is crystallized out of concentrated sulfuric acid. These were first described by Ercolani et al. (19) and examined using FTIR. The Mossbauer spectra at Case (Fig. 5) show large differences in the quadrupole splittings for the FePc and the two μ-oxo species. These are due to differences in the spherical symmetry of the electronic charge distribution around the iron center, the largest splitting being associated with the largest degree of asymmetry. Despite the major diffrence in the Mossbauer spectra, the cyclic voltammetry of FePc and its two μ-oxo derivatives obtained by mixing the materials in dry form with high area Vulcan XC-72 carbon yielded a common set of voltammetric peaks (Fig. 6), providing evidence for the presence of a single type of surface species for the macrocycle in its various forms.

The electrochemical activity of these dispersed specimens for O_2 reduction in alkaline media usig the thin porous coating-rotating disk technique was found to be essentially the same for both μ-oxo derivations. Although initially lower in activity the bulk monomeric FePc showed comparable activity to μ-oxo(1) and (2) only after polarizing the electrodes at fairly negative potentials. It is interesting to note that the activity associated with the μ-

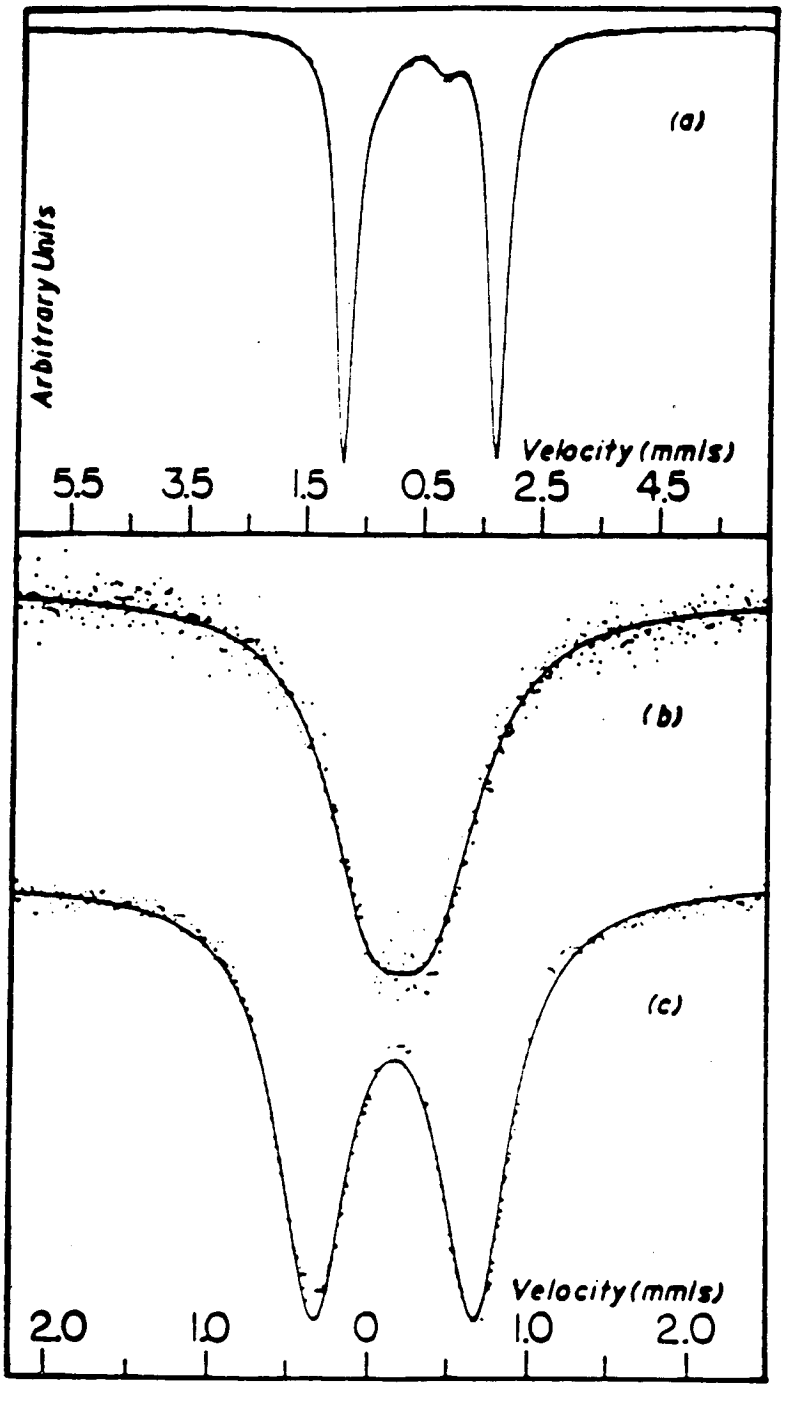

Figure 5. Mossbauer spectra of a) FePc, b) FePc μ-oxo (1), and FePc μ-oxo (2).

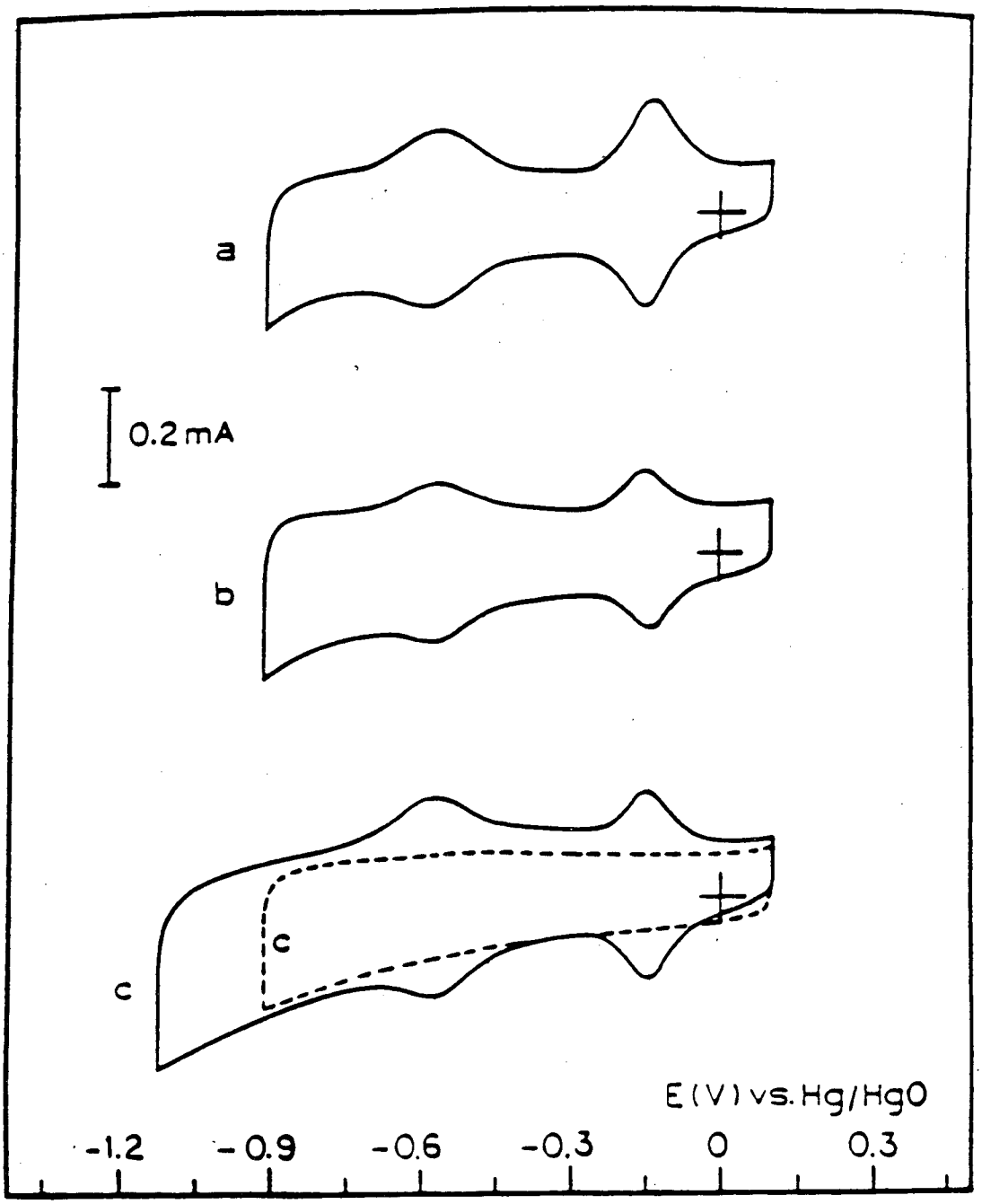

Figure 6. Cyclic voltammograms of a) 7% w/w FePc μ-oxo (1), b) 7% w/w FePc μ-oxo (2), and c) 7% w/w FePc dispersed on Vulcan XC-72 carbon in a N_2 saturated 1 M NaOH solution. Scan rate = 20 mV s^{-1}. Room temperature.

oxo(1) species was comparable to that obtained with Powercat 2000 (Fig. 6), a commercially available Pt-based catalyst and much higher than that of the Vulcan XC-72 carbon without catalyst. The ring currents for the activated FePc and the two μ-oxo forms of the macrocycle were found to be very low, particularly for FePc-μ-oxo(1), for which the results are shown in (Fig. 7). This could indicate that the overall reduction occurs via a direct 4-electron mechanism This possibility, however, cannot be confirmed employing the thin coating electrode technique since the peroxide may undego decomposition within the porous matrix generating O_2, which can then be further reduced to yield effectively four electrons per dioxygen molecule. Significant differences in activity were observed for the materials in gas-fed electrodes of the type used in fuel cells in 4 M NaOH at 60°C. Based on the experimental results obtained and quantum mechanical arguments at Case, the following conclusions can be drawn.

1) Mossbauer experiments conducted in this (20) and other laboratories (21) indicate that four distinct species can be found in FePc specimens either in bulk form or dispersed on carbon supports from a number of solvents. These have been assigned to the standard monomeric form of FePc (δ = 0.39 mm s^{-1} vs. α-Fe, Δ = 2.62 mm s^{-1}), two μ-oxo compounds (1.δ = 0.25,Δ = 0.38 ; 2.δ = 0.18, Δ = 1.00) and a fourth species (δ = 0.35, Δ = 0.71) believed to correspond to very small amorphous particles or microcrystals of FePc. The information so far obtained does not appar to provide conclusive evidence for the presence of individual FePc molecules bound directly to the support.

ii) Cyclic voltammetry experiments involving the standard monomeric FePc and the two μ-oxo derivations in the form of small crystals mixed with carbon yielded a common set of two well defined peaks (E_1 = -

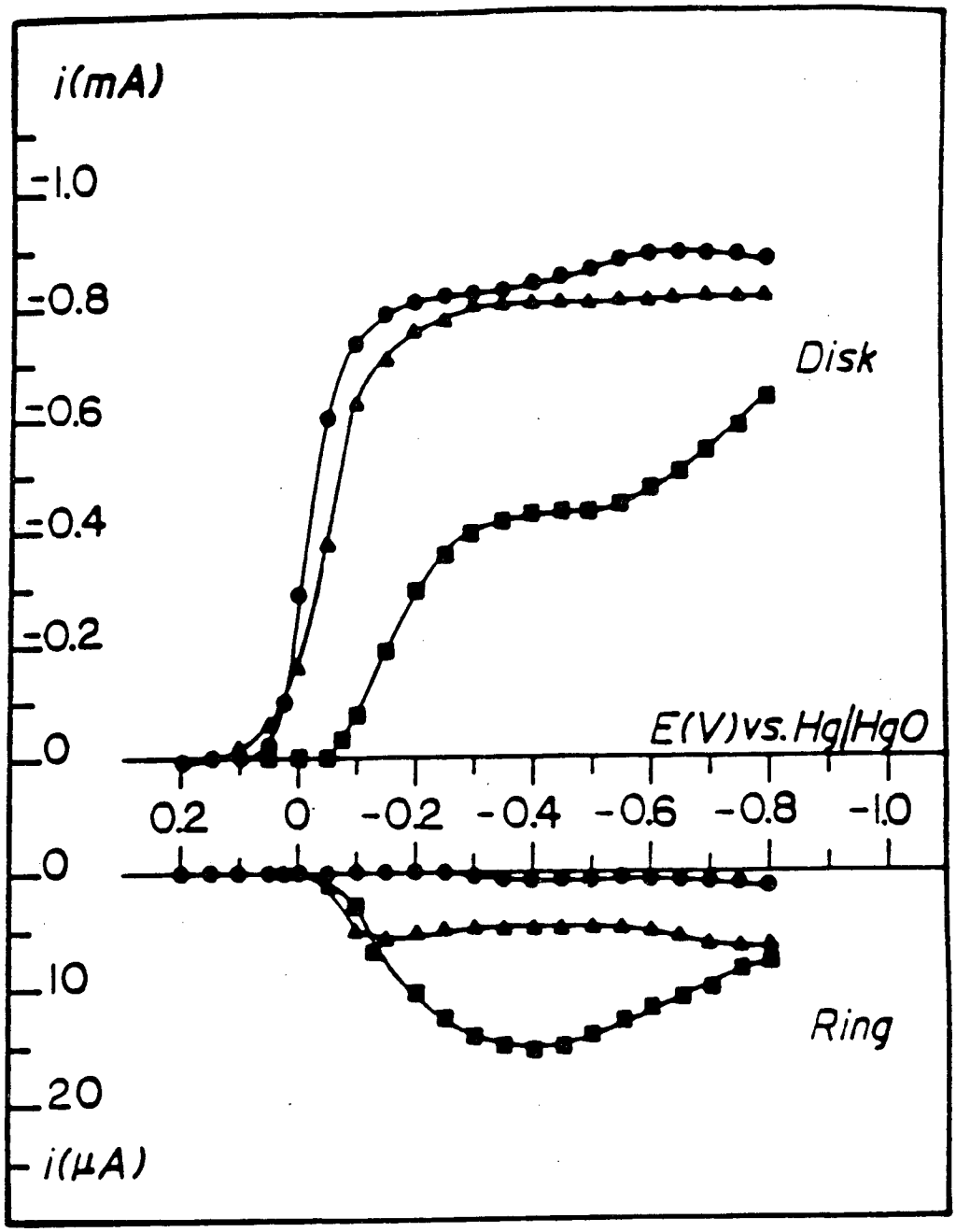

Figure 7. Ring-disk polarization curves for O_2 reduction on (●) 7% w/w FePc μ-oxo (1)/XC-72 carbon, (▲) Powercat 2000, and (■) Vulcan XC-72 carbon in 1 M NaOH. Rotation rate = 2500 rpm, room temperature. Electrode geometrical area = 0.196 cm^2. Gold ring at +0.13 V vs. Hg/HgO. Collection efficiency = 0.38.

0.15 V, E_2 = -0.55 V vs. Hg/HgO, OH^-). This indicates that despite the major differences in their spectral properties the redox characteristics of all forms of the FePc examined are associated with a single FePc surface species. The potentials at which these peaks are observed are in excellent agreement with those of two surface states reported by Barendrecht and coworkers (22) for FePc films, vapor deposited on smooth carbon surfaces.

iii) Quantum mechanical calculations and symmetry and overlap arguments reported elsewhere (23) indicate that Fe(II)Pc has an optimum electronic configuration for interacting with dioxygen. The bonding would involve charge transfer from the electron rich metal center to the O_2-π^* orbital leading to an overall weakening for the O-O bond in an end-on configuration. Evidence in support of this view has been provided by matrix isolation techniques from which an O_2-FePc adduct with this geometry has been unambiguously characterized (24). The fact that the onset for O_2 reduction appears to occur at potentials more positive than that associated with the Fe(III)Pc/Fe(II)Pc redox process may be explained by the high reactivity of the reduced form of the catalyst in direct analogy with the arguments put forward by Anson and Shigehara (25) in the case of a number of iron porphyrins.

iv) The strength of the axial interactions between the iron(II) center in FePc and O_2 and its reduction intermediates and products is expected to depend quite critically on the nature of the orbitals involved. It is thus likely that the affinity of Fe(II)Pc for dioxygen may be very high compared to that for other species. This may be of critical importance to the electrocatalysis involving a single type of iron site. Such model would make it necesary to invoke a metal spin crossover mechanism to explain the high activity of FePc for O_2

reduction as suggested by Savy and coworkers (25). The details of this work are given in Reference 20.

5. Molecular Orbital Calculations

In an effort to obtain theoretical insight into O_2 electrocatalysis by transition metal macrocycles,molecular orbital calculations have been performed using the semiempirical atom superposition-electron delocalization (ASED-MO) theory [18]. Transition metal macrocycles of the porphyrin (P) and phthalocyanine (Pc) type have been analyzed starting from a primitive fragment of the Me-N_4-type catalyst and building up larger ring molecules containing various substituents. From this unit the electron accepting properties of the ligand have been analyzed as a function of a change in the topology of this unit and as a function of a change on the metal-ligand (Me-N) bond length. It has been found that the energy gap defined as ΔE between the occupied d_{xz}, d_{yz} metal orbitals and the empty $e_g(\pi^*)$ ring orbital indirectly controls the ability of the transition metal macrocycle to activate O_2. Two of the most used electrocatalysts for O_2 reduction [e.g., porphyrin (P) and phthalocyanine (Pc)] have an electron acceptor $e_g(\pi^*)$ orbital nearly at the same relative energy with respect to the d_{xz}, d_{yz} metal orbitals. This should result in a similar electron population at the metal for both complexes and thus, in their electrocatalytic properties. The larger Me-N bond length in porphyrins, however, decreases the metal-to-ligand back bonding and increases the electronic charge at the metal. This may be one of the reasons for the μ-oxo formation in porphyrins. It is possible that by attaching appropriate substituents at the para position of the phenyl ring, the stability of the μ-oxo dimer may be decreased.

Metal porphyrins provide a unique opportunity to modify the electronic properties at the metal via a substitution at the meso positions of the ring

since the 18 π-electron system can be directly perturbed. This has been done by attaching phenyl rings and substituted phenyl rings at the meso position of the porphyrin. Steric constraints, however, orient these phenyl groups nearly perpendicular to the molecular plane and, thus, decrease the π resonance between the porphyrin ligand and the phenyl groups. One way of decreasing this steric constraint could be to increase the phenyl-macrocycle distance by interposing a -C≡C- group between both rings.

Figure 8.

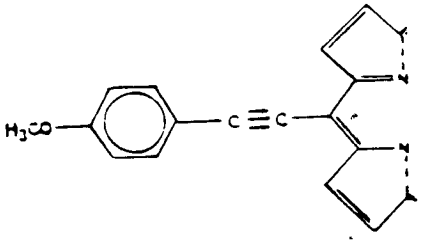

The planarity expected between the macrocycle ligand and the four phenyl rings should then increase the effect of the substituent in the para position of the phenyl groups.

MO considerations indicate that for the transition metal phthalocyanines, the increase in the number of π-electrons associated with the naphthalocyanines and polymeric phthalocyanines probably will not significantly improve the catalytic activity towards dioxygen since the charge density at the metal is only slightly modified. Structural factors, however, may play a role in the catalytic activity of phthalocyanines for dioxygen reduction. Further theoretical and experimental work on face-to-face phthalocyanines may provide important information for understanding the factors controlling O_2 reduction in such binuclear complexes.

6. Catalytic Effects of Simultaneously and Sequently Adsorbed Water-Soluble Transition Metal Macrocycles

An approach recently initiated at Case for the preparation of binuclear transition metal macrocycles is based on work of Linschitz and coworkers (26)

who have examined such diporphyrins spectroscopically (uv-visible absorption and ESR). Their approach simply involves the spontaneous association of water-soluble anionic and cationic macrocycles. In principle, mixing aqueous solutions of macrocyclic ligands of comparable molecular dimensions with peripheral positive and negative charges leads to the precipitation of a one-to-one stoichiometric salt due to molecular shape and charge compatibility.

Thus water soluble tetrasulfonated phenyl porphyrin (TSPP) and tetramethyl pyridyl porphyrin (TMPyP) have been synthesized and characterized at Case (Fig. 9). These porphyrins have also been metallated and the electrochemical studies on their redox behavior and the O_2 reduction kinetics have been investigated.

Preliminary studied with water soluble iron compounds of a positively charged porphyrin (TMPyP) and a negatively charged phthalocyanine (TsPc) both sequentially and simultaneously adsorbed on graphite, did not show significant gains in the catalytic activity for O_2 reduction in 0.1 M NaOH over the better catalytically active macrocycle individually (e.g., FeTsPc in this case). However, with cobalt compounds of the same positively charged porphyrin and negatively charged phthalocyanine, the activity of the sequentially adsorbed macrocycles is somewhat better than the simultaneously adsorbed macrocycles in this case.

Adsorbed layers containing both the anionic mesotetra (sulfonated phenyl) porphyrin (TSPP) and the cationic mesotetra (N-methyl-4-pyridyl) porphyrin (TMPyP) were also formed on a pyrolytic graphite substrate. Preliminary results with cobalt compounds have shown no preponderance in the catalytic activity for O_2 reduction in alkaline solutions over the individually adsorbed transition metal macrocycles. The results indicate that the ligands used may not possess sufficient structural compatibility to form the desired sandwich type species with proper spacing for binding the oxygen molecule. More work needs to be done involving both anionic and cationic macrocyclic ligands of

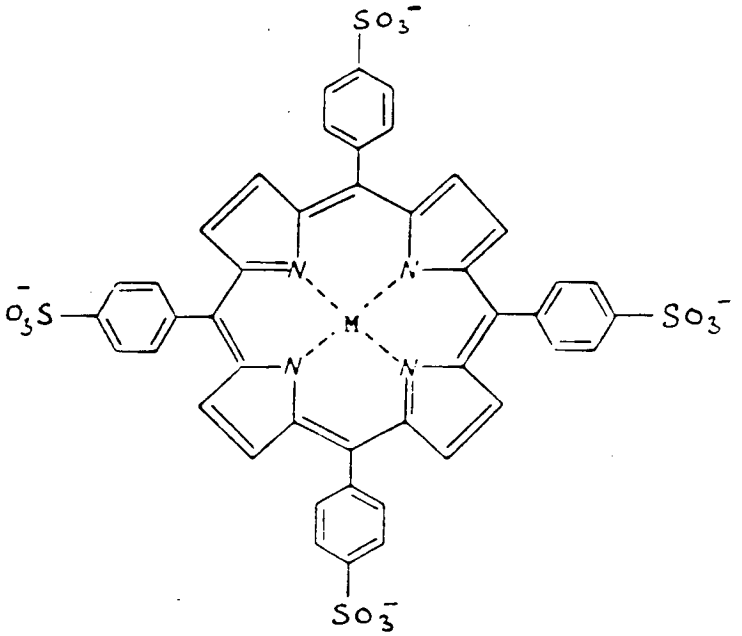

Metallo-tetra(sulfophenyl) porphyrin (MeTSPP)

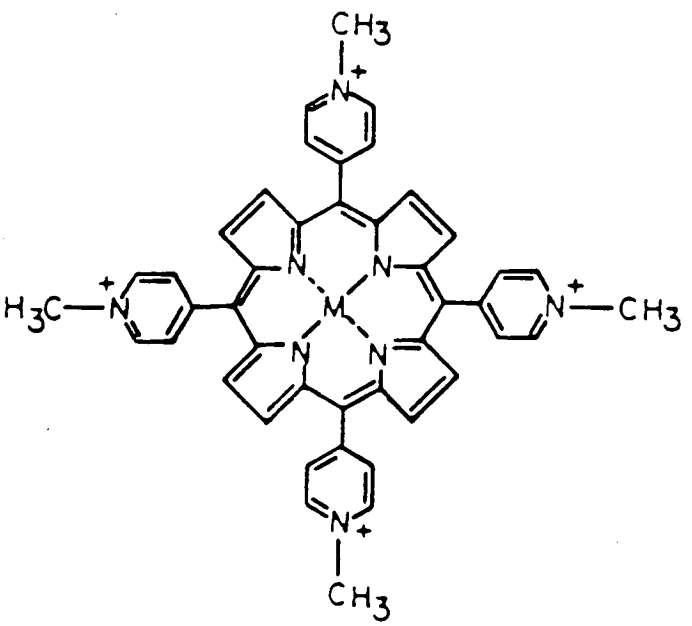

Fig. 9. Metallo-tetra(methylpyridyl) porphyrin (MeTMPyP)

comparable molecular dimesnions.

7. Adsorption Studies of Macrocycles

To understand better the factors involved in the fabrication of macrocycle catalyzed high area carbon electrodes, the adsorption isotherms have been determined for the adsorption of macrocycles on high area carbons from organic solvents. The Case group has examined the adsorption of cobalt tetramethoxy phenyl porphyrin (CoTMPP) on XC-72 and Shawinigan black from acetone solution. The isotherms (Fig. 10) and the corresonding Langmuir plots show that the adsorption is Langmuirian. The maximum amount adsorbable on the surface cannot be determined directly from the curves since they have not completely levelled off at high concentration. A plot of the same data in reciprocal form, i.e., reciprocal of the amount adsorbed vs. the reciprocal of the concentration, will yield the maximum amount adsorbable as the extrapolated intercept at $1/c = 0$ i.e., infinite concentration. The values thus obtained were 0.069 gg^{-1} for XC-72 and 0.020 gg^{-1} for SB. Having calculated the theoretical area of CoTMPP to be 3.9 nm^2 for the flat configuration, (Fig. 11) one can calculate the fraction of a monolayer which is covered. Taking 67 m^2g^{-1} for SB and 216 m^2g^{-1} for XC-72, the fractional coverages were 0.95 and 0.88 respectively. These values are surprisingly close to the unit monolayer coverage, given the uncertainty in the estimation of the molecular area, the measurements of the BET surface area and in the assumption that all the BET area is available for adsorption.

8. Voltammetry and O_2 Reduction Studies of Mono- and Binuclear Metal Chelates of Tetradentate Schiff Base Ligands

A number of mono- and binuclear metal chelates of tetradentate Schiff base ligands derived from aromatic diamines and O-hydroxyaromatic aldehydes have been made available from Tanta University (Egypt). In these compounds the metal is not coordinated in an N_4 center as in the porphyrins and phthalocyanines but

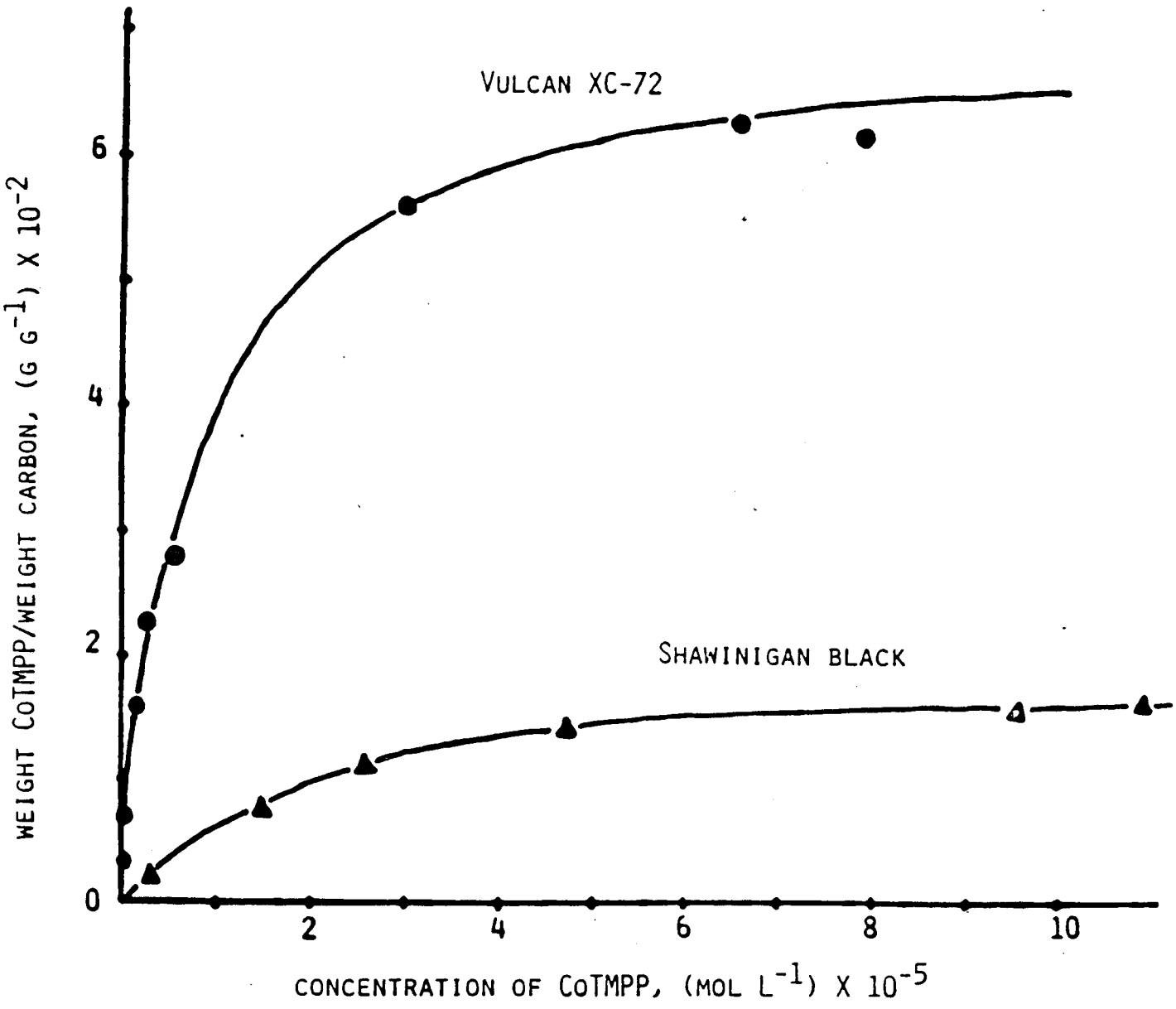

FIG. 10. ADSORPTION ISOTHERMS FOR THE ADSORPTION OF CoTMPP ON CARBONS FROM ACETONE SOLUTION AT 25°C.

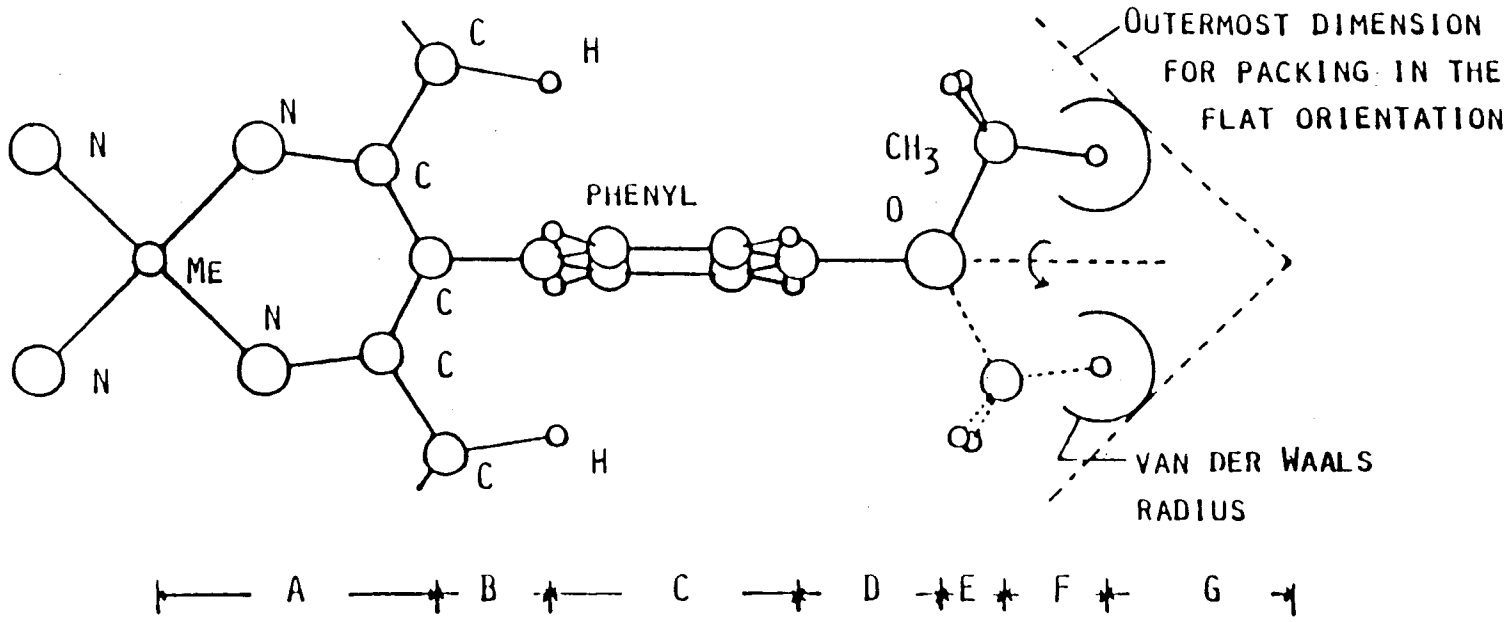

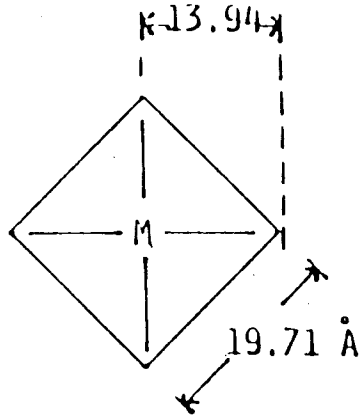

A	:	3.43 Å
B	:	1.39 Å
C	:	2.79 Å
D	:	1.36 Å
E	:	0.72 Å
F	:	1.08 Å
G	:	3.17 Å
TOTAL	:	13.94 Å

TOTAL AREA = 388.5 $Å^2$

FIG. 11. MOLECULAR DIMENSIONS FOR METALLATED TETRAMETHOXY PHENYL PORPHYRINS, SHOWING THE OUTER DIMENSIONS FOR ADSORPTION IN THE FLAT ORIENTATION, BASED ON FREE ROTATION OF THE METHOXY GROUP.

is coordinated to both N and O atoms. Some of these complexes have been characterized electrochemically at Case using cyclic voltammetry and the rotating disk electrode technique. The electrocatalytic activity of these complexes for O_2 reduction in acid and alkaline electrolytes has also been examined. In general it can be seen that the charge associated with the voltammetric peaks for the adsorbed metal chelates on pyrolytic graphite is small, corresponding typically to 3-10 $\mu C/cm^2$, as would be expected for 0.3-1.0 monolayer of the complexes. The redox properties appear quite normal, but a detailed interpretation of the voltammograms requires supplementary uv-visible and other spectroscopic data plus the voltammetry curves for the solution phase species. The activities for O_2 reduction of the metal chelates used in this study are much smaller than those of the iron and cobalt porphyrins and phthalocyanines. One of the reasons for the low catalytic activity may be the lack of π electron delocalization in the ligand structure symmetrically about the central metal ion, which results in non-planarity of the molecule.

B. Heat and Radiation-Treated Macrocycle Catalysts

1. Heat-treated Macrocycle Catalysts

A large portion of the DOE-LBL research done at Case in conjunction with the Eltech Project (Contract No. W-7405-ENG-48) has involved the examination of the heat-treated transition metal macrocycles because of their demonstrated high activity and stability for O_2 reduction in alkaline and acid electrolyte.

Heat-treated transition metal macrocycle catalysts such as Fe- and Co-tetramethoxyphenyl porphyrins (TMPP) dispersed on high area carbons have shown high activity for O_2 reduction in alkaline and acid electrolytes with good stability in concentrated alkaline solutions. The transition metal need not be present in the macrocycle during the heat treatment. Metal-free macrocycles such as H_2TMPP can be heat-treated and the transition metal subsequently

adsorbed on the surface even in-situ from the alkaline electrolyte. The combined use of Fourier transform infrared, transmission electron microscopy, Mossbauer, X-ray diffraction, Magnetic susceptibility and pyrolysis gas chromotograph-mass spectroscopy has provided new insight into the effects of heat treatment. The macrocycles partially decompose while retaining the pyrrole nitrogen. The pyrrole nitrogens then provide binding sites for adsorbed transition metal such as Co and Fe with the catalytic activity due mostly to the transition metal in an atomic state of dispersion.

a. Effect of heat treatment of the Macrocycle

In the case of CoTMPP dispersed on XC-72 carbon, the effect of 800°C HT on the polarization curves for O_2 reduction in the gas-fed porous electrodes is not very pronouced in short-term tests but the stability of the electrode is, however, increased considerably with 800°C HT (27). The curves exhibit ~21 mV separation between the air and O_2 polarization curves which is predicted on the basis of the Nernst equation using the respective O_2 partial pressures. The Tafel slopes (~-37 mV/decade) are also consistent with peroxide decomposition as rate-determining. FeTMPP/XC-72 shows large improvements in activity and stability with 800°C HT. However, the rate-determining step is not as clearly understood and may involve the initial O_2 reduction step. The Tafel slope for the non-heat-treated FeTMPP on XC-72 was ~-50 mV/decade. Over part of the potential range, the air and O_2 curves are separated by a factor of 5 in current density, which would be expected for first order rate control by O_2.

b. Role of Transition Metal

Contrary to reports of the Iliev (28) and Wiesener (29) groups, it has been found at Case that the transition metal is necessary for high O_2 reduction activity but that the metal-free porphyrin can be used, as long as some source of either Fe or Co exists, such as in the activated RB carbon or an added metal hydroxide before or after the heat treatment. The metal-free porphyrin H_2TMPP

has been found to be not active for O_2 reduction in either acid or alkaline electrolytes even after heat treatment on carbon blacks not containing significant transition metal impurities. The Iliev (30) and Wiesener (31) research groups have shown that cobalt acetate heat treated together with H_2TMPP and carbon produces a catalyst with almost the same O_2 reduction behavior as for the heat-treated CoTMPP on carbon. They also produced active catalysts using different sequences of addition of cobalt acetate and H_2TMPP with the heat treatment done at various stages (31). The Case group found that cobalt or iron hydroxides could be substituted for the acetates and the subsequent heat treatment with H_2TMPP on carbon would result in highly active catalysts for O_2 reduction in acid (32) and alkaline solutions (33). It was also found that cobalt hydroxide could be added after the heat treatment of the H_2TMPP on carbon and highly active catalysts would result (32-34). With the Fe(III) hydroxide added after the H_2TMPP heat treatment there is a measurable increase in the O_2 reduction performance but not as good as was observed for the Co(II) hydroxide addition. It is thought that this difference has to do with the difficulty in maintaining the Fe(II) state, which is necessary for interaction with the ligand structure.

In some cases more than one transition metal hydroxide was added to H_2TMPP on carbon after the heat treatment with additional gains in performance being noted in KOH electrolyte (34, 36) (Fig. 12). More than one metal hydroxide were added in some cases to the metal-free macrocycle on carbon prior to the heat treatment. For example, both iron and cobalt hydroxides were added to H_2TMPP on XC-72 and then heat-treated to 450°C. The O_2 reduction performance is quite promising (Fig. 13).

In order to establish the role played by the various components of the heat-treated cobalt-porphyrin-carbon catalyst system in the O_2 reduction pro-

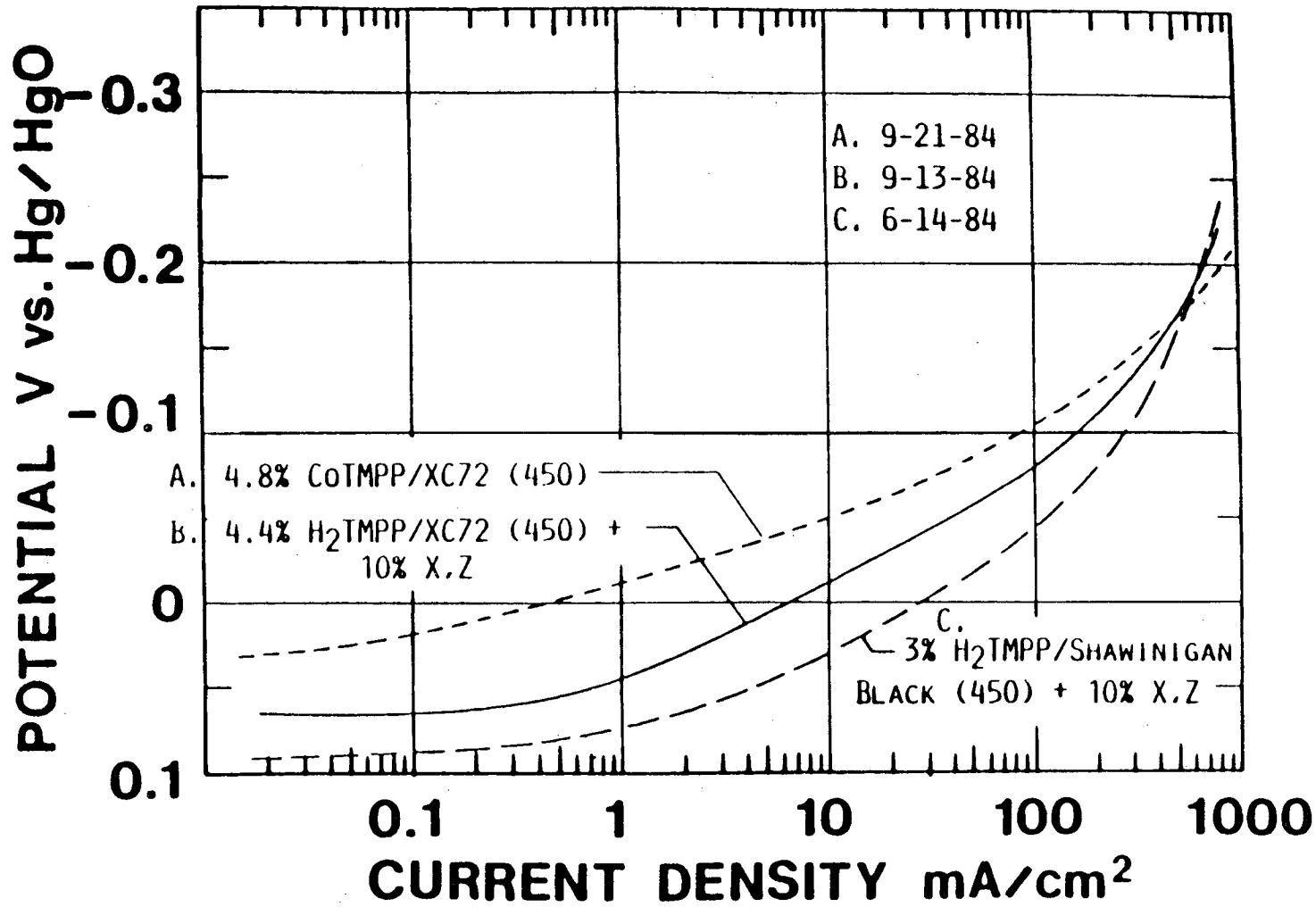

FIG. 12. POLARIZATION CURVES FOR O_2 REDUCTION WITH POROUS O_2-FED (1 ATM) ELECTRODES IN 4 M NAOH AT 60°C. ELECTRODES A AND B CONTAINED 27.1 MG CM^{-2} MACROCYCLE/CARBON AND 11.6 MG CM^{-2} TEFLON T30B, WHILE ELECTRODE C CONTAINED 27.1 MG CM^{-2} MACROCYCLE/CARBON AND 9.0 MG CM^{-2} TEFLON. ELEMENTS X AND Z WERE ADDED AS THE HYDROXIDES. THE MACROCYCLE/CARBONS WERE HEAT-TREATED AT 450°C FOR 2 H IN FLOWING AR.

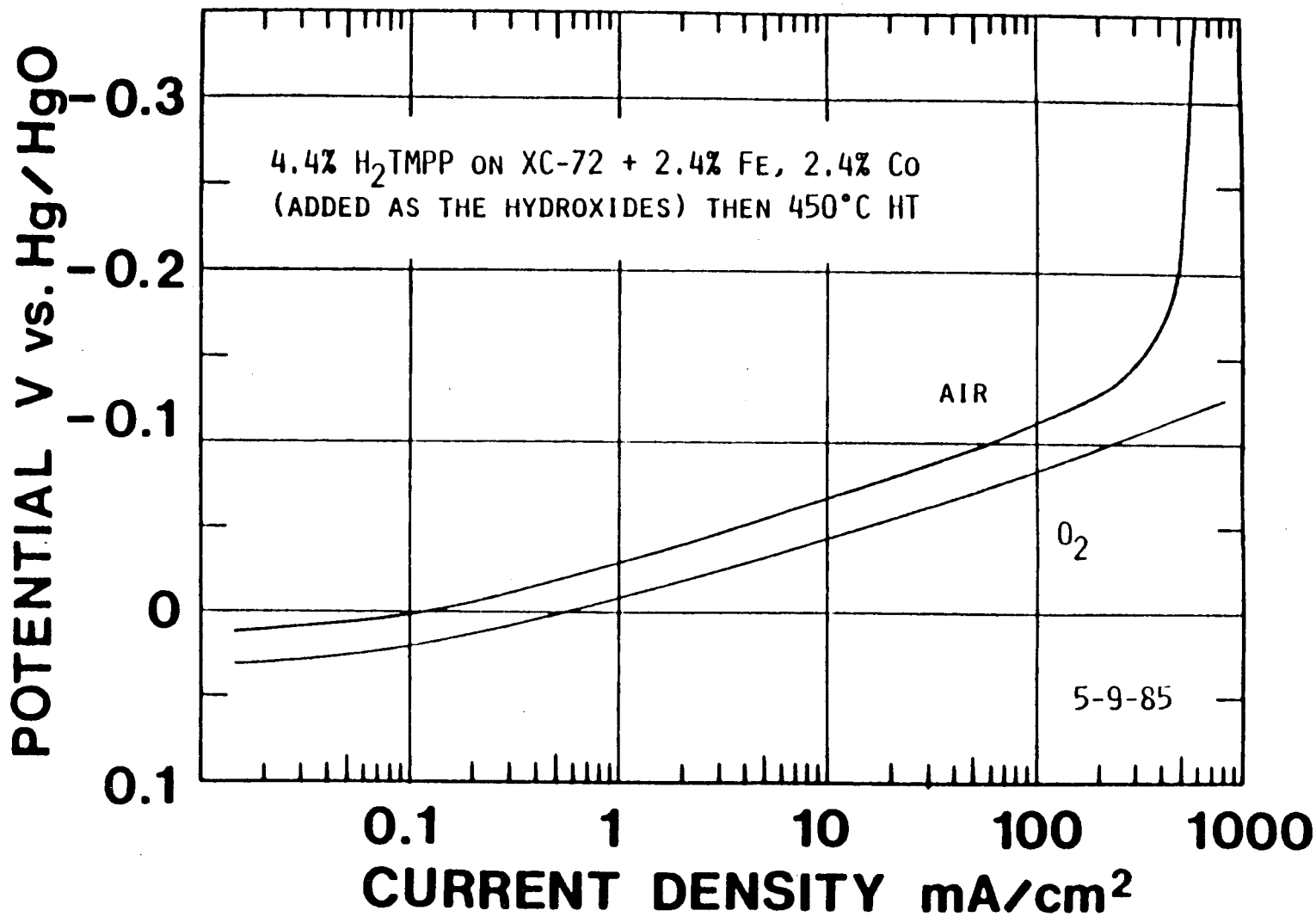

FIG. 13. POLARIZATION CURVES FOR O_2 REDUCTION WITH A GAS-FED (1 ATM) ELECTRODE IN 4 M NaOH AT 60°C. THE ELECTRODE CONTAINED 14.6 MG CM^{-2} CATALYST/CARBON AND 6.2 MG CM^{-2} TEFLON T30B AND WAS HEAT-TREATED AT 280°C FOR 2 H IN FLOWING HE.

cess in alkaline solutions, kinetic studies have been conducted using the rotating ring-disk electrode technique (35). These measurements have been carried out on catalysts prepared from the metal-free H_2TMPP, CoTMPP and $Co(OH)_2$, supported on carbon black (Shawinigan) attached to pyrolytic graphite disk as a thin Teflon-bonded coating with the heat treatment being either before or after the deposition of the hydroxide (Fig. 14). Hydrogen peroxide decomposition rates were also measured for this series of formulations using the gasometric method. It has been shown that $H_2TMPP/SB + Co(OH)_2$ as well as the CoTMPP/SB, both heat-treated at 450°C, possess similar O_2 reduction activity and catalyze both the reduction of O_2 to HO_2^- and the decomposition of HO_2^- (Table II). The interpretation of the results is that the $Co(OH)_2$ interacts with the H_2TMPP even after the latter has been heat-treated and that the product of this interaction is more active for O_2 reduction than the SB carbon itself and more active for peroxide decomposition than the $Co(OH)_2$. The experiments suggest that the high catalytic activity of heat-treated macrocycle/transition metal systems may be due to the transition metal adsorbed on a modified carbon surface perhaps through surface nitrogen atoms. The catalysis may be due principally to adsorbed transition metal-N sites. The details are given in Reference 35.

c. Adsorption Experiments

Another approach to the adsorption of the transition metal on the heat-treated metal-free macrocycle-carbon surface is to have the reaction take place in a suspension of the macrocycle-carbon in a solvent such as acetic acid or dimethyl formamide, much as in the usual procedure of the metallation of porphyrins (37,38). This approach was successful in the case of cobalt. Approximately 0.24 moles of cobalt were adsorbed per mole of H_2TMPP, which had been heat-treated on XC-72 carbon at 450°C, when the reaction was performed in

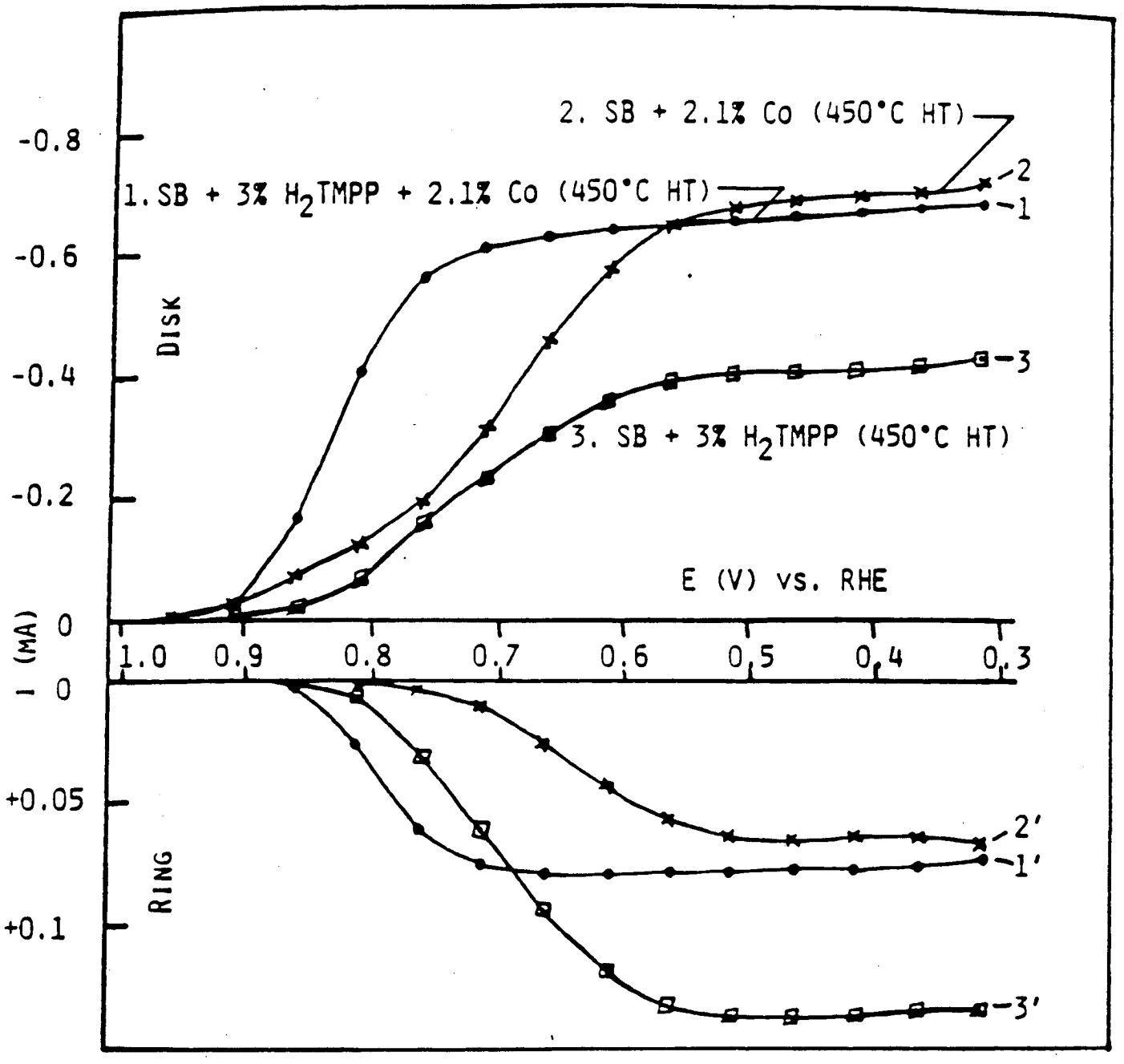

FIG. 14. DISK CURRENTS (O_2 REDUCTION) AND RING CURRENTS (HO_2^- OXIDATION) FOR ROTATING ELECTRODES WITH THIN (~5 MG CM^{-2} OR ~50 μM) POROUS TEFLON-BONDED COATINGS ON PYROLYTIC GRAPHITE (0.2 CM^2). THE COATINGS CONTAINED 10 WGT.% TEFLON T30B. THE PT RING (N = 0.37) WAS SET AT 1.11 V VS. RHE. THE ROTATION RATE WAS 900 RPM. SB = SHAWINIGAN ACETYLENE BLACK.

TABLE II

KINETIC PARAMETERS FOR O_2 REDUCTION WITH HEAT-TREATED CoTMPP, H_2TMPP AND $Co(OH)_2$ ON SHAWINIGAN BLACK IN 0.1 M NAOH AT 25°C.

MATERIAL	$E_{1/2}$, V vs. SCE[A]	I, mA at -0.25 V[A]	n[A]	K_p, $(G\ s)^{-1}$ X 10^{-2} (B
1. SB (450°C HT)	-0.225	0.095	2.15	0.04
2. SB (450°C HT) + 0.21% Co	-0.225	0.110	2.30	0.26
3. SB + 0.21% Co (450°C HT)	-0.265	0.155	3.00	3.80
4. SB + 2.1% Co (450°C HT)	-0.285	0.170	3.62	5.72
5. SB (450°C HT) + 3% H_2TMPP	-0.285	0.050	1.92	0.14
6. SB + 3% H_2TMPP (450°C HT)	-0.265	0.130	2.23	0.10
7. SB + 3% H_2TMPP (450°C HT) + 0.21% Co	-0.190	0.335	3.08	11.0
8. SB + 3% H_2TMPP +0.21% Co (450°C HT)	-0.180	0.355	3.08	26.2
9. SB + 3% H_2TMPP + 2.1% Co (450°C HT)	-0.170	0.425	3.62	53.2
10. SB + 3% CoTMPP (450°C HT)	-0.170	0.435	3.54	46.0
11. SB (450°C HT) + 3% H_2TMPP	-0.190	0.365	2.69	2.92

A. FROM RRDE (THIN POROUS COATING) MEASUREMENTS AT 400 RPM. THE n VALUE AT -0.50 V IS BASED ON A LEVICH COEFFICIENT OF 6.5×10^{-3} mA $RPM^{-1/2}$ PER ELECTRON IN 0.1 M NAOH (REF. 78).

B. HYDROGEN PEROXIDE DECOMPOSITION PSEUDO-FIRST ORDER RATE CONSTANT.

boiling glacial acetic acid (ca. 120°C) with ca. 1mM cobalt acetate. The O_2 reduction activity of the resulting material was much higher than if the carbon without the macrocycle was given identical heat treatment and chemical treatment with Co^{2+}-glacial acetic acid, and very close to the activity of heat-treated CoTMPP/XC-72. However, when the same treatment is carried out with iron maintained in the +2 valency state (H_2 atmosphere), the subsequent O_2 reduction activity of the resulting material was only slightly higher than the carbon alone, given the same treatment and much less than heat-treated FeTMPP/XC-72. To achieve high activity, the iron should be present during the heat treatment of the macrocycle/carbon samples. Thus in contrast to the behavior with cobalt, iron may catalyze a kind of transformation of the macrocycle/carbon which is qualitatively different from that obtained with either cobalt or metal-free macrocycle.

Adsorption experiments were also conducted in-situ with a gas-fed electrode in 4 M NaOH at 60°C by adding cobalt chloride directly into the caustic. In air-saturated solution, the $Co(OH)_2$ and $Co(OH)_3$ are readily air-oxidized, and resulting $Co(OH)_3$ and Co_3O_4 precipitate. An electrode made from, heat-treated H_2TMPP on XC-72 improved considerably over the span of 1.5 h after the addition of $CoCl_2$ to the caustic. This experiment again demonstrates the critical role played by the transition metal in the O_2 reduction catalysis. It also suggests methods for preventing the loss of the cobalt from air electrodes during long-term operation.

d. Extraction Experiments

Earlier extraction experiments with cobalt and iron tetramethoxy phenyl porphyrins using hot glacial acetic acid showed that CoTMPP extracted after 800°C heat treatment on XC-72 carbon exhibited somewhat lower activity for O_2 reduction than the unextracted samples but still much higher than for the

carbon or metal-free macrocycle (H_2TMPP) alone. Only part of the transition metal is removed, however.

Extraction experiments were also done with CoTMPP on steam-activated Shawinigan black (SASB) (800°C HT) using nitrogen saturated 4 M NaOH at 60°C as the extractant. Approximately 13 to 25% of the original Co was removed after 20 h. This length of time was allowed since the solubility of $Co(OH)_3$ is relatively low under these conditions, ca. 1.1 mM. The solid was washed with dilute caustic and water, then filtered on a Gelman Vinyl Metrical filter membrane (PVC, 5 μm pore size). The polarization curve showed only a slight shift as compared with the non-extracted material. The extraction probably removes mostly the metal oxides and leaves the majority of the metal in a complexed from which is catalytically active. The existence of the metal oxides is inferred from Mossbauer and electron microscopic results of Scherson and co-workers (39-40) and from cyclic voltammetry curves (42).

Further extraction experiments have been carried out with non-heat-treated and heat-treated Co-TMPP samples adsorbed on steam-activated Shawinigan black (SASB) using acetone. Co-TMPP can be completely extracted (Soxhlet extraction) from a non-heat-treated sample on carbon. The uv-visible spectrum of the Co-TMPP was unchanged after this procedure. A sample heat-treated at 300°C, however, showed a sharp decrease in the amount of extractable Co-TMPP. The spectra obtained for samples heat-treated at 350°C ± 25°C showed that all of the absorption bands shifted toward longer wavelengths (Fig. 15). For samples heat-treated at temperatures >400°C there was no detectable Co-TMPP extracted. The fact that changes occur at temperatures as low as 300°C, at which pyrolysis-mass spectral data (41) have shown no evidence for the release of gaseous products, indicates that Co-TMPP may undergo some type of chemical binding to the carbon surface in which products are not released.

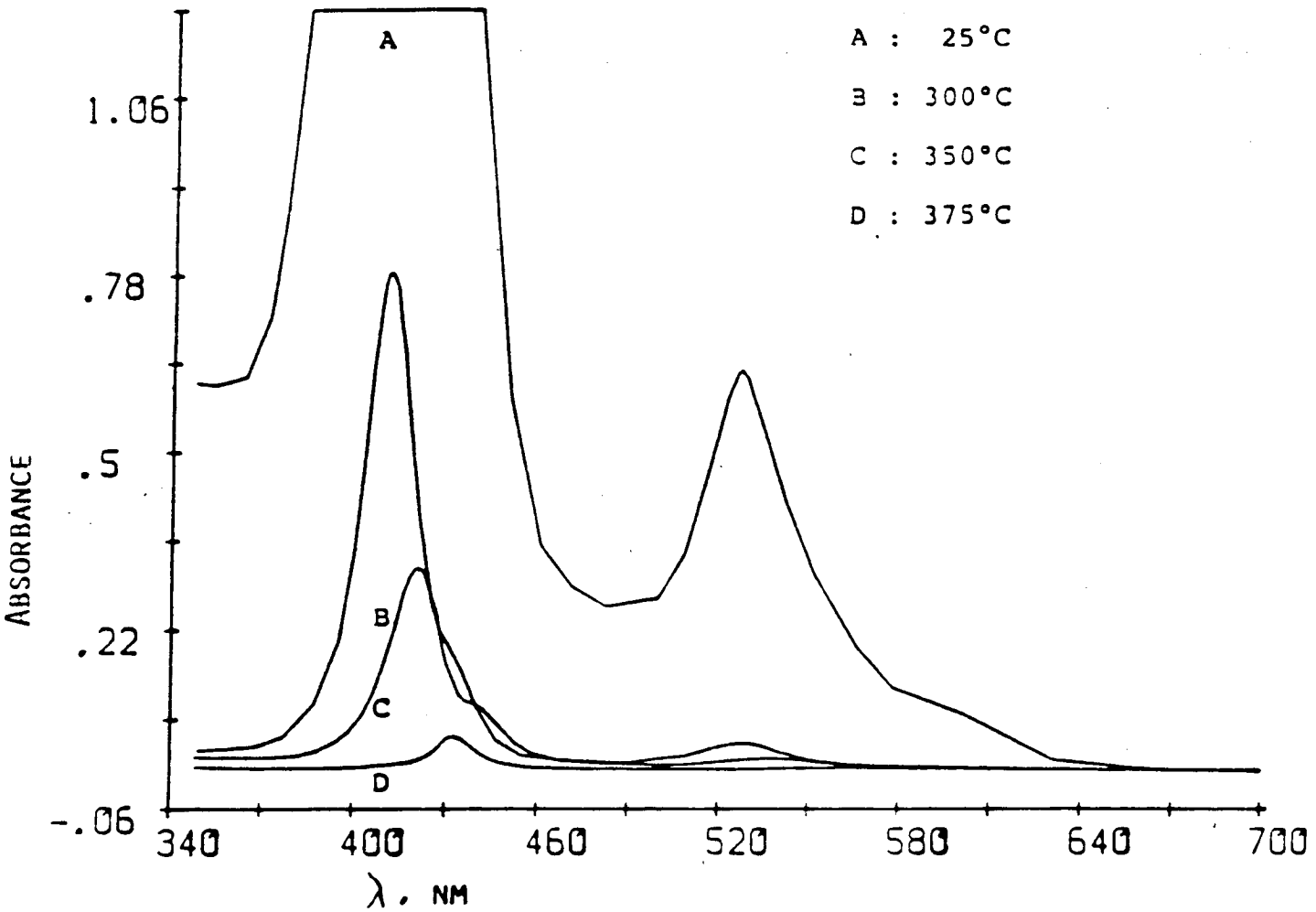

Figure 15. UV-visible absorption spectra of acetone-extracts (20 mg/25 ml, Soxhlet extraction, 1 h) from heat treated 9.3% CoTMPP on steam-activated Shawinigan black (25°, 300°, 350°, 375°C, Ar, 2 h)

e. Naturally-occurring Macrocycles

There has been some emphasis on finding lower-cost catalysts for O_2 reduction and one possible approach is to use natural products such as hemoglobin or the iron porphyrin found in hemoglobin such as hemin or hematin. Hemin (Fig. 16) adsorbed on RB carbon and heat-treated at 800°C exhibited polarization for O_2 reduction which was very similar to that of FeTMPP/RB. Hemoglobin has also shown promising results. The macrocycle portion of the molecule is a small part of the total structure (~1% by weight). Even so, the catalytic activity in alkaline solutions is quite high.

Kinetic studies of O_2 reduction have been carried out using the rotating ring-disk electrode technique on the naturally occurring macrocycles (hemin, hematin and hemoglobin) supported on deashed RB carbon (800°C HT) and attached to a pyrolytic graphite disk as a thin Teflon-bonded coating. The ring-disk data particularly for hemin on RB carbon (800°C HT) (Fig. 17) show practically no solution phase peroxide at low polarization in alkaline solutions indicating that the O_2 reduction approaches 4-electrons.

f. Characterization of Heat-treated Macrocycles

A number of electrochemical and non-electrochemical methods including spectroscopic methods have been used at Case to characterize the heat-treated macrocycles. Some of the important results are given below:

1. Pyrolysis-gas chromatography-mass spectrometry (41)

The slow and flash pyrolysis-mass spectrometry and and pyrolysis-gas chromatography-mass spectrometry experiments have indicated that i) the fraction of volatile nitrogen to non-nitrogen containing species generated during thermal treatment is much higher for the metal-free than for the cobalt and iron-μ-oxo TMMPs. This effect is especially pronounced when the macro-

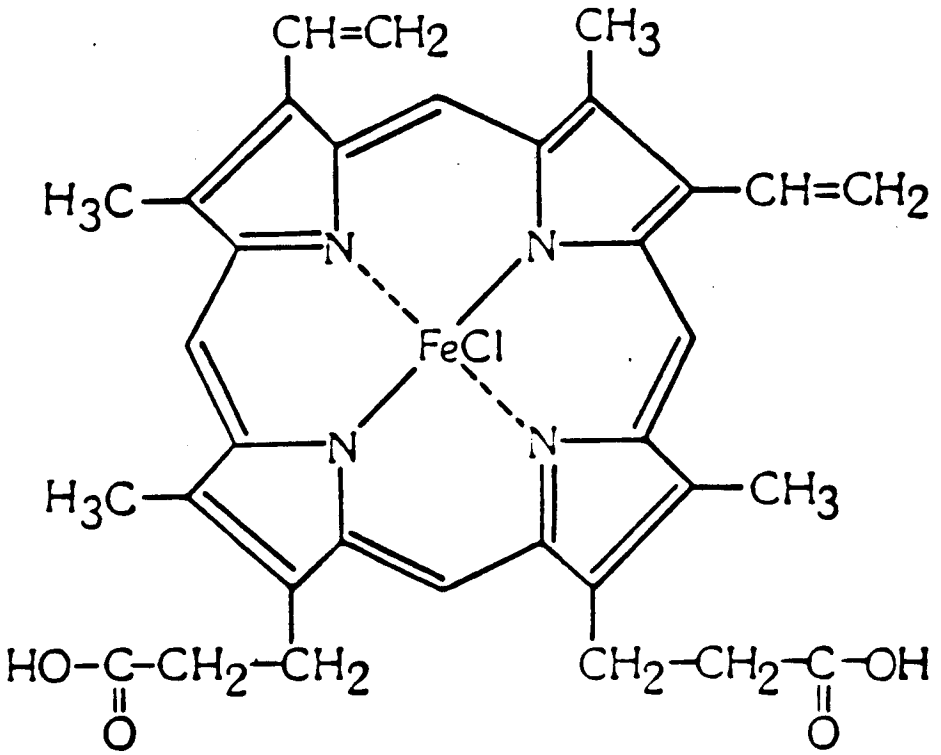

FIG. 16. STRUCTURAL FORMULA FOR HEMIN [CHLOROPROTOPORPHYRIN IX IRON (III)].

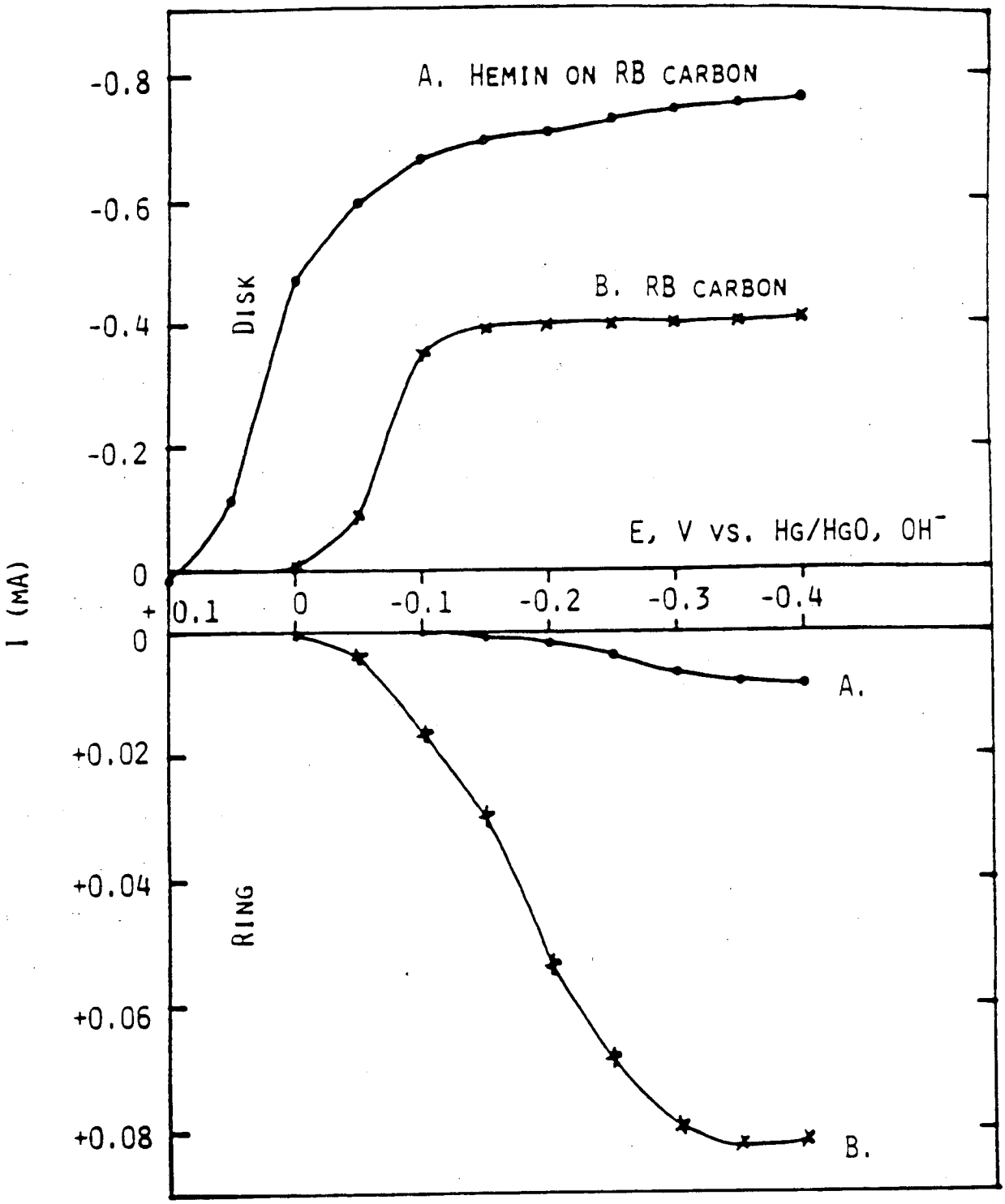

FIG. 17. DISK CURRENTS (O_2 REDUCTION) AND RING CURRENTS (HO_2^- OXIDATION) FOR ROTATING ELECTRODES WITH THIN (~50 μM) POROUS TEFLON-BONDED COATINGS MADE FROM A) 10% HEMIN ON RB CARBON (800°C HT) AND B) RB CARBON IN 0.1 M NAOH AT 25°C. THE DISK AREA WAS 0.2 CM^2. THE COATINGS CONTAINED 10% TEFLON T30B. THE PT RING (N = 0.37) WAS SET AT +0.1 V. THE ROTATION RATE WAS 2500 RPM.

cycles are supported on Vulcan XC-72 high area carbon. These results are consistent with microgravimetry analysis of the same supported macrocycles before and after heat treatment at 800°C for which the amount of nitrogen was higher for the metallated compounds than for the metal-free analog and ii) high molecular weight volatile fragments can be detected only in the case of H_2TMPP and to a much less extent for $(FeTMPP)_2O$. These consist of a pyrrole attached to substituted benzene group and thus do not correspond to the compounds reported earlier by other workers. The details are given in Reference 41.

2. Mossbauer Spectroscopy

Mossbauer spectra have been obtained for heat-treated $(FeTMPP)_2O$ dispersed on carbon. The room temperature Mossbauer spectrum for the $(FeTMPP)_2O$ dispersed on XC-72 and heat-treated at 800°C for two hours under a flowing inert gas atmosphere was found to consist of a broad asymmetric singlet. Comparison of the actual spectrum with the curve obtained by the statistical fit of the data to a single Lorentzian superimposed on the experimental points reveals the asymmetry. In order to gain insight into the nature of the species present in the material, Mossbauer measuremnts were conducted at 50 K and 5.7 K (Fig. 18). A spectrum was also recorded at the latter temperature in the presence of an external magnetic field of 6 T (Fig. 19). The results obtained bear some resemblance to those reported by van Veen et al. (43) and Bett et al. (44) for similar heat-treated compounds. The broad magnetic pattern is most likely due to relaxation effects. Similar Mossbauer spectra without applied magnetic field, have been observed by Maricondi et al. (45) for compounds of the form FeTPPX where X represent a halide group bound to the complex in the axial position. This provides some evidence that part of the iron in this pyrolyzed material may be present as Fe(III) in a high spin state.

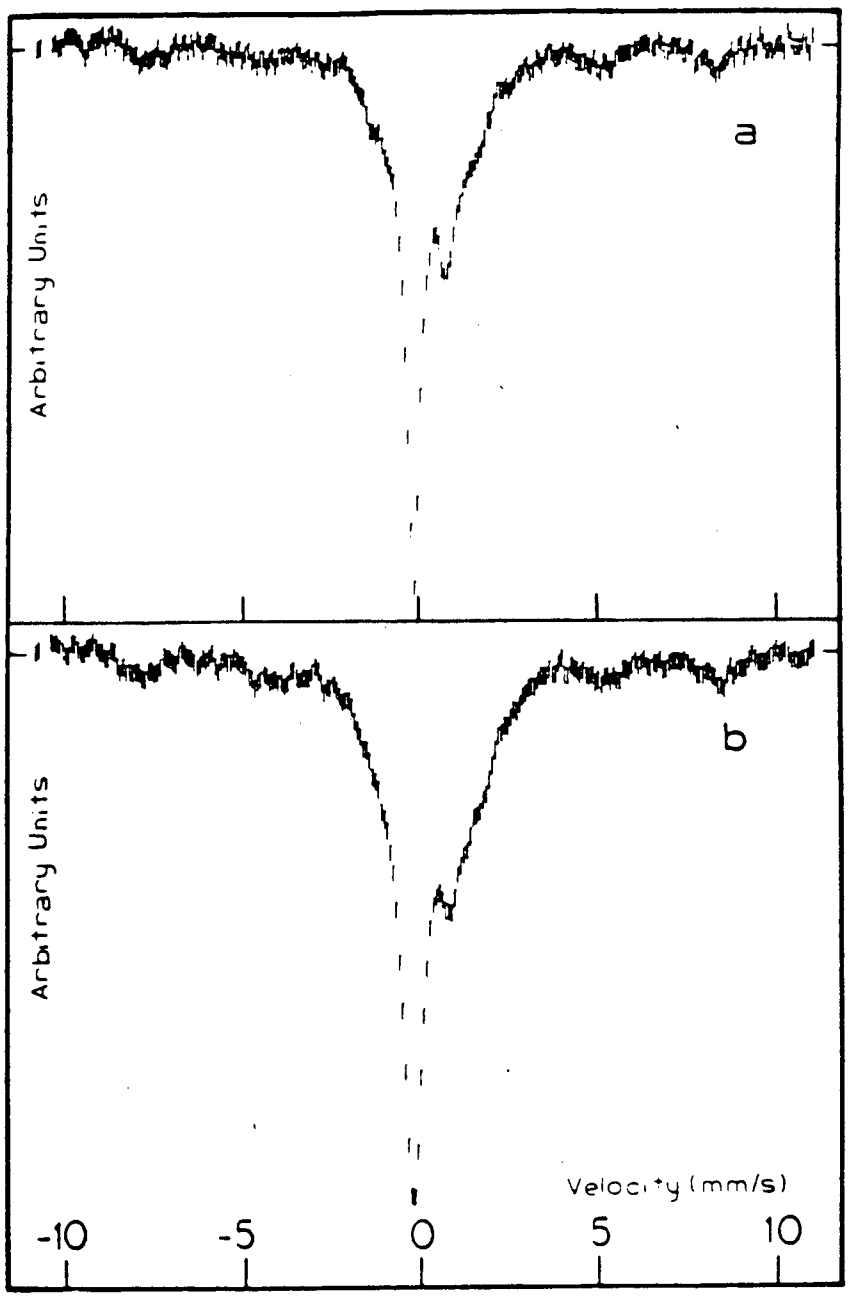

Figure 18. Mossbauer spectra of 4.8% w/w $(FeTMPP)_2O$ dispersed on Vulcan XC-72 carbon and heat-treated at 800°C for 2 hours in Ar. Spectra recorded at a) 50 K and b) 5.7 K.

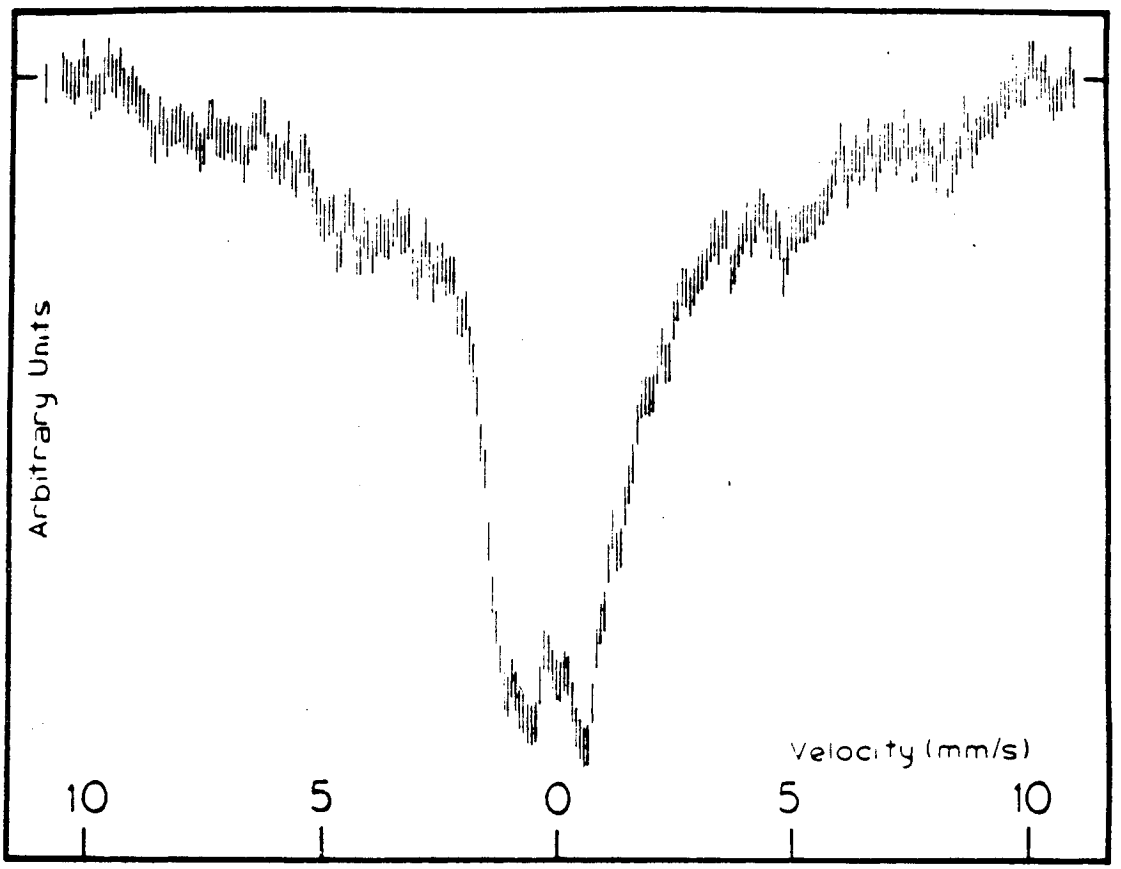

Figure 19. Mossbauer spectrum of 4.8% $(FeTMPP)_2O$ dispersed on Vulcan XC-72 carbon and heat-treated at 800°C for 2 hours in Ar. Spectrum recorded at 5.7 K and 6 T.

It is well known that as the particle size of a magnetic material is decreased, the internal field becomes too small to split effectively the magnetically degenerate states (46). This leads to a collapse of the lines associated with the allowed nuclear transitions yielding in the limit a singlet. It is thus possible that the prominent feature observed in the spectra may be either metallic iron or some of its oxides in highly divided form. The first of these possibilities may be excluded, however, in view of the results obtained by Niemantsverdriet et al. (46) who obtained strong evidence that small particles of hydrogen-reduced iron supported on high area carbon undergo complete oxidation upon exposure to air during the Mossbauer measurements. In earlier experiments conducted in this laboratory (39), the Mosbauer spectra of the heat-treated materials were quite different exhibiting six distinct peaks, and the parameters clearly fitted γ-Fe_2O_3. This oxide was the only iron containing species detected in the Mossbauer spectra of $(FeTMPP)_2O$ supported on carbon specimens heat-treated at temperatures between 600°C and 800°C. This assignment was later verified by transmission electron microscopy and electron diffraction (47) for which the single crystals observed indexed precisely as γ-Fe_2O_3.

The differences between the Mossbauer results obtained in previous work at CWRU (39) and those presented here may be attributed to the use of less stringent purification and adsorption procedures as well as of a much more rudimentary pyrolysis system involved in the earlier studies. It is not clear at this point whether these oxides observed in the ealier work were generated during the pyrolysis due to the presence of traces of O_2 in the thermal treatment apparatus arising from leaks or from the decomposition of surface functional groups. These oxides may have also been produced from the metallic iron in highly dispersed form upon exposure to the atmosphere at room temperature after the heat treatment.

3. Transmission Electron Microscopy - Preliminary Results (42)

The non-heat-treated $(FeTMPP)_2O$ dispersed on XC-72 was found to exhibit iron-containing particles of about 600 nm across. These most likely correspond to crystals of the macrocycle providing evidence that some of the materal undergoes crystallization during the adsorption as the solvent is evaporated. After heat treatment as 800°C, large clusters containing carbon particles with diameters between 10 and 50 nm and iron-containing single crystals were observed. Crystals of the intact macrocycle, however, were no longer evident. The crystals were equiaxed, and in many cases faceted with diameters of 50 to 70 nm. Most of the crystals showed evidence of a surrounding layer of about 10 nm thick which may be presumed to be amorphous. Electron diffraction patterns obtained from these crystals could not be indexed as either γ-Fe_2O_3, α-Fe_2O_3 or FeO nor as any of the common nitrides.

The CoTMPP specimens before pyrolysis contained large prismatic crystals about 100 nm long wich were unstable under the electron beam allowing observation only for a few seconds before disappearing. After the heat treatment, numerous Co-containing cyrstals dispersed in an amorphous carbon matrix were found. The imaging of these particles, primarily because of their size (about 3 nm in diameter), was found to be very difficult. The crystallography of the particles could not be generally determined because of the superposition of diffraction patterns originating from many particles. Nevertheless, some of the patterns contained higher index of relflections that could be indexed as hexagonal Co_2O_3. It was reported in an earlier communication (48) that the emission Mossbauer spectra of ^{57}CoTMPP dispered in Vulcan XC-72 heat treated at 800°C for 2 h yielded features with parameters very silimar to those expected for a mixture of cobaltous oxides.

4. Fourier Transform infrared spectroscopy (49)

Due to the sensitivity problem, most of the published work in this area has used macrocycles either supported on alumina or unsupported. In similar work done at Case greater sensitivity was achieved than in the published work since a Fourier Transform instrument (Mattson Cygnus 25) was used. The spectra (Fig. 20) were obtained in the diffuse transmission mode using KBr pellets containing approximately 0.5% of the solid macrocycle. With the heat-treated samples, the sensitivity was much decreased possibly due to partial carbonization of the material. IR band assignments were arrived at after comparison of a number of studies of unsubstituted porphyrins and tetraphenyl porphyrins. It must be emphasized that there is no complete agreement to the assignments, however, by the various workers.

With that caveat in mind, one can examine the changes in the spectral features with the heat treatment. At 350°C, the methyl groups are ejected. The bands characteristic of the pyrrole rings shift and broaden at 400°C but remain visible. At 500°C and above individual bands are no longer distinguishable, indicating that the structure is modified considerably. With FeTMPP the μ-oxo linkage appears to have broken below 300°C.

5. Magnetic Susceptibility (50)

Magnetic susceptibility measurements have shown that bulk CoTMPP, both with and without heat treatment at 400°C, is paramagnetic, although the effective magnetic moment is less than expected for Co(II), indicating an antiferro magnetic interaction. The CoTMPP adsorbed on XC-72, both with 400°C HT and without HT did not effect the intrinsic diamagnetic properties of the XC-72 greatly. After a 800°C HT, however, both the bulk CoTMPP and CoTMPP on XC-72 became ferromagnetic, probably indicating the presence of metallic cobalt, although cobalt oxide can not be ruled out at present (Tabe III). The

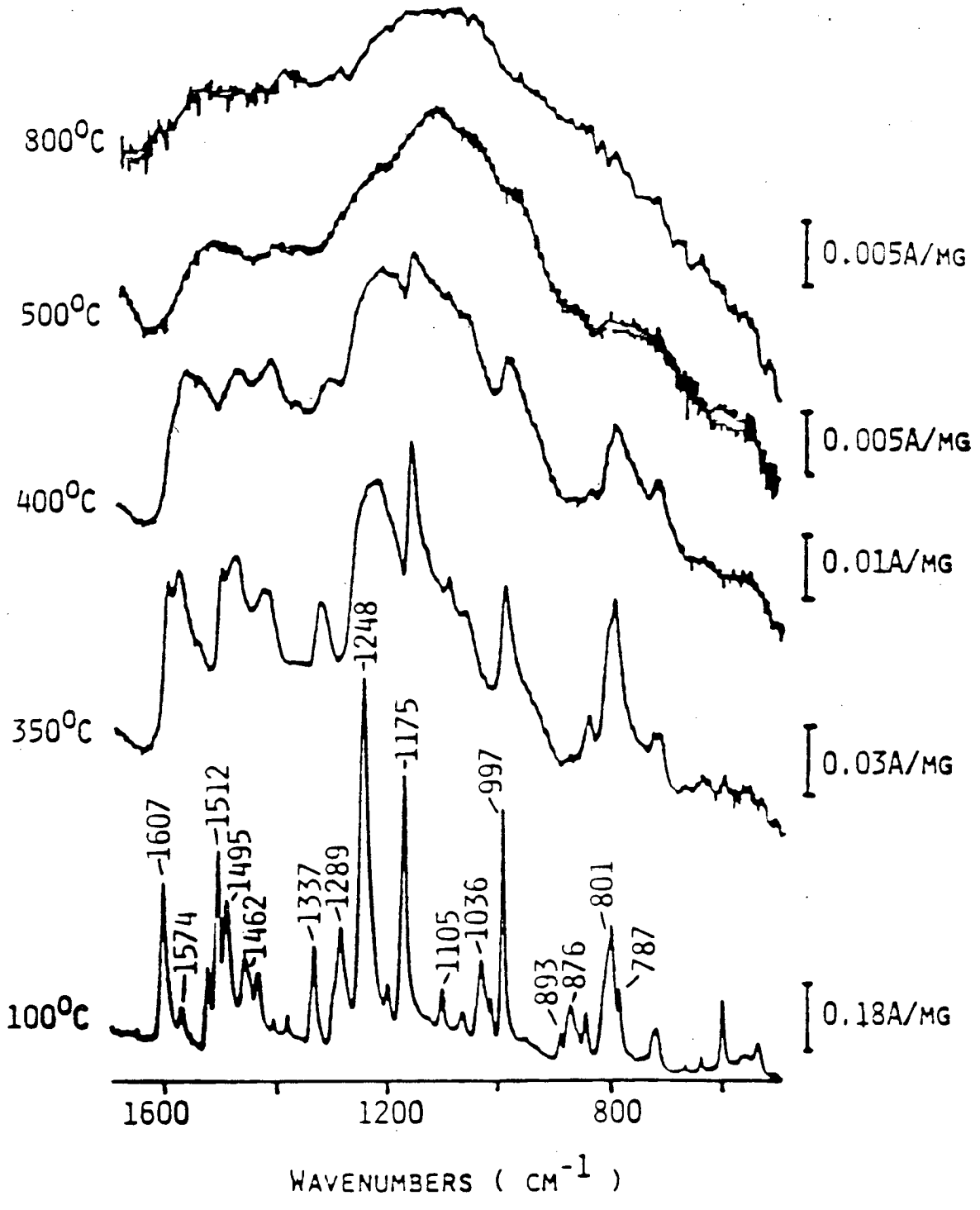

FIG. 20. ABSORPTION FTIR SPECTRA FOR $(FeTMPP)_2O$ HEAT-TREATED AT VARIOUS TEMPERATURES. (KBR PELLET TECHNIQUE)

TABLE III

MAGNETIC SUSCEPTIBILITIES FOR HEAT-TREATED CoTMPP IN BULK CRYSTALLINE FORM OR ADSORBED ON XC-72 CARBON

MATERIAL	HTT, °C	MAGNETIC SUSCEPTIBILITY PER UNIT WEIGHT, EMU $G^{-1} \times 10^{-6}$	MAGNETIC SUSCEPTIBILITY PER MOLE, EMU $MOL^{-1} \times 10^{-6}$	EFFECTIVE MAGNETIC MOMENT, BOHR MAGNETONS	ASSIGNMENT
CoTMPP	-	3.02	3010	2.7	PARAMAGNETIC
"	400	3.02	3010	2.7	PARAMAGNETIC
"	800	1650	1,020,000	49	FERROMAGNETIC
XC-72 CARBON	800	-0.44	-5.3	-	DIAMAGNETIC
4.9% CoTMPP ON XC-72	-	-0.90	-	-	DIAMAGNETIC
"	400	-0.80	-	-	DIAMAGNETIC
"	800	31.8	400,000	31	FERROMAGNETIC

bulk CoTMPP exhibited a higher molar magetic susceptibility than the adsorbed CoTMPP, normalized to the amount of CoTMPP present. This result is consistent with formation of metal or oxide particles, because this process would tend to be easier with the bulk metal or oxide material due to the stacking of the macrocycles.

6. Electrochemical Measurements

Cyclic Voltammetry

The cobalt and iron μ-oxo TMPP dispersed in Vulcan XC-72 without heat treatment yielded cyclic voltammetry curves in 0.05 M H_2SO_4 (Fig. 21-b and 21-c, respectively) exhibiting rather reversible peaks, using thin-porous coating technique. The peak observed for CoTMPP at ~+0.50 V vs. SCE in 0.05 M H_2SO_4 seems to involve the metal center. Anson et al. (51) observed a redox process at +0.54 V vs. SCE for monomeric cobalt porphyrin adsorbed on pyrolytic graphite in 1 M CF_3COOH, and attributed it to the Co(III)/Co(II) redox couple. In addition, such a redox couple also has been observed to occur at +0.45 V vs. SCE 0.1 M $HClO_4$ for cobalt (tetra-methylpyridyl)porphine adsorbed on gold, using in-situ electroreflectance technique (52). In the case of the iron derivative, the redox process at ~-0.1 V vs. SCE in 0. 05 M H_2SO_4 also appears to involve the metal center. A voltammetry peak at a potential essentially identical to that shown in Curve c, Fig. 21 was obtained by Shigehara and Anson (53) for the closely related iron tetraphenyl porphyrin, FeTPP, adsorbed on pyrolytic graphite electrodes, in 0.1 M $HClO_4$ + 0.1 M $NaClO_4$ solutions, and they assigned it to the Fe(III)/Fe(II) redox process. More recently, Meyer and coworkers (54) have reported such process at $E_{1/2}$ = -0.23 V vs. SCE for the water-soluble iron tetrasulfonated phenyl porphyrin, FeTsPP, in 0.1 M H_2SO_4 solutions.

The charges under the voltammetric peaks showed in (Fig. 21b and 21c),

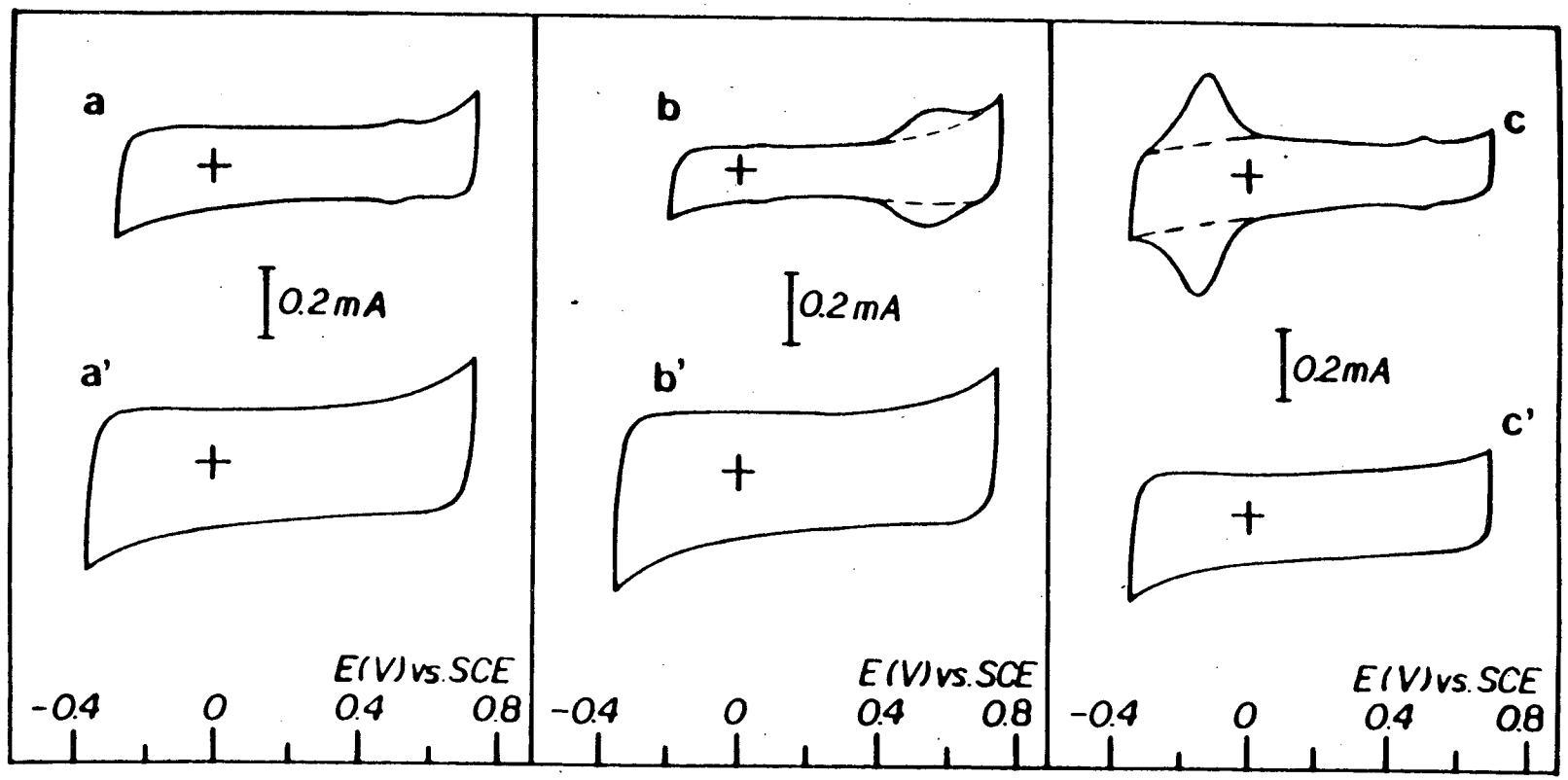

Figure 21. Cyclic voltammograms of a thin porous coating electrode containing a) 4.4% w/w H_2TMPP, b) 4.7% w/w CoTMPP, and c) 4.8% $(FeTMPP)_2O$ dispersed on high area Vulcan XC-72 carbon in 0.05 M H_2SO_4. The curve at the top of each figure corresponds to the supported material without heat treatment whereas that at the bottom was obtained with the same specimen after heat treatment at 800°C for 2 hours in Ar (see text). Scan rate: 20 mV/s. Electrode cross sectional area: 0.196 cm^2.

evaluated by integration of the area under each peak taking into account the background currents (dashed lines in Fig. 19), yielded values of 0.7 and 1.3 mC for the coablt and iron derivatives of TMPP, respectively. At the best, however, these values can only be considered as estimates because of the difficulty of establishing the background corrections. Cathodic peaks were used in the calculations because they were generally better defined. The amount of the macrocycle-carbon mixture involved in this type of thin porous coating electrode has been estimated to be (0.5 $\pm$ 0.1) mg for all electrodes, based on dry weight of applied weight of the Teflon-macrocycle-carbon mixture. Hence, taking into account the percent by weight of the complexes, only about 25% and 45% of all cobalt and iron TMPP molecules, respectively, are electrochemically active in acid media. The results in alkaline media, to be presented later, have shown that ~45% (cobalt) to ~60% (iron) of all molecules present are active. The accuracy in these calculations is very poor, however. These observations probably indicate that part of the complexes are not involved in the electron transfer processes, possibly due to wetting problems inside the electrode structure and/or possibly the restraints on ion migration within the microporous structure within the activated particles.

Two voltammetric peaks were observed both for the Co and Fe porphyrins in 0.1 M NaOH (Fig. 22b and 22c, respectively). That at -0.7 V vs. SCE for the iron and at +0.1 V for the Co most probably involve the metal centers. A similar shift was reported by Shigehara and Anson[53] in the case of the FeTPP by comparing the peak potentials at pH 1 and 12. The voltammety peak at about -1.2 V, common to both metal containing specimens (see Fig. 22b and 22c), appears to involve orbitals with mostly ring character. Evidence in support of this view was obtained by comparing the results obtained with those of the H_2TMPP which yielded a single peak in essentially the same voltage region in alkaline solutions (Fig. 22a). In addition, a peak in this potential region

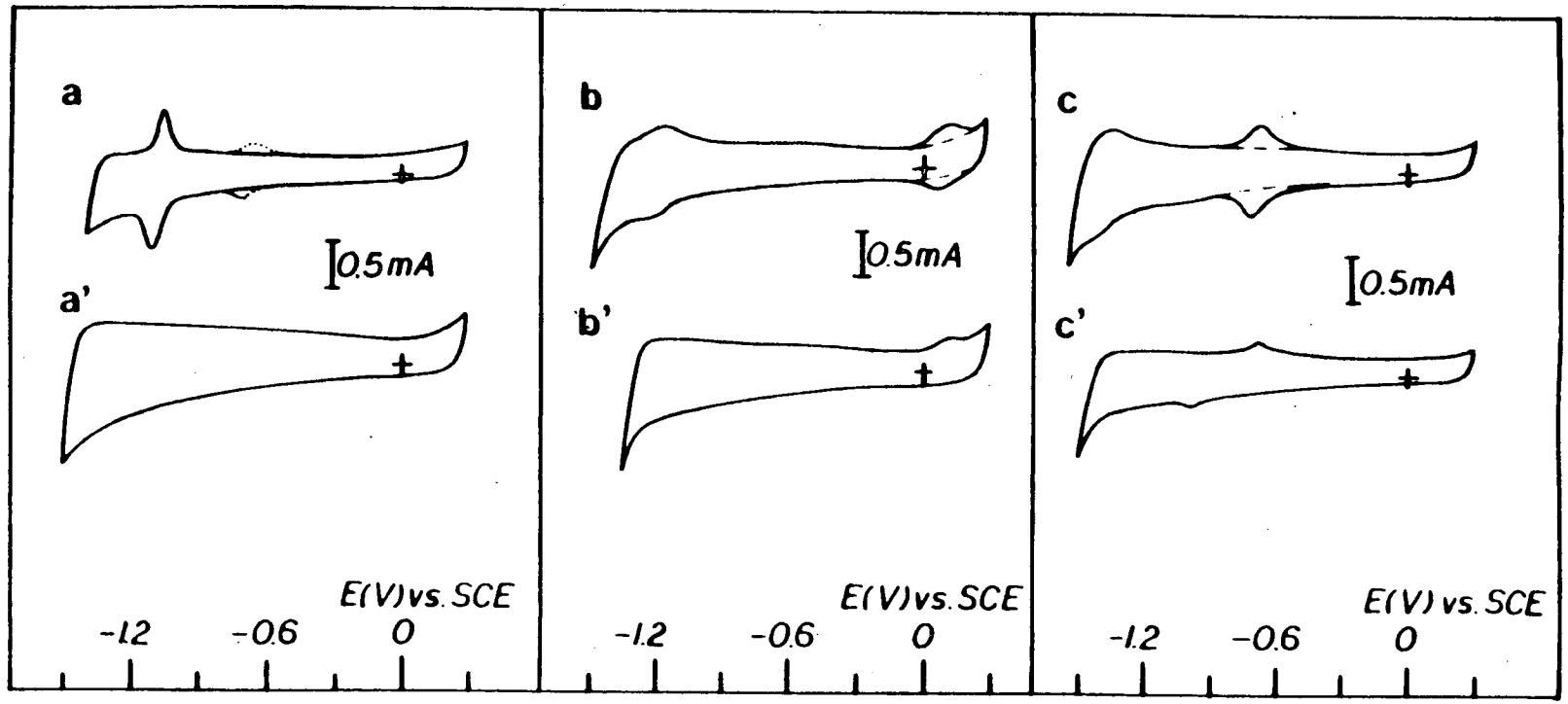

Figure 22. Cyclic voltammograms of a thin porous coating electrode containg a) 4.4% w/w H_2TMPP, b) 4.7% w/w CoTMPP, and c) 4.8% w/w $(FeTMPP)_2O$ dispersed on high area Vulcan XC-72 carbon in 0.1 M NaOH (see caption Fig. V-9 for additional details. The voltammetry features at about -0.7 V in curve a were obtained after the electrode had been cycled or polarized at potentials negative to the peak at -1.1 V and are mostly likely related to redox processes involving the products of the electrochemically induced decomposition of the dispersed macrocycle (see text).

has also been observed for FeTsPc (55) and iron tetrapyridino porphyrazine, FeTPyPz in 0.1 M NaOH and attributed to the reduction of the macrocycle ring.

The metal-free derivative appears to be unstable when polarized at potentials more negative to that at which the voltammetric feature was found to occur, i.e. at -1.07 V vs. SCE, generating additional peaks in subsequent cycles as shown by the dotted lines in Fig. 22a. It is also interesting to note than when comparing H_2TMPP with the cobalt and iron derivatives in this potential region, the mean value of the peak potential shifts in the cathodioc direction in the order: H_2TMPP (-1.07 V vs. SCE), CoTMPP (-1.2 V), $(FeTMPP)_2O$ (-1.38 V). a similar behavior was observed for these compounds adsorbed on OPG electrode.

The voltammetry observed after heat treatment of these materials at 800°C in acid media yielded featureless curves (Fig. 21a', b' and c'). This may be regarded as very surprising since most Fe and Co species would have been expected to undergo redox processes in the potential window examined and provided additional evidence that these materials undergo profound changes in their structure when exposed to such high temperatures. Some insight into the nature of the heat-treated CoTMPP/XC-72 and $(FeTMPP)_2O$/XC-72 samples, was gained from the cyclic voltammetry in 0.1 M NaOH (Fig. 22b' and 22c', respectively). Specifically, the potentials at which the peaks were observed for the iron macrocycle specimen (see Curve c', Fig. 22) correspond almost precisely to those attributed on the basis of in-situ Mossbauer measurements (9) to the reaction:

$$e^- + FeOOH(amorphous) \text{ --------> } Fe(OH)_2(crystalline)$$

This indicates that one of the iron containing species in this particular heat treated material when in contact with the alkaline solution is amorphous FeOOH. In the case of the cobalt sample the peak at ~0.1 V vs. SCE observed in the

scan in the positive direction (see Curve b', Fig. 22) appears most likely to be due to the oxidation of $Co(OH)_2$. Additional evidence in support of this view was provided by the fact that a specimen prepared by simply precipitating cobalt hydroxide onto XC-72 carbon yielded (56) a voltammogram which exhibited a small anodic peak in 0.1 M NaOH, at essentially the same potential as that in (Fig. 22b') for the heat-treated CoTMPP. Furthermore, the scan in the negative direcion, upon reversing at 0.3 V vs. SCE, did not produce any clearly defined peaks in direct analogy with curve b' in(Fig. 22). It is also interesting to note that the capacitive currents, which can be attributed to the carbon substrate, appear to increase for all specimens after the heat treatment. This may be due to an increase in the carbon surface area, although other factors such as a modification in the hydrophobic-hydrophilic character of the material may also be involved.

On the basis of the evidence presented that for alkaline solutions, it is proposed that substantial fractions of the iron and cobalt centers in $(FeTMPP)_2O$ and CoTMPP dispersed in Vulcan XC-72 after heat treatment at 800°C do not remain in the N_4-center. The metals seem instead to act as catalysts for reactions involving the macrocyclic ring and possibly the carbon substrate, in the former case generating non-volatile nitrogen containing structures. It is possible, however, that upon contact with an electrolyte solution the transition metal species undergo dissolution and subsequently adsorb or coordinate to the thermally formed nitrogen sites on the carbon surface. Preliminary evidence in support of this view has been provided by the substantial increase in the electrocatalytic activity for O_2 reduction in alakline media of H_2TMPP dispersed and heat-treated at 450°C (35) or 800°C (33) after addition of cobalt by precipitation of the corresponding hydroxide in the carbon matrix.

Oxygen Reduction Polarization Curves

The electrocatalytic properties of the Fe-μ-oxo-, Co-, and H_2TMPP for O_2 reduction were investigated with the thin porous coating technique using the rotating ring-disk electrode. The results obtained for the materials before and after heat treatment are shown in (Figs. 23 and 24), respectively, for alkaline and Figs. 25 and 26, respectively, for acid media. The polarization curves obtained with pure carbon are also given in these figures for comparison.

Thin Porous Coating Electrodes - Alkaline Electrolytes

The onset for O_2 reduction in 0.1 M NaOH at room temperature for the non-heat-treated TMPP compounds, was found to be about 150 mV more positive for the CoTMPP than for the other materials, as shown in Fig. 23. The limiting current, however, was highest for the iron μ-oxo, for which the ring currents associated with the oxdation of hydrogen peroxide produced at the disk were found to be very small compared with the other macrocycles. The H_2TMPP material yielded very similar results to those with pure XC-72 carbon.

After heat treatment, the activities for the metal free and CoTMPP were not found to change appreciably (see Fig. 24). In the case of the iron sample, however, a sizable shift in the onset potential for O_2 reduction towards more postivie potential was observed, without appreciable changes in the magnitude of the convective diffusion limiting current. It is interesting to note that the ring currents for the oxidation of HO_2^- for this specific compound, were essentially zero for low overpotentials, $0.0\ V < E_{disk} < -0.4\ V$ and very small in the region $-0.4\ V < E_{disk} < -1.0\ V$ vs. SCE.

Thin Porous Coating Electrodes - Acid Electrolyte

In contrast to the results obtained in alkaline media, the polarization curves of the Fe-μ-oxo and CoTMPP without heat treatment were found to be essentially identical in 0.05 M H_2SO_4, with only slight differences in the

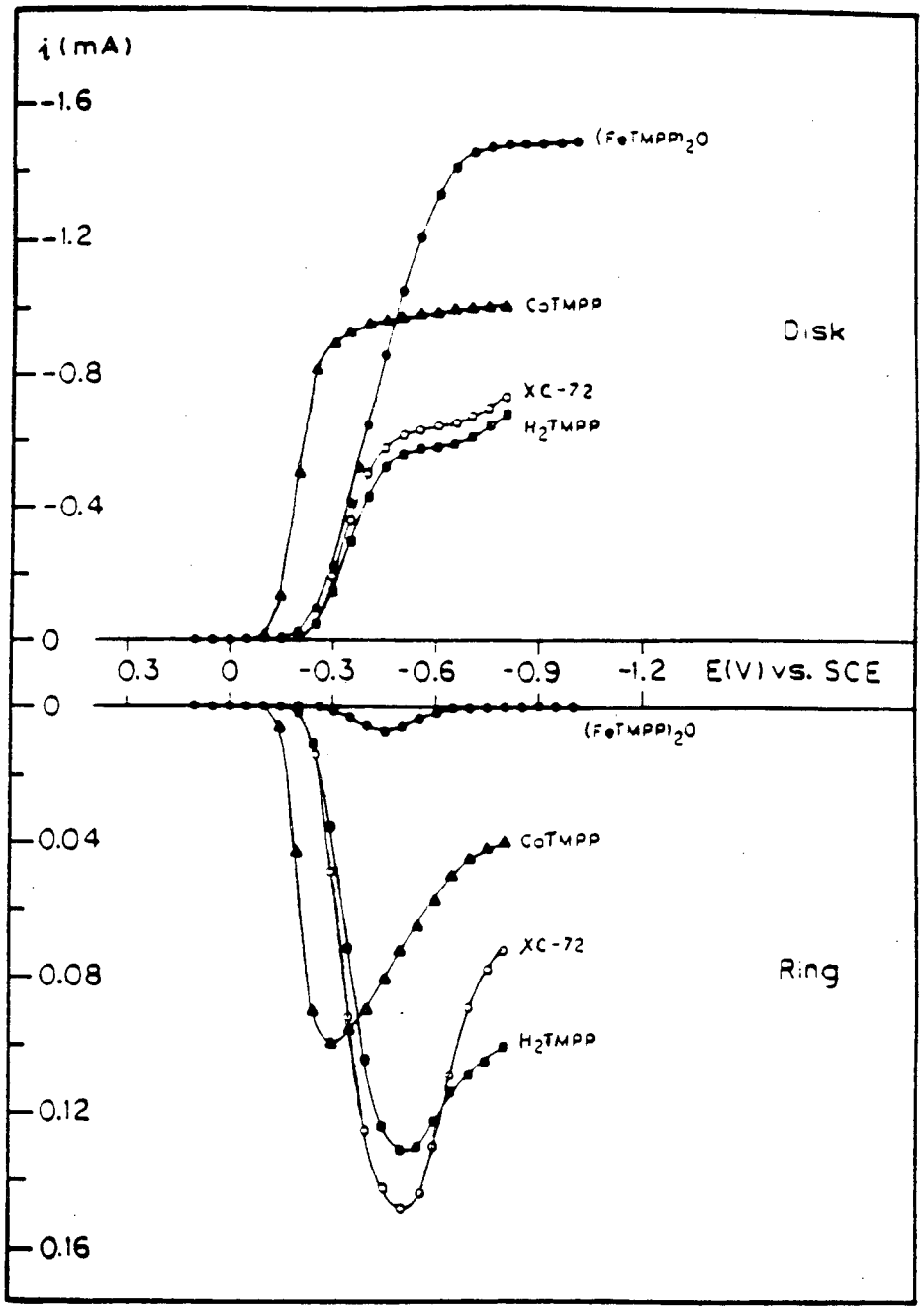

Figure 23. Ring-disk polarization curves for O_2 reduction on a thin porous coating disk electrode containing (O) Vulcan XC-72 carbon, (■) 4.4% w/w H_2TMPP/XC-72, (▲) 4.7% w/w CoTMPP/XC-72, and (●) 4.8% w/w $(FeTMPP)_2O$/XC-72 in 0.1 M NaOH. Electrode cross sectional area: 0.196 cm^2, rotation rate: 2500 rpm, room T, Au ring at +0.1 V vs. SCE, collection efficiency: 0.38.

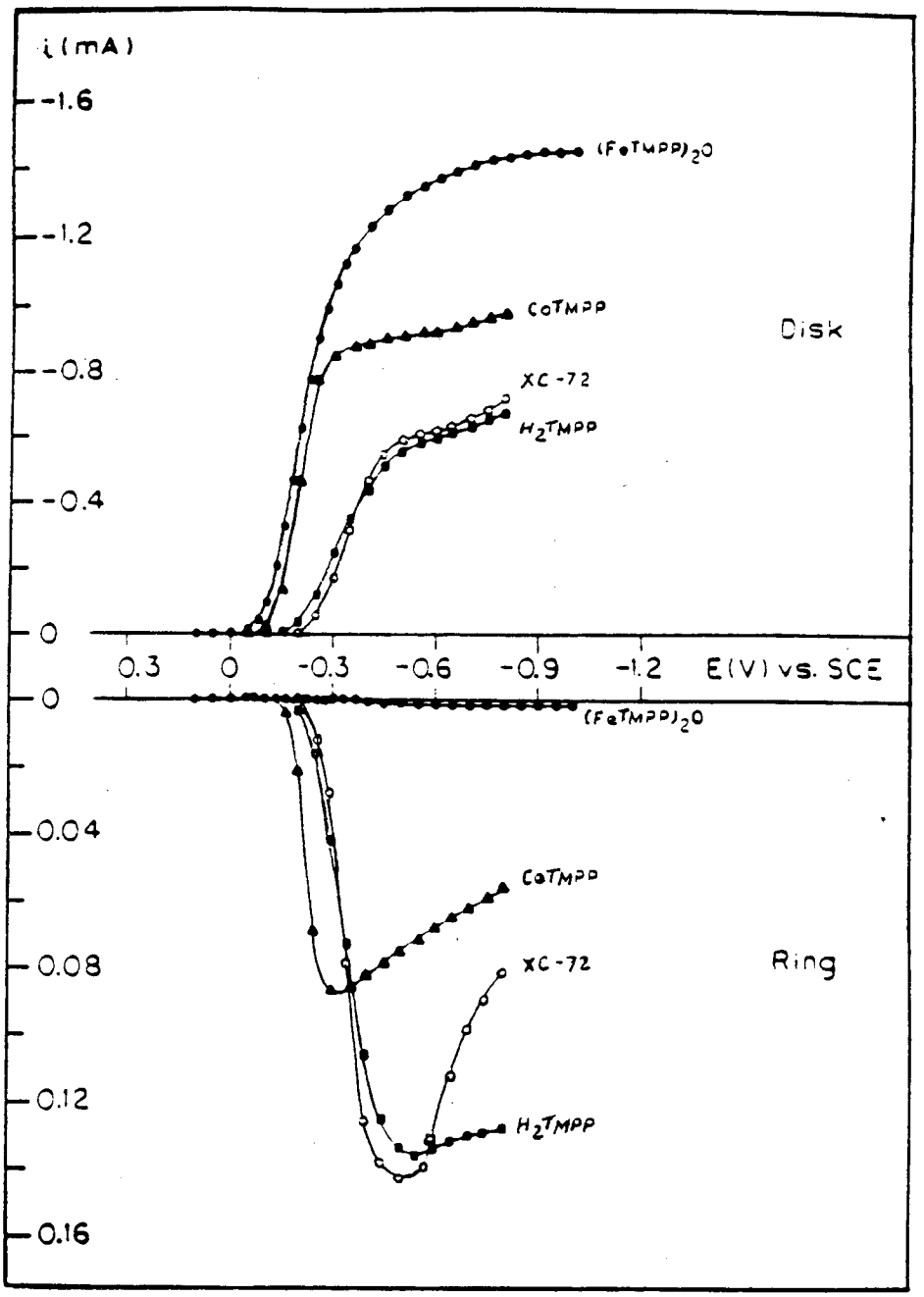

Figure 24. Ring-disk polarization curves for O_2 reduction on a thin porous coating disk electrode containing heat-treated (800°C, 2 hours in Ar) (O) Vulcan XC-72 carbon, (■) 4.4% w/w H_2TMPP/XC-72, (▲) 4.7% w/w CoTMPP/XC-72, and (●) 4.8% w/w $(FeTMPP)_2O$/XC-72 in 0.1 M NaOH (see Caption Fig. V-11 for additional details).

magnitude of the ring currents (see Fig. 25). Furthermore, a significant amount of H_2O_2 are produced with $(FeTMPP)_2O$ as well as CoTMPP. Very similar, although much lower activities were observed for the H_2TMPP and XC-72 carbon. As was the case in 0.1 M NaOH, an appreciable improvement in the activity for O_2 reduction was observed for the iron speciman after pyrolysis without, however, a significant shift in the onset potential (see Fig. 26).

7. Peroxide Decomposition (57)

There have been a number of reports in the literature concerning the dependence of the peroxide decomposition rate upon the heat treatment temperature, but most have been for acid solutions (see e.g. Refs. 58 and 59). These have shown that the catalytic activity for the macrocycle typically increases with heat treatment temperatures, goes through a maximum and finally decreases. In results obtained at Case, the activity increases monotonically with temperature (Table IV). For CoTMPP/XC-72 beore HT, the activity is relatively high and then increases by a factor of ca. 3 for the 800°C HT material. For FeTMPP/XC-72 before HT, the activity is quite low and then increases at 800°C to a value similar to that for the CoTMPP/XC-72 (800°C HT).

e. **Heat-treated Macrocycles - Model**

On the basis of the O_2 polarization measurements and the various characterization techniques, a consistent model emerges which can partially explain the processes occuring during the heat treatment of the tetramethoxy phenyl porphyrins and may also help to explain their behavior as catalysts for O_2 reduction.

1. Heat treatment of these macrocycles at 800°C drastically alters their structure, but a significant amount of nitrogen remains on the surface which can complex the iron or cobalt.

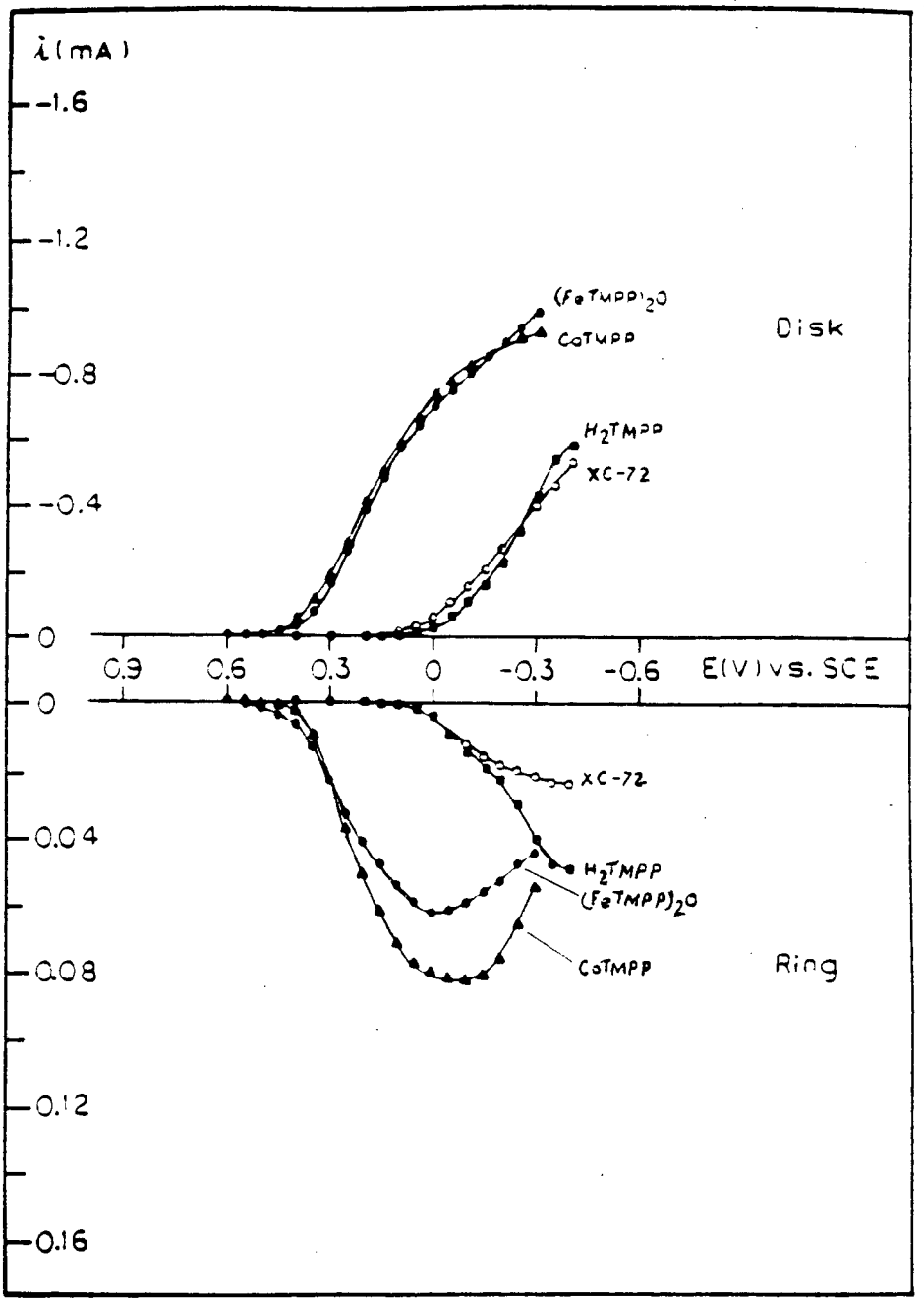

Figure 25. Ring-disk polarization curves for O_2 reduction on a thin porous coating electrode containing (O) Vulcan XC-72 carbon, (■) 4.4% w/w H_2TMPP/XC-72, (▲) 4.7% w/w CoTMPP/XC-72, and (●) 4.8% w/w $(FeTMPP)_2O$/XC-72 in 0.05 M H_2SO_4. Electrode cross sectional area: 0.196 cm^2, rotation rate: 2500 rpm, room T, Pt ring at +1.1 V vs. SCE, collection efficiency: 0.38.

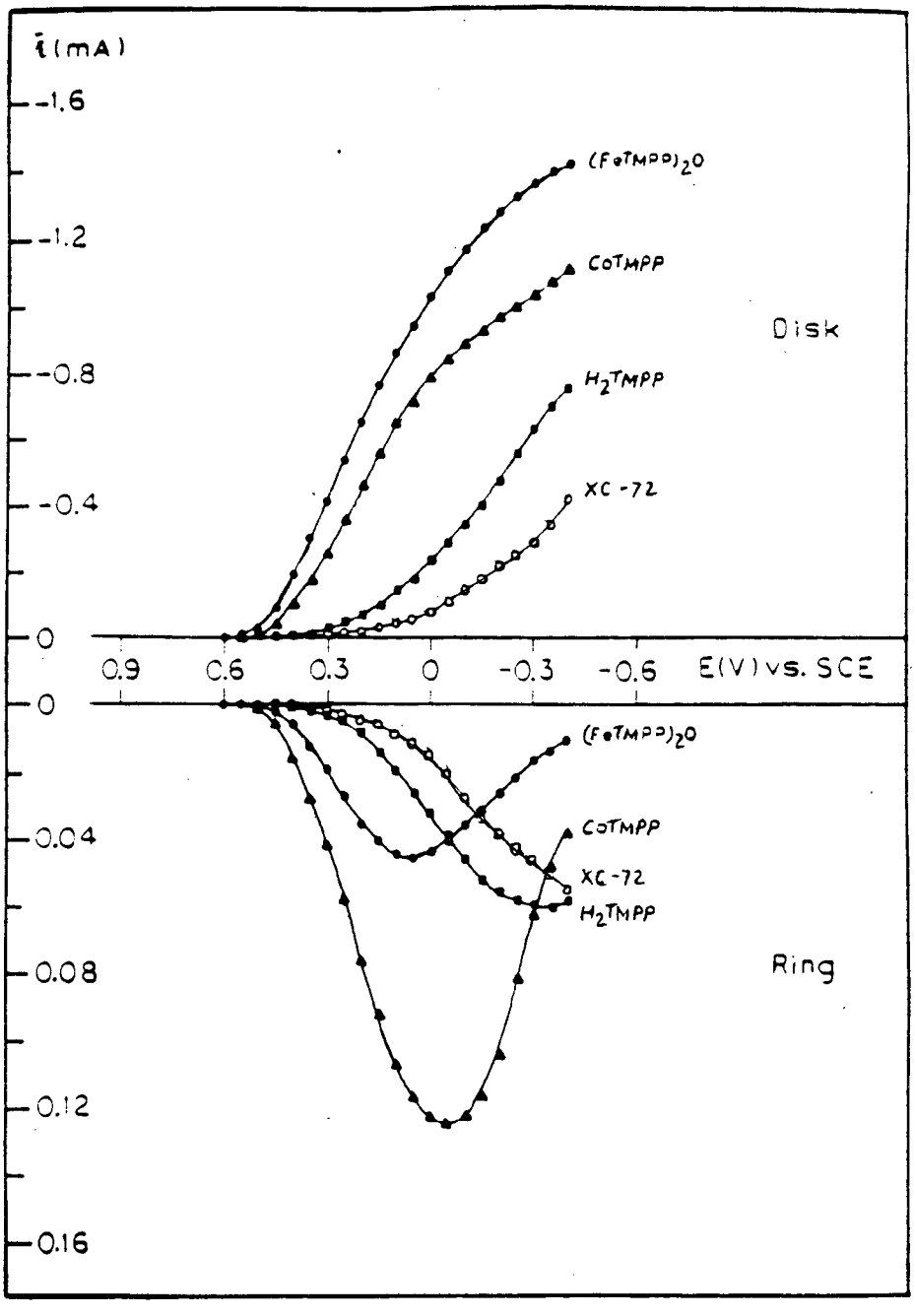

Figure 26. Ring-disk polarization curves for O_2 reduction on a thin porous coating electrode containing heat-treated (800°C, 2 hours in Ar) (○) Vulcan XC-72 carbon, (■) 4.4% w/w H_2TMPP/XC-72, (▲) 4.7% w/w CoTMPP/XC-72, and (●) 4.8% w/w (FeTMPP)$_2$O/XC-72 in 0.05 M H_2SO_4. (see caption Fig. V-13 for additional details).

2. Due to the disturbance of the structure, a part of the transition metal content no longer remains in complexed form and is easily converted to the oxide form upon contact with oxygen. These metal oxides are converted to the hydrated form upon contact with the alkaline electrolyte.

3. Although the transition metal oxides, especially cobalt, possess some activity for peroxide decomposition, the major portion of the catalytic activity for O_2 reduction is due to the complexed form of the metal.

4. The complexation of cobalt can take place after the heat treatment of the metal-free TMPP on the carbon, from either acetic acid or alkaline solution. Iron may be difficult to complex in this way because of its tendency to remain in the Fe(III) state, which would slow down the kinetics of complexation.

5. The increase in O_2 reduction performance for the heat-treated FeTMPP (800°C HT) vs. the non-heat-treated sample is partially due to a large increase in the peroxide decomposition activity.

2. Radiation-Treated Macrocycle Catalysts

Attempts have also been made using γ-radiation to graft the transition metal macrocycles onto the carbon surfaces with a view to enhancing the stability of the macrocycle/carbon catalysts. The deaerated samples of CoTMPP and cobalt octaethyl porphyrin (CoOEP) on steam-activated Shawinigan black (SASB) were exposed to ^{60}Co-γ radiation up to a maximum dose of 10 Mrads. However, the gas-fed porous electrodes and the thin porous coated rotating disk electrode measurements (O_2 polarization and voltammetry) showed no significant differences in the behavior of radiated and unradiated samples in alkaline and acid electrolytes. Further, it has been found that the CoTMPP could be quanti-

tatively Soxhlet-extracted with acetone from its radiated samples, showing no evidence for grafting of the macrocycle onto the carbon surface. Possible reasons for the lack of interactions are: 1) it may be difficult to form long-lived localized free radicals on the carbon surface due to its good electronic conductivity and 2) it may also be difficult to produce localized free radials on the macrocycle periphery due to delocalization or charge transfer with the carbon.

C. Heat-Treated Nitrogen-Containing Polymers-Based Catalysts

The source of the catalytic activity in the heat-treated macrocycles is believed to be the atomically dispersed transition metal adsorbed on the electrode surface through nitrogen functionality. The interaction between the transition metal and the nitrogen originally part of the pyrrole ring is an important factor. Transition metal porphyrins contain four pyrrole nitrogens coordinated to the metal ion, but it is not established whether this Me---N_4 structure remains intact after the heat treatment. This structure may persist at 550°C, but it is questionable at 800°C. Even at the latter temperature, however, most of the pyrrole nitrogen is retained after the pyrolysis of the Co- and FeTMPP and is available to serve as bindig sites on surface for transition metal species, which can in turn interact catalytically with O_2. On the basis of this model (Fig. 27) it should be possible to use a starting material which is simpler and cheaper than the relatively expensive macrocycles such as the porphyrins. Such a material should have the following attributes: 1) nitrogen-containing functional groups which can coordinate transition metal ions; 2) lack of volatility; 3) stability and 4) low cost and ease of preparation.

1. Pyrrole Black-Based Catalysts

One such material is polypyrrole, which when chemically prepared is termed

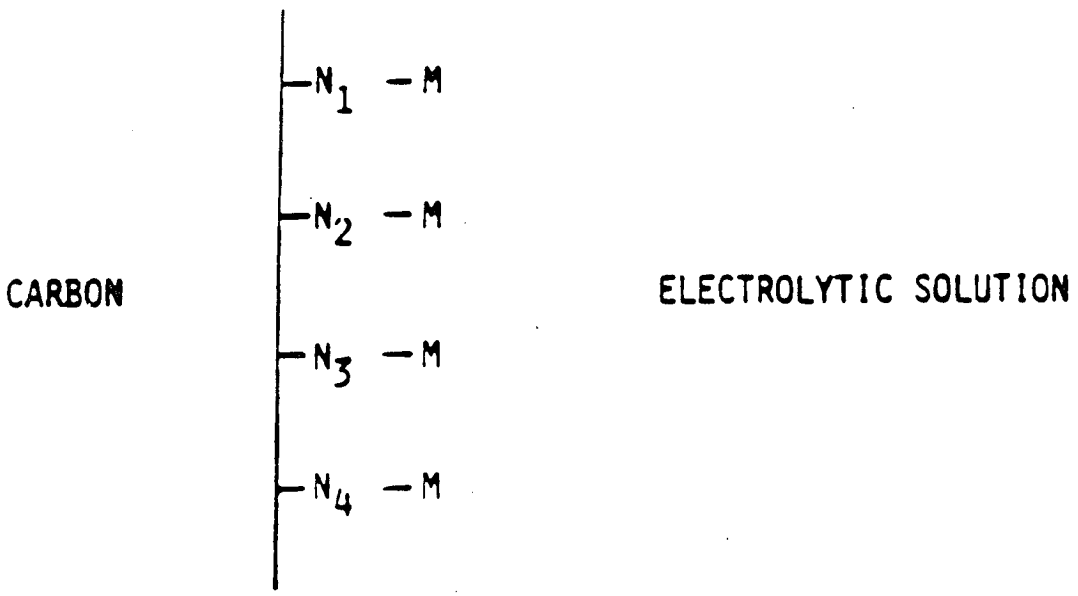

FIG. 27 NITROGEN ADSORPTION SITES FOR TRANSITION METAL IONS ON A CARBON SUBSTRATE.

pyrrole black (PB) (Fig. 28). Pyrrole black prepared by chemical oxidation of pyrrole with peroxide has been heat treated (800°C) in an inert atmosphere in the presence of Fe(II) acetate or Co(II) acetate. This catalyst has shown high activity for O_2 reduction in alkaline and acid electrolytes. The activity is comparable with heat-treated FeTMPP or CoTMPP supported on RB carbon, which have been found at Case to be among the best electrocatalysts for O_2 reduction. The activity of Teflon-bonded gas-fed electrodes made from Fe/PB and Co/PB was examined as a function of the HT temperature. The activity was measured as a current density at -0.100 V vs. Hg/HgO, OH^- and was found to increase greatly with heat treatment between 400°C and 700°C. The activity was similar for 800°C, 850°C and 900°C HT for Fe/PB, with a slight maximum at 850°C. The 950°C HT material showed a slight loss of activity and stability. It may be noted that the heat-treated FeTMPP/C catalyst also shows much higher activity after 800°C HT than after 450°C.

Similar results are obtained for Teflon-bonded gas-fed electrodes made from Co/PB. There is a sharp increase in activity up to 700°C HT. The activity is very similar for 700°C, 800°C and 900°C HT. In the case of CoTMPP/C, the effect of HT on the polarizaiton curves for O_2 reduction in gas-fed porous electrodes is not very pronounced in short-term tests (hours). The stability for the electrodes is, however, increased considerably with 800°C HT (27). Thus the Fe appears to be playing a direct role in modifying the catalytic properties during heat treatment both for FeTMPP/C and the Fe/PB catalysts.

The results show (Fig. 29) that materials produced by the heat treatment of pyrrole black mixed with transition metal salts are promising catalysts for the electroreduction of O_2 in both alkaline and acid electrolytes. Their activity is comparable to that of transtion metal macrocycles heat-treated on carbon. Some optimization of mass transport and/or electronic conductivity is

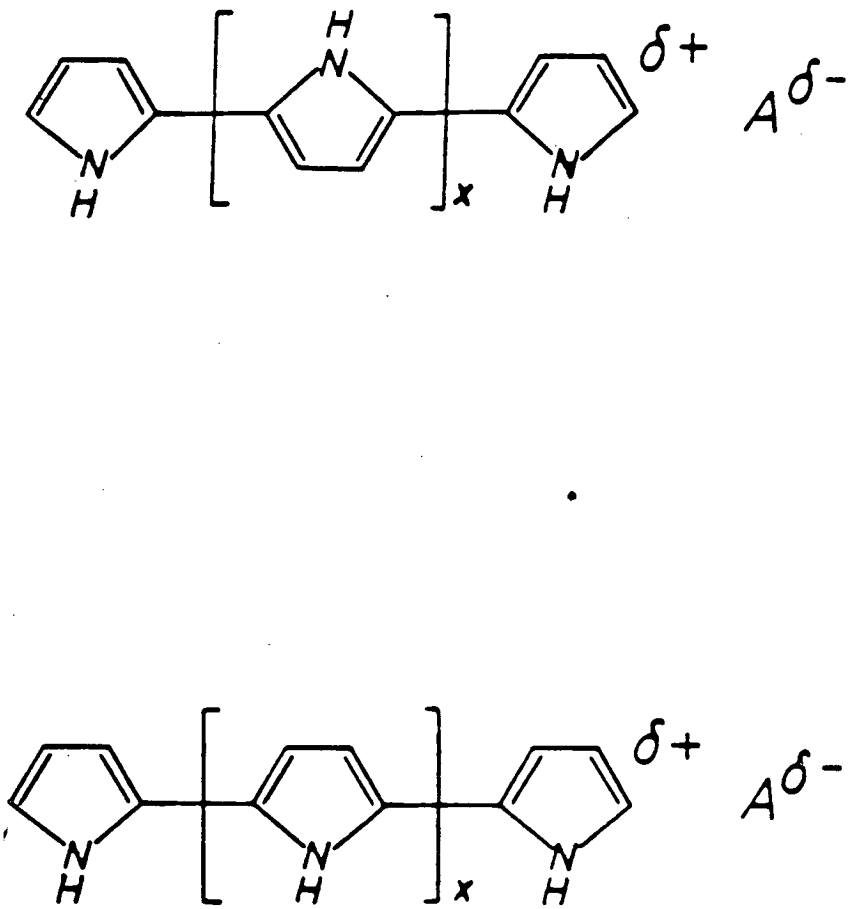

FIG. 28. STRUCTURES FOR THE TRANS (ABOVE) AND CIS (BELOW) FORMS OF POLYPYRROLE.

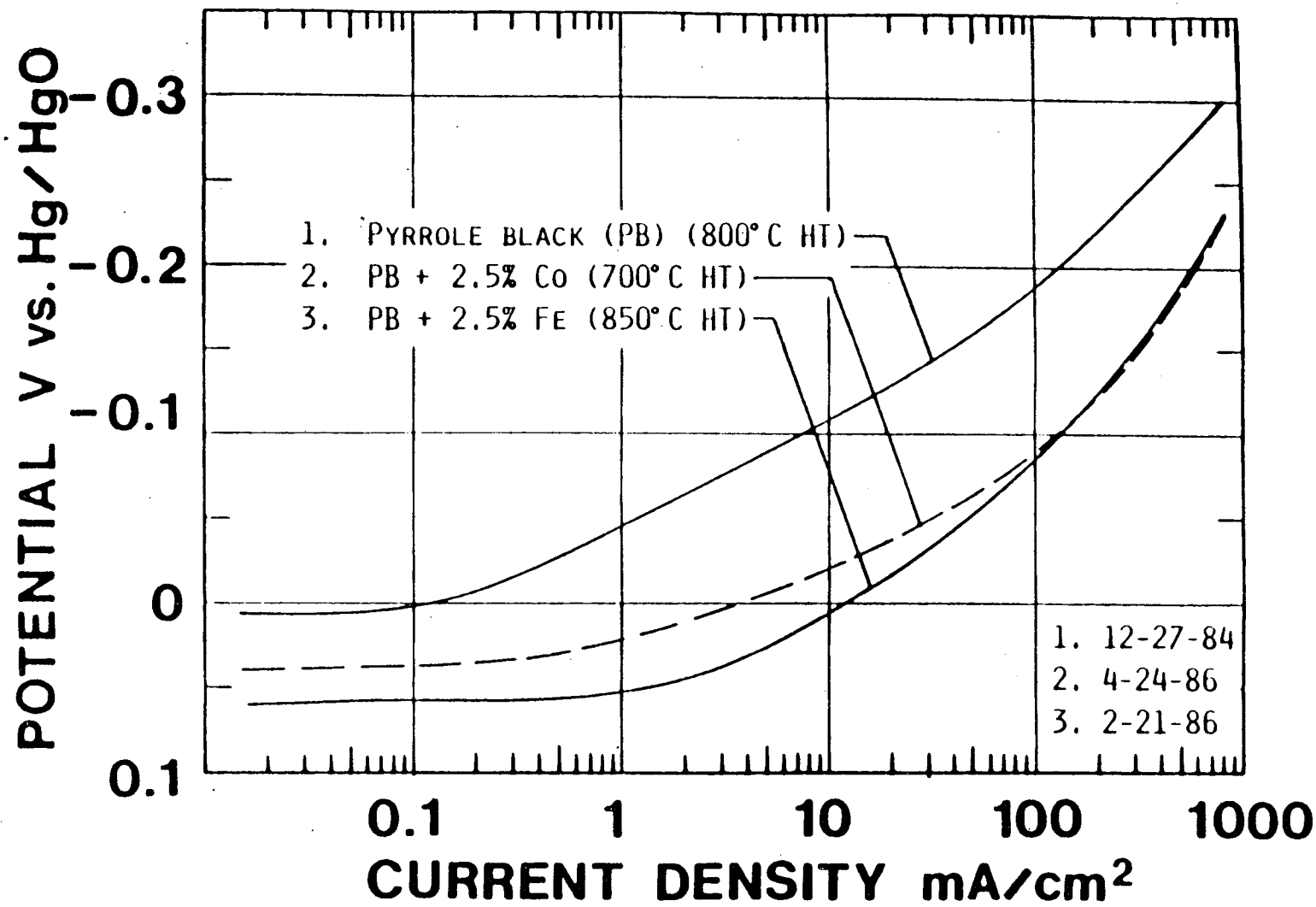

FIG. 29. POLARIZATION CURVES FOR O_2 REDUCTION WITH POROUS O_2-FED (1 ATM) ELECTRODES IN 4 M NaOH AT 60°C. THE ELECTRODES CONTAINED 14.6, 15.0 AND 15.0 MG CM^{-2} CATALYST AND 3.6, 6.4 AND 5.0 MG CM^{-2} TEFLON T30B FOR CURVES 1, 2 AND 3 RESPECTIVELY. Co AND Fe WERE ADDED AS THE ACETATES.

still needed. The details of this work are given in Reference 58.

2. Polyacrylonitrile-Based Catalysts

In order to see if other nitrogen-containing polymers can also be used in the preparation of active catalysts for O_2 electroreduction, expierments have been conducted with polyacrylonitrile (PAN) (Fig. 30). In the present study the catalysts were prepared by heat-treating polyacrylonitrile mixed with transition metal salts and carbon at various temperatures. The reduction of O_2 catalyzed by such materials was studied in concentrated alkaline and acid electrolytes in porous gas-fed electrodes and by TPC electrode technique.

The catalysts were prepared by dissolving the PAN together with either the Co(II)or Fe(II) acetates in dimethylformamide (DMF), mixing in the carbon black and then removiong the DMF by distillation under N_2. The solid was then heat-treated. Heat treatment of the various catalysts samples was performed in a horizontal tube furnace under continuous flow of purified argon (Matheson, H.P. grade). The samples were allowed to cool while still under flowing argon.

The activity of Teflon-boned gas-fed electrodes made from 10% PAN, 2.5% Co(II) acetate and XC-72 carbon was studied as a function of the heat treatment temperature (HTT). The activity was measured as a current density at -0.1 V vs. Hg/HgO, OH^- and was found to increase greatly with heat treatment between 500°C and 800°C with a maximum at 800°C. The 900°C HT material showed lower activity and stability as compared with the 800°C HT material (Fig. 31).

Similar results were obtained from Teflon-bonded gas-fed electrodes made from 40% PAN, 5% Fe(II) acetate and XC-72 carbon. There is an increase in activity up to 850°C HT. The activity is very similar for 850°C, 900°C and 950°C HT (Fig. 31). As seen earlier with heat-treated transition metal macrocycles and pyrrole black-based catalysts, the transition metal or the nitrogen-containing polymer alone on carbon does not produce a good catalytic material

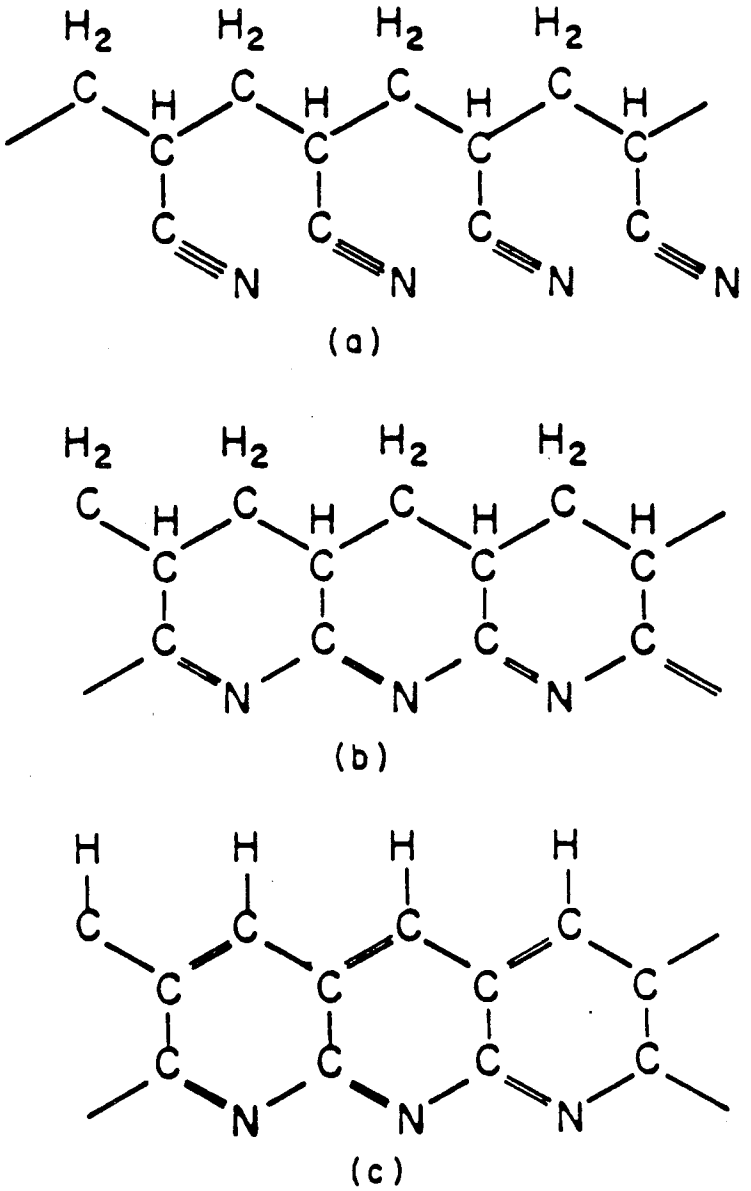

FIG. 30. STRUCTURES OF POLYACRYLONITRILE A) BEFORE PYROLYSIS, B) AFTER THE FIRST STAGE OF PYROLYSIS, FORMING A SINGLY CONJUGATED STRUCTURE AND C) AFTER THE SECOND STAGE OF PYROLYSIS, FORMING A DOUBLY CONJUGATED LADDER. (SEE TEOH ET AL., MOL. CRYST. LIQ. CRYST., 1982, VOL. 83, PP. 297-306.)

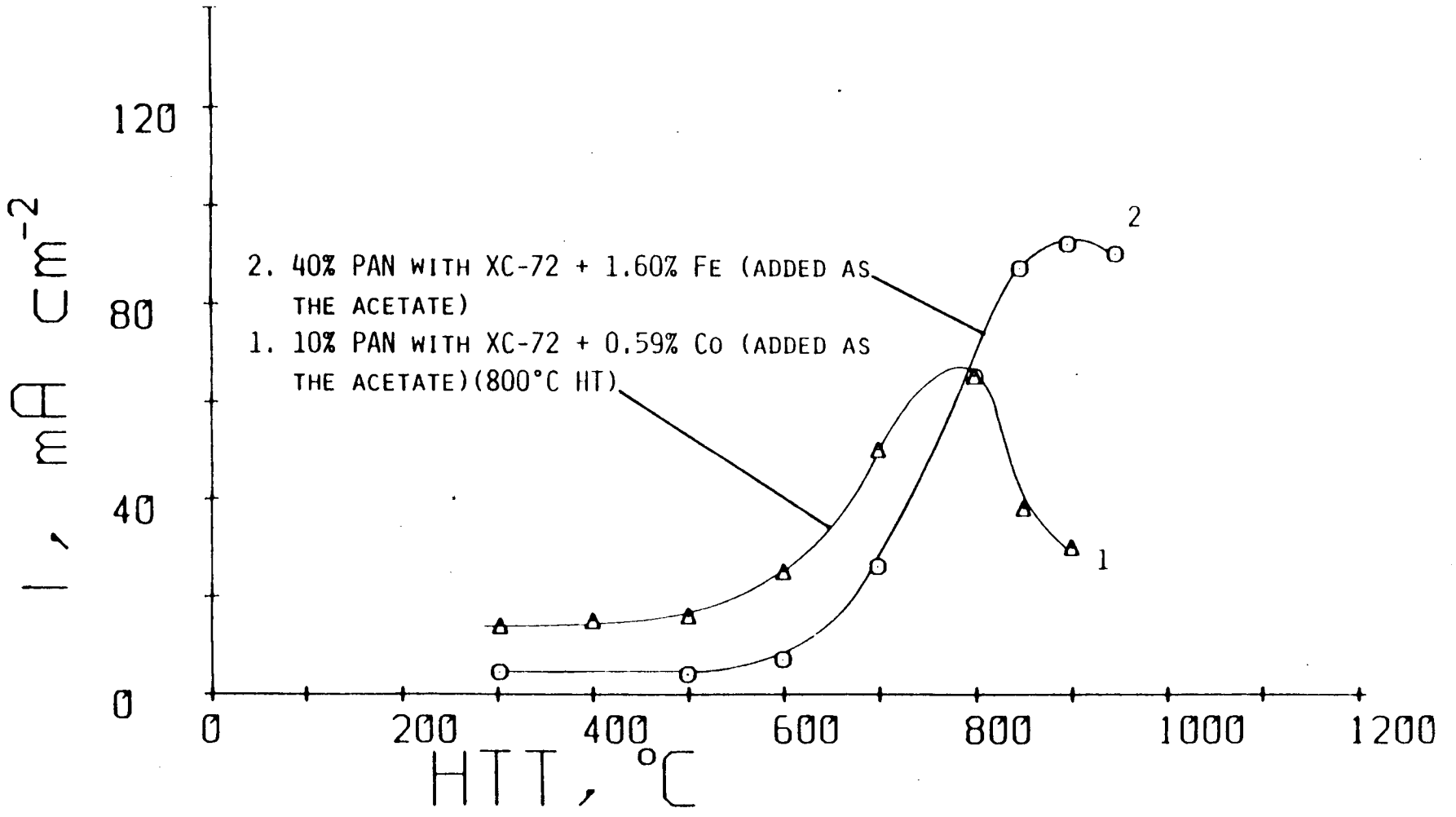

FIG. 31. CURRENT DENSITY AT -0.100 V VS. Hg/HgO,OH$^-$ FOR O_2 REDUCTION IN 4 M NaOH AT 60°C USING TEFLON-BONDED POROUS O_2-FED (1 ATM) ELECTRODES. CURVE 1: 10% PAN, 2.5% Co(II) ACETATE (0.59% AS Co) AND XC-72 CARBON (WT.% BASED ON XC-72 WT.); CURVE 2: 40% PAN, 5.0% Fe(II) ACETATE (1.60% AS Fe) AND XC-72 CARBON. ELECTRODES WERE HEAT-TREATED AT VARIOUS TEMPERATURES IN FLOWING Ar FOR 2 H.

after the heat treatment. The presence of both the transition metal and the nitrogen-containing polymer before the heat treatment with carbon is an important factor for good catalytic activity (see Fig. 32).

The structure of the PAN after the heat treatment is not known with any certainty. The structral investigations which have appeared in the literature have not involved materials which have been heat-treated in the presence of transition metal salts. Such studies may still shed light on the types of structures which may be present in the transition metal-containing materials. Teoh et al. (59) have observed changes in the IR spectra, after heating PAN films to temperatures up to 435°C in vacuum, which are consistent with conversion to a singly and then a doubly conjugated structure (Fig. 30). A temperature of 390-435°C is critical; the electrical conductivity of the material increases dramatically above this temperature (59).

If the transition metal-containing heat-treated PAN materials contain the fused pyrido rings which have been concluded for the material without the transition metal, the nitrogens of these rings could act as adsorption or coordination sites for transiton metal ions. These adsorbed metal ions could then act as catalytic sites for O_2 reduction to peroxide and for peroxide decomposition.

Similar processes could occur in the formation of the materials reported by Hinden and Gauger (60) in which Ir, Ru and Pt salts were used in the pyrolysis of PAN to form coatings for anodes used in electrowinning cells in acid electrolytes.

FTIR studies at Case of PAN samples without and with the transition metal indicate the disappearance of the nitrile groups after heat treatment with evidence for the production of pyrido-rings (Fig. 33). Elemental analysis show that a considerable amount of the nitrogen (~50%) is retained even after the heat treatment at 800°C. This catalyst system (Co + PAN + XC-72) functions

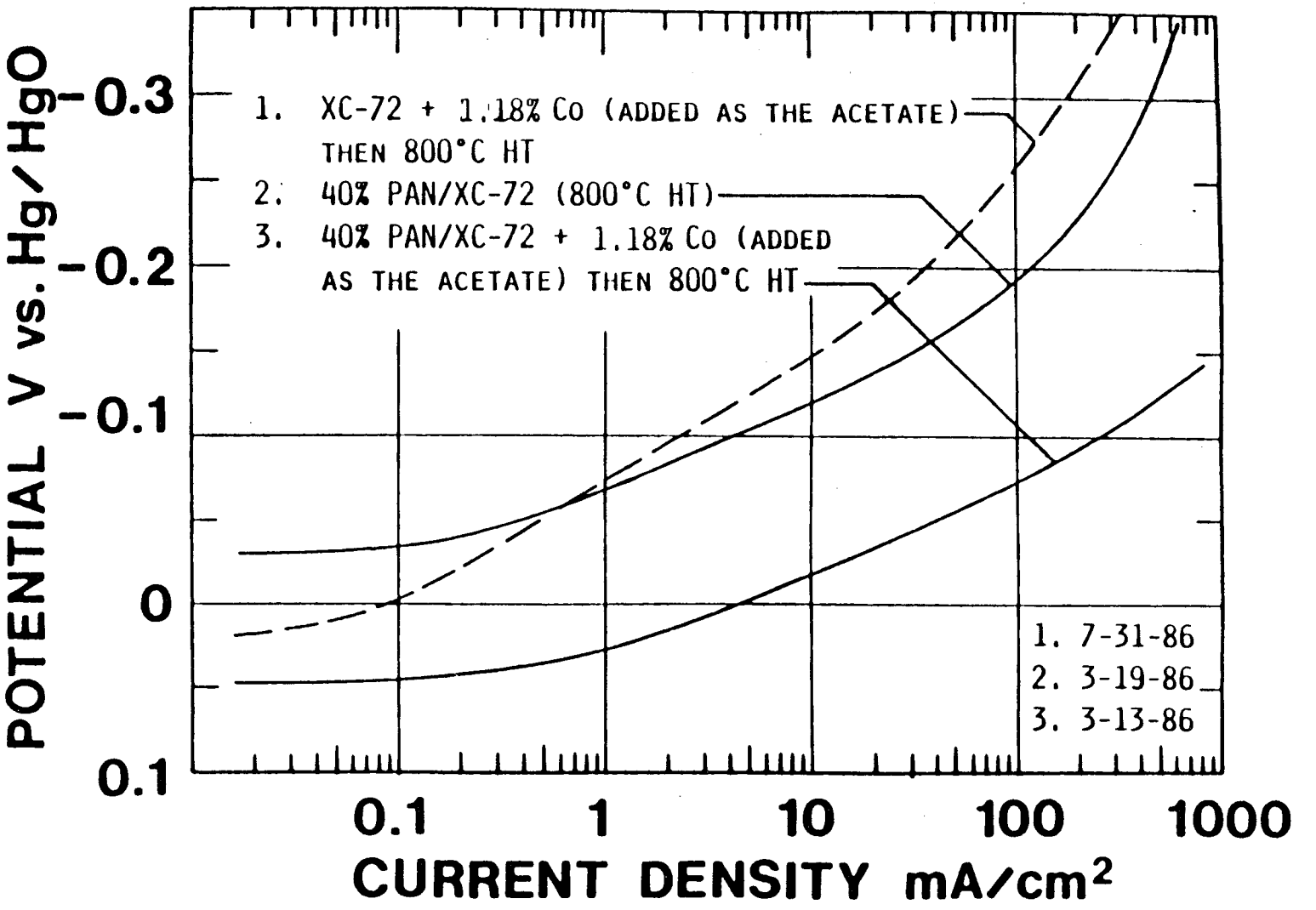

FIG. 32. POLARIZATION CURVES FOR O_2 REDUCTION WITH O_2-FED (1 ATM) ELECTRODES IN 4 M NaOH AT 60°C. THE ELECTRODES CONTAINED 15.0 MG CM^{-2} CATALYST/CARBON AND 6.4 MG CM^{-2} TEFLON T30B AND WERE HEAT-TREATED AT 280°C FOR 2 H IN FLOWING HE.

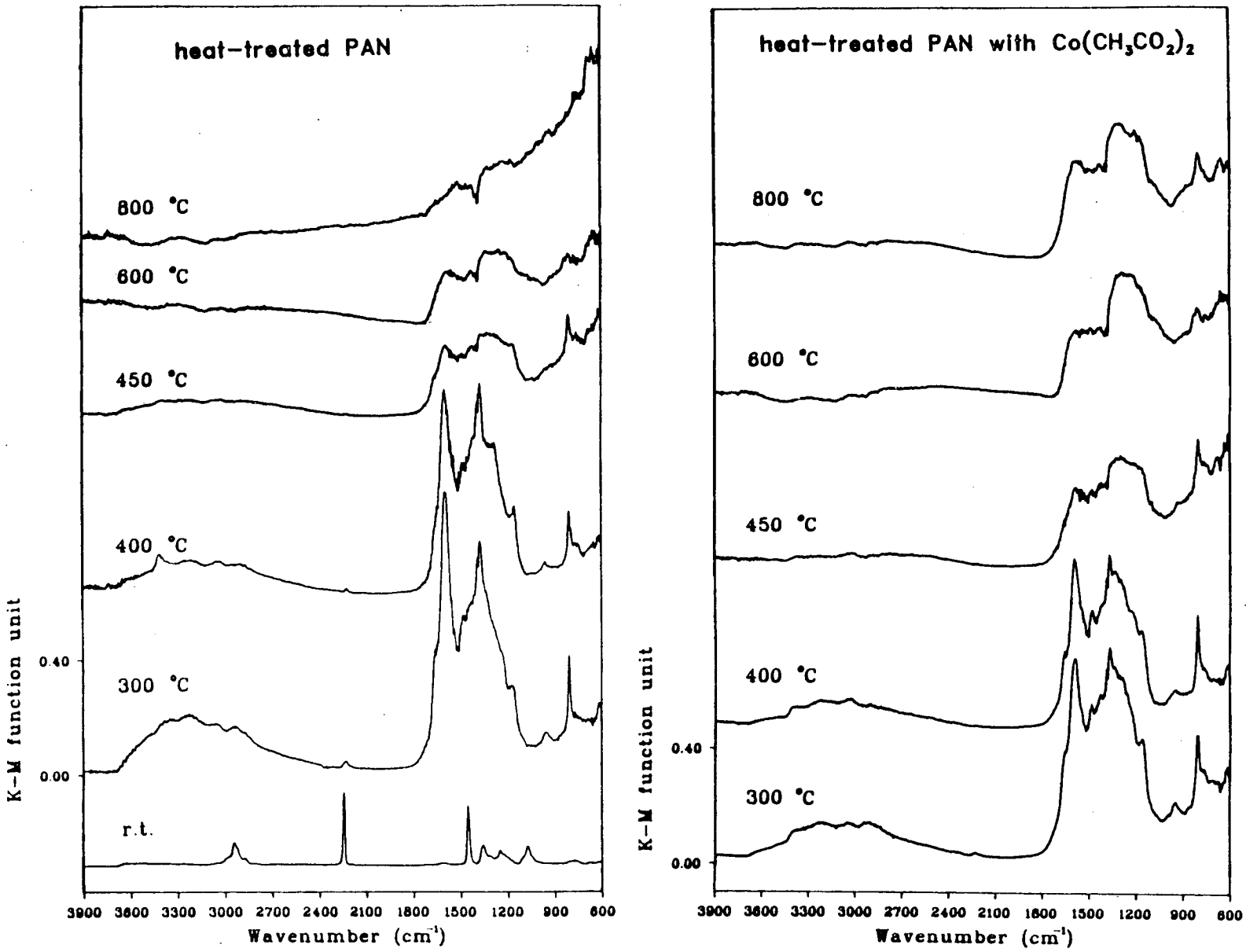

Fig. 33. **Diffuse reflectance FTIR spectra of heat-treated polyacrylonitrile samples at various temperatures with and without cobalt acetate.**

through a peroxide mechanism similar to that involved with the heat-treated cobalt porphyrins and has comparable activity but much lower cost. The comparison of the catalytic activity of the heat-treated CoTMPP, PB and PAN-based catalysts for O_2 reduction in alkaline and acid solutions is given in (Figs. 34-37). Experiments are also being conducted to determine the long term stability. The details are given in Reference 61.

D. Use of Ionically Conducting Polymers in Porous Electrodes

Ionically conducting polymers are being considered both as replacements for fluid electrolytes within the porous active layer of the gas-fed electrodes and also as an additional porous outer layer. The former has the advantage of affording a medium in which some of the macrocycles as well as oxide catalysts and even the carbon supports may be more stable. The latter has the advantage of also impeding O_2 gas generation on the outer surface of the electrode in the anodic mode, forcing gas to exit from the active layer through the gas wick structure into the rear (gas-side) of the electrode. Such electrodes will take a substantial gas overpressure on the rear side.

The use of Nafion as an overlayer on electrode surfaces has been proposed by the Case group to increase the rate of O_2 reduction in acid solutions due to the relatively high O_2 solubility in the Nafion. Experiments have been done recently at Case in which this prediction has been partially realized. Adsorbed Co-TsPc on a pyrolytic graphite electrode surface was used with an overlayer of Nafion containing additional dissolved CoTsPc. It was found, however, that the presence of CoTsPc in the Nafion phase was necessary in order for the enhancement effect to be exhibited. The macrocycle in the bulk Nafion may suppress the loss of the adsorbed CoTsPc from the OPG surface and also provides further catalytic sites for O_2 reduction to peroxide (the predomiant process with this macrocycle).

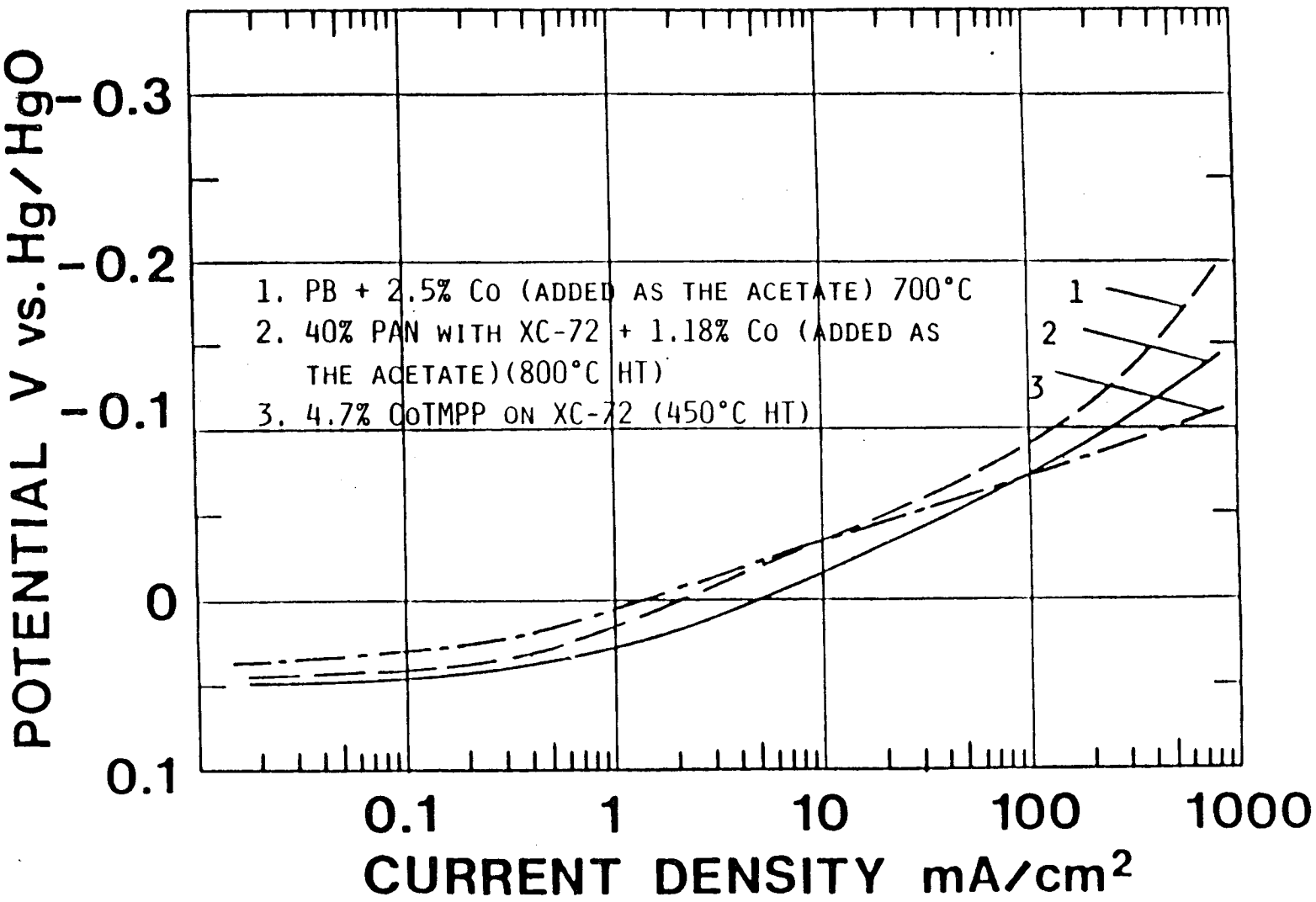

FIG. 34. POLARIZATION CURVES FOR O_2 REDUCTION WITH POROUS O_2-FED (1 ATM) ELECTRODES IN 4 M NAOH AT 60°C. CATALYST/CARBON 15.0 MG CM^{-2} AND 6.4 MG CM^{-2} TEFLON FOR EACH ELECTRODE.

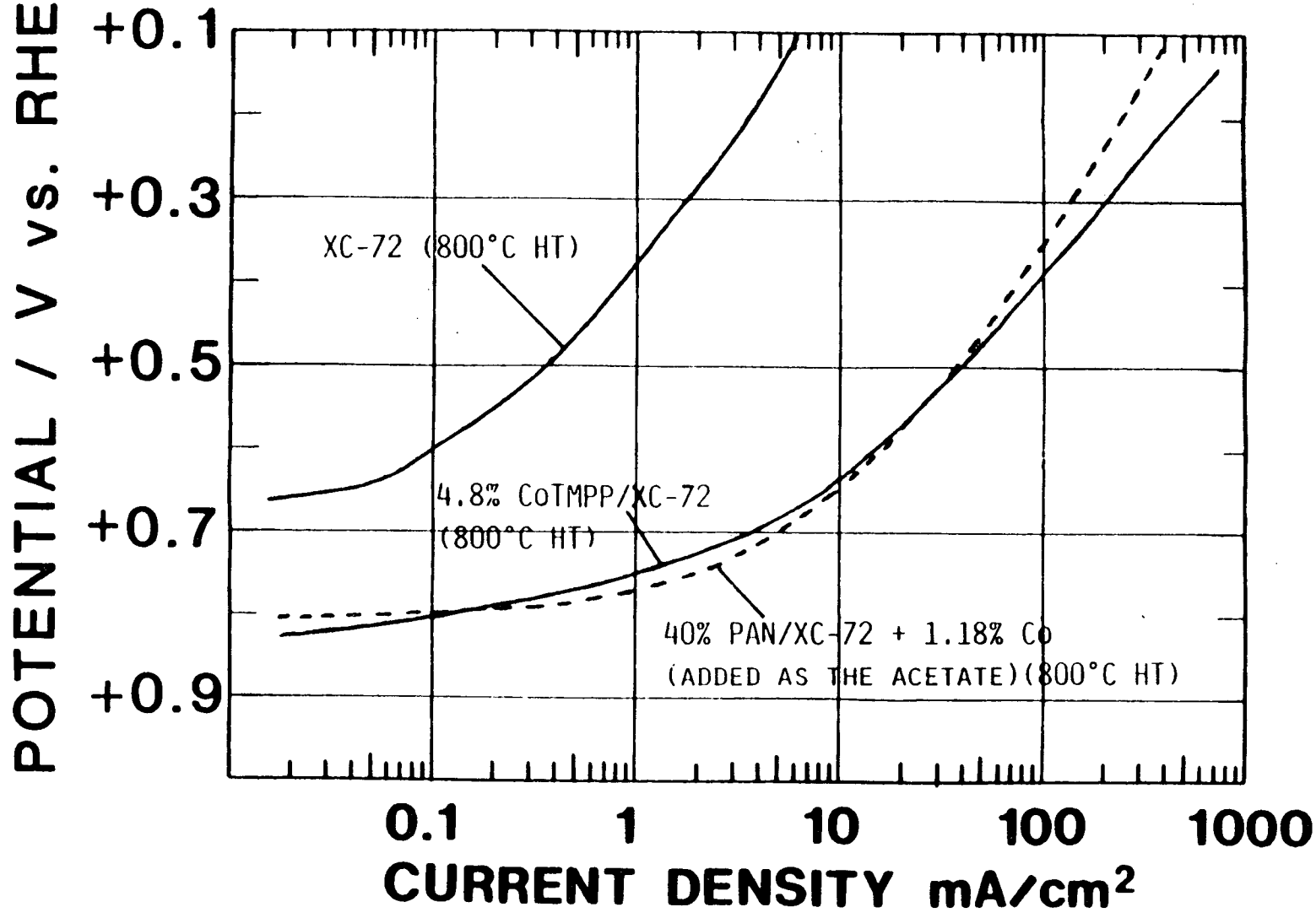

FIG. 35. POLARIZATION CURVES FOR O_2 REDUCTION WITH POROUS O_2-FED (1 ATM) ELECTRODES IN 85% H_3PO_4 AT 100°C. ALL THE CURVES CONTAINED 14.6 MG CM^{-2} CATALYST/CARBON AND 6.2. MG CM^{-2} TEFLON.

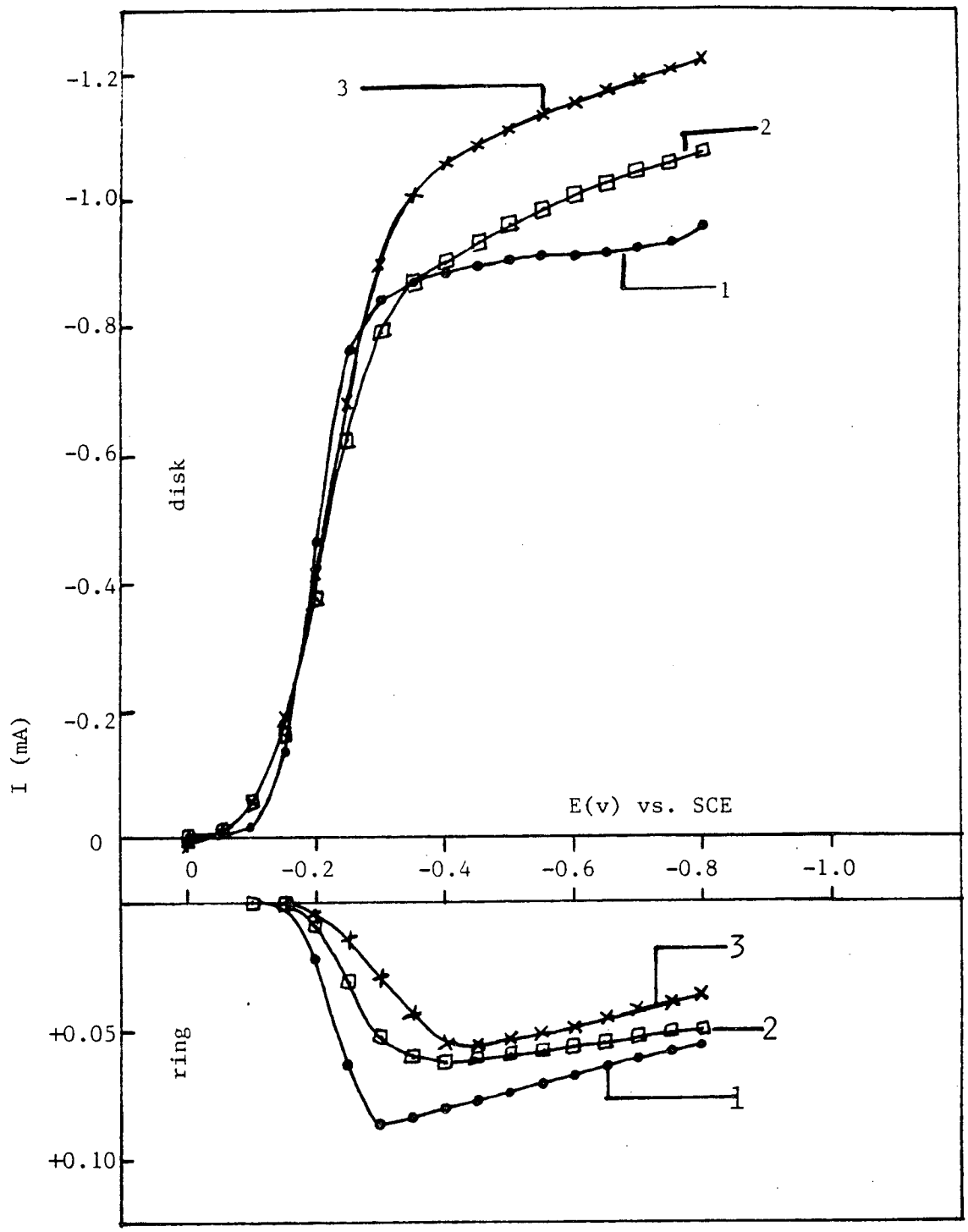

FIG. 36. ROTATING RING DISK CURRENTS FOR O_2 REDUCTION (1 ATM) ON A TPC ELECTRODE IN 0.1 M NAOH AT 25°C. DISK AREA (GEOMETRICAL) = 0.2 CM^2. RING, PT (N = 0.37) RING POT. = +0.1 V. ROTATION = 2500 RPM. TEFLON EMULSION = 10%.

1 - 5% COTMPP/XC-72 (800°C HT)

2 - PB + 2.5% CO (ADDED AS THE ACETATE) (800°C HT)

3 - 40% PAN + 1.18% CO (ADDED AS THE ACETATE)/XC-72 (800°C HT)

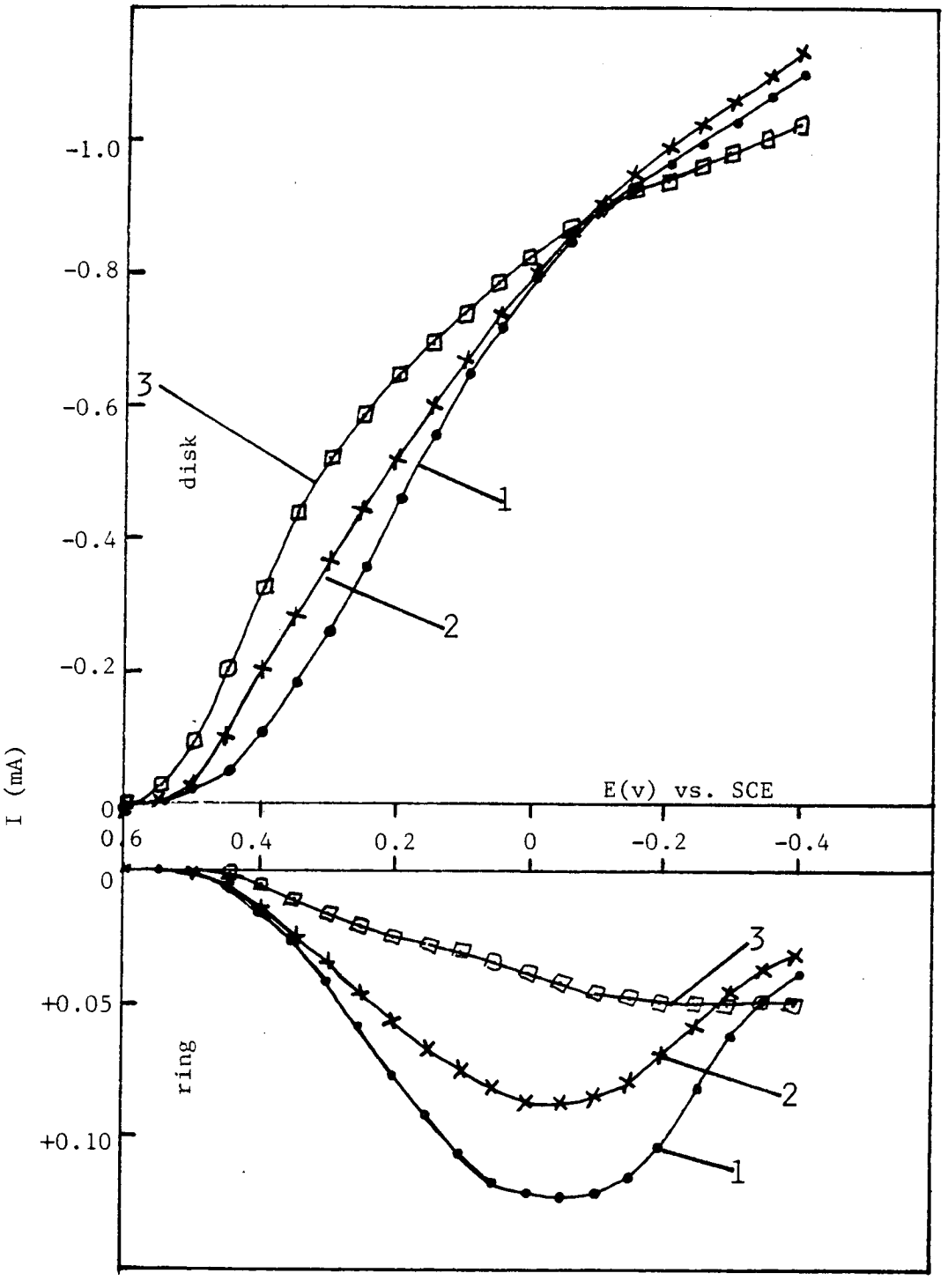

FIG. 37. ROTATING RING-DISK CURRENTS FOR O_2 REDUCTION (1 ATM) ON A TPC ELECTRODE IN 0.05 M H_2SO_4 AT 25°C. DISK AREA (GEOMETRICAL) = 0.2 CM^2. RING, PT (N = 0.37), RING POT. = +1.1 V. ROTATION = 2500 RPM. TEFLOM EMULSION = 10%

1 - 5% COTMPP/XC-72 (800°C HT)

2 - PB + 2.5% CO (ADDED AS THE ACETATE) (800°C HT)

3 - 40% PAN + 1.18% CO (ADDED AS THE ACETATE)/XC-72 (800°C HT)

The use of ionically conductive polymer phases incorporated into active layers of porous gas-fed electrodes is being pursued at Case in order to help stabilize the transition metal macrocycle catalysts in both acid and alkaline electrolytes. Some of these catalysts are relatively active for O_2 reduction but are also relatively unstable in 85% H_3PO_4 at 100°C, probably due to the loss of the transition metal into the bulk electrolyte (Fig. 38).

Another approach is to cover the solution side of the active layer with an ionomeric membrane. This approach has been tried in alkaline solution using a caustic-resistant anion exchange membrane (Ionics, Inc., Watertown, MA AR108-U01) with an active layer made from heat-treated CoTMPP on steam activated Shawinigan black. The polarization curves are essentially the same with and without the membrane up to ~200 mA cm^{-2} (Fig. 39) with IR correction for the resistance external to the active layer (including the membrane). Long term stability remains to be checked but is expected to be improved. Furthermore, the polymer permits the gas-fed electrodes to withstand substantial overpresure on the gas-side without blowing bubbles into the electrolyte* (Fig. 40).

One further approach to the problem of impeding the loss of the transition metal ion from the catalyst does not involve polymers but instead involves the use of bulk transition metal oxides to buffer the solution phase concentration of the dissolved species within the electrode.

E. Improvements with Gas-Fed O_2 Cathodes

Recent modifications in the fabrication of gas-fed electrodes and the subsequent polarization measurements at Case have led to a marked improvement and extension of the linear range in the Tafel plots. The modifications in

* This work was also partially supported by Gould, Inc., Ocean Systems Division.

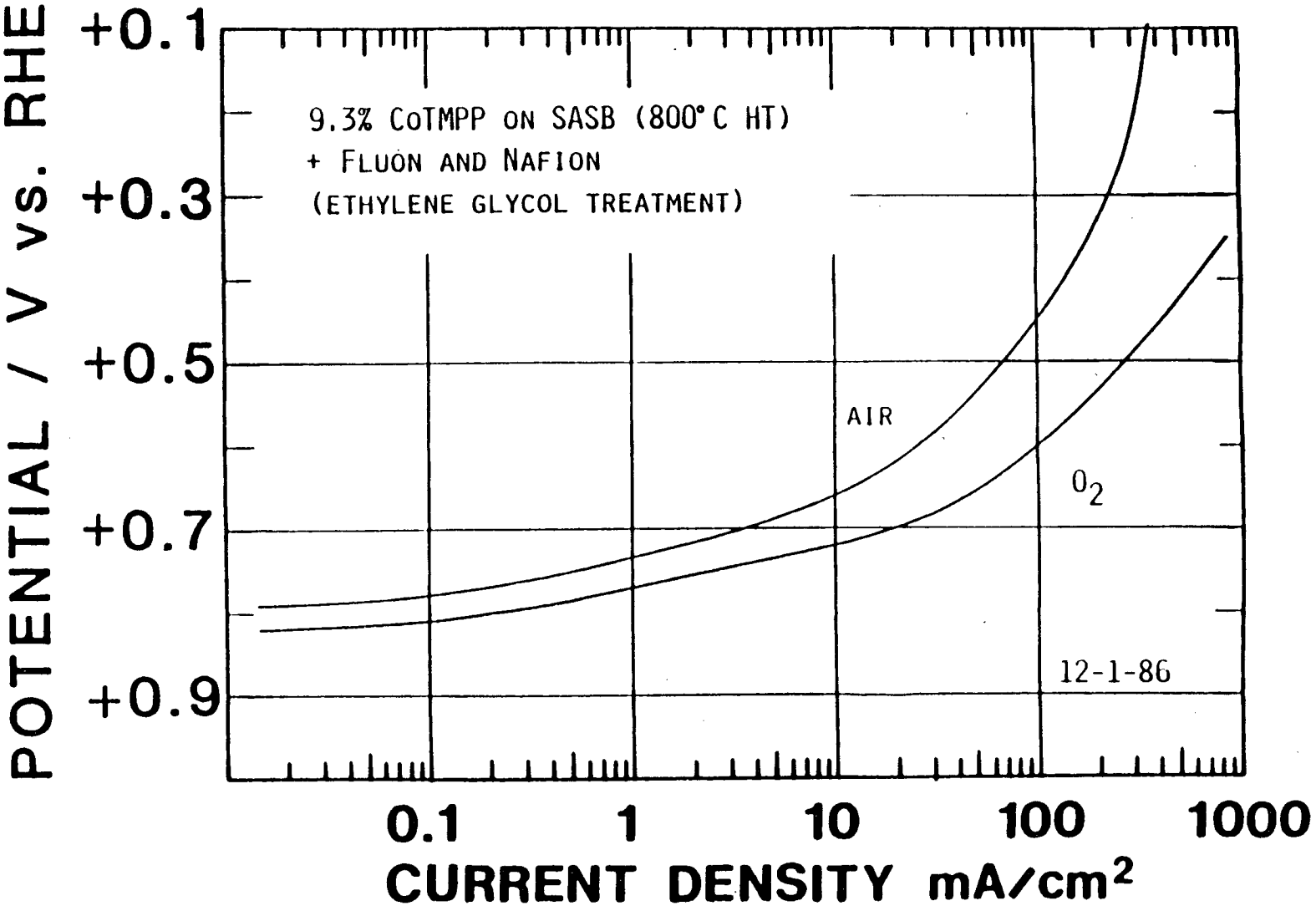

FIG. 38 POLARIZATION CURVES FOR O_2 REDUCTION WITH A GAS-FED (1 ATM) ELECTRODE IN 85% H_3PO_4 AT 85°C. THE ELECTRODE CONTAINED 15.0 MG CM^{-2} CATALYST/CARBON AND 11.0 MG CM^{-2} EACH OF UNDIALYZED FLUON AND BASE-TREATED NAFION AND WAS HEAT-TREATED AT 145°C FOR 9 H IN FLOWING HE.

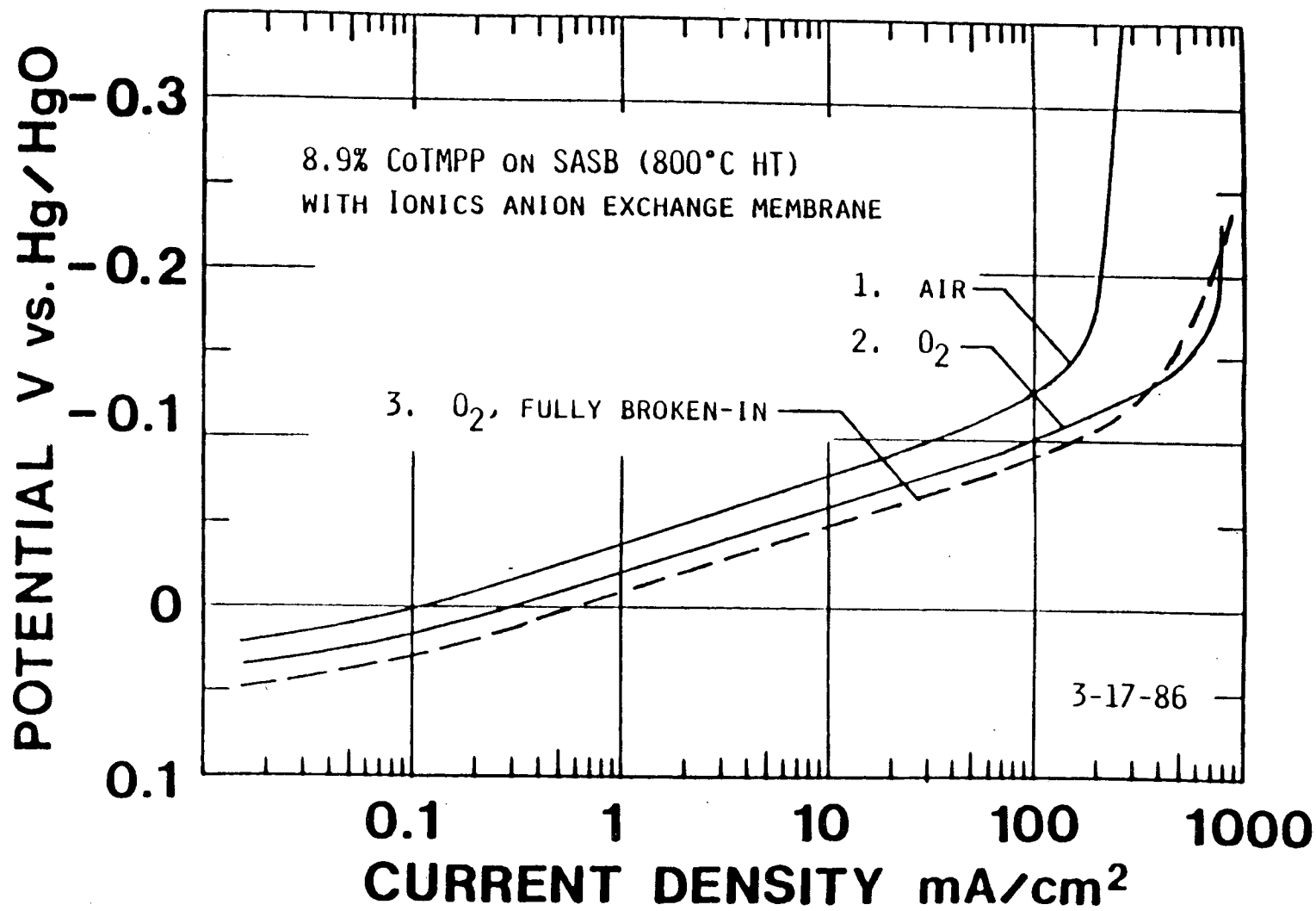

FIG. 39. POLARIZATION CURVES FOR O_2 REDUCTION WITH A POROUS GAS-FED (1 ATM) ELECTRODE IN 4 M NaOH AT 60°C. THE ELECTRODE CONTAINED 15.0 MG CM^{-2} CATALYST/CARBON AND 6.4 MG CM^{-2} TEFLON T30B AND WAS HEAT-TREATED AT 280°C FOR 2 H IN FLOWING HE, AFTER WHICH THE Ionics MEMBRANE WAS PRESSED ON THE ACTIVE LAYER.

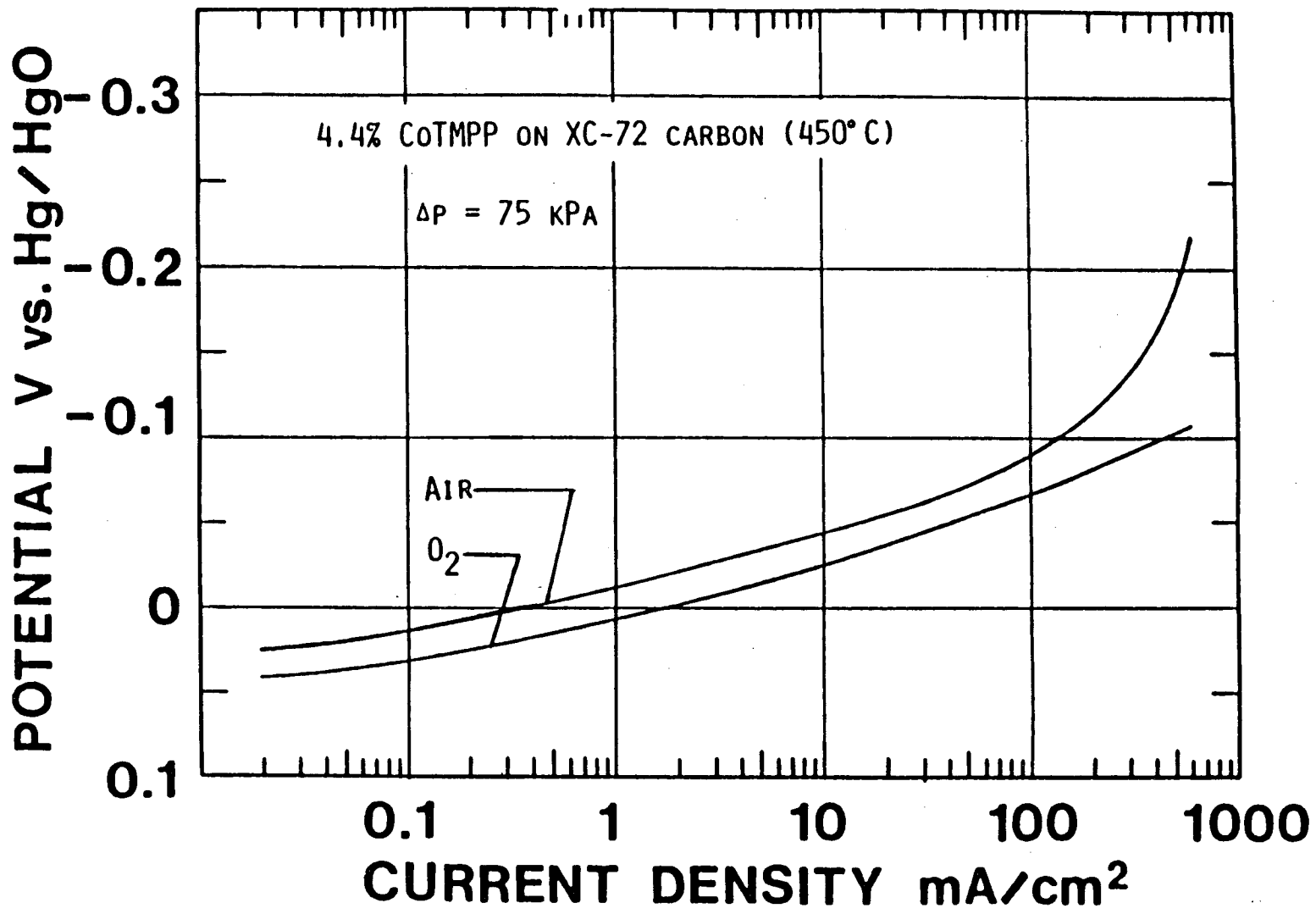

FIG. 40. O_2 REDUCTION POLARIZATION CURVES (AFTER 15 HOURS WITH ΔP = 75 KPA OF O_2 AND AT 100 MA CM^{-2} AND THEN PASSING H_2 AT 27 KPA FOR ~1 HOUR FOR GAS-FED ELECTRODE (ΔP = 75 KPA) WITH ANION EXCHANGE MEMBRANE (FIRST COATED WITH DDAC AND THEN PRESSED WITH IONICS MEMBRANE) OVER ACTIVE LAYER IN A MIXTURE OF ALKALINE SOLUTIONS (0.5 M LIOH IN 2:1 (V/V) 50% NAOH AND 45% KOH) AT 80°C. TOTAL ACTIVE LAYER (CATALYST + CARBON + TEFLON) = 29.58 MG CM^{-2}; CATALYST: 0.92 GM CM^{-2}; TEFLON: 8.75 MG CM^{-2}.

electrode fabrication have included the use of thinner active layers (10-15mg cm^{-2}) and the use of the conductive, hydrophobic backing material of the Electromedia Corporation. The improvements in the polarization measurements have involved optimization of the placement of the Luggin Capillary to minimize the IR drops and more accurate compensation of the remaining ohmic loss. The latter has involved the use of fast-action potentiostat in a galvanostatic interruptor mode to establish the ohmic drop external to the porous active layer.

A new steam-activated Shawinigan acetylene black (SASB) has become available from the Electromedia Corporation which has a BET surface area 190 m^2g^{-1}. It can be used in place of Cabot Vulcan XC-72 (250 m^2g^{-1}) with virtually identical results (Fig. 41), but the electrodes are much easier to fabricate with SASB than with XC-72 because of their differing interaction with Teflon.

A new fluorocarbon emulsion (Fluon) has become available which may be more effective for the fabrication than the traditionally used duPot Teflon T30B. The latter contains 6% of the surface active agent Triton X-100, which has been found in work at CWRU to poison the catalytic activity for O_2 reduction of some electrode surfaces, as well as to impede the homoflocculation of the Teflon particles. This duPont Teflon emulsion also includes a minor amount of a second surfactant (undisclosed) to improve its wetting properties. The Fluon emulsion manufactured by Imperial Chemical Industries contains only 0.14% of an octaonate surfactant, which can be removed by dialysis with the emulsion still retaining short term stability. It was found that an electrode fabricated using Fluon (undialyzed) without the customary 280°C heat treatment functions as well as those fabricated with Teflon with the 280°C heat treatment. If Teflon is used without this treatment, it performs rather poorly. This is probably because the heat treatment serves both to remove the triton X-100 as

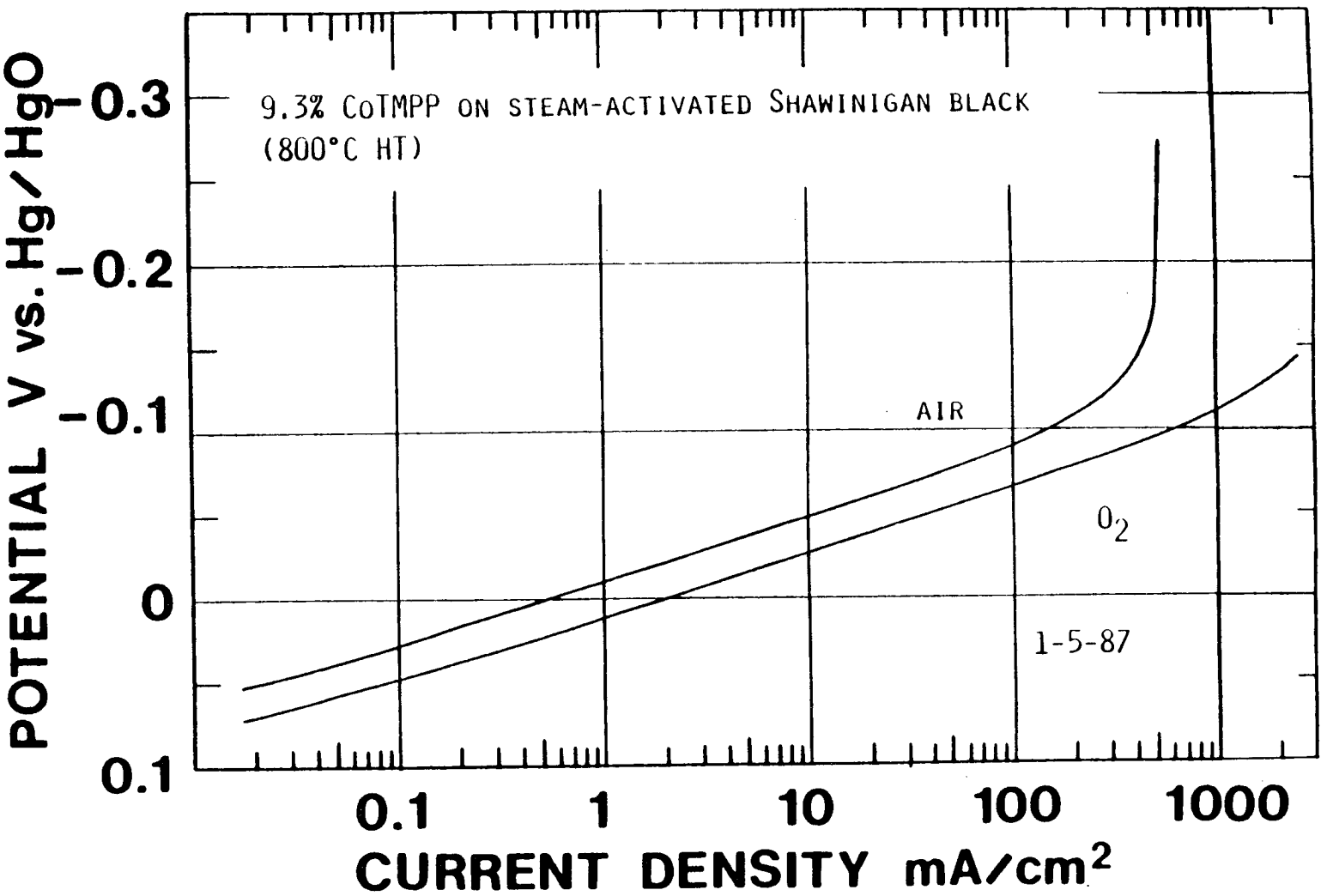

FIG. 41. POLARIZATION CURVES FOR O_2 REDUCTION WITH GAS-FED (1 ATM) ELECTRODES IN 4 M NaOH AT 60°C. THE ELECTRODE CONTAINED 14.6 MG CM^{-2} CATALYST/CARBON AND 5.7 MG CM^{-2} TEFLON T30B AND WAS HEAT-TREATED AT 305°C FOR 2 H IN FLOWING HE.

well as to "pre-sinter" the Teflon particles (the melting range of PTFE is 360-390°C).

F. Perovskite Electrocatalysts

The perovskites have not generally been found to be very active catalysts for O_2 reduction when used in oxygen cathodes either with or without high area carbon. Some of the higher area compounds have considerable activity for peroxide decomposition and O_2 generation, however. When used in conjunction with heat-treated macrocycles, even ones without a transition metal center, some of the perovskites show excellent performance for O_2 reduction. This section will focus on peroxide decomposition, while results of O_2 reduction and generation measurements on gas-fed electrodes will be presented in the next section, covering bifunctional O_2 electrodes.

The peroxide-decomposing properties of the perovskites have received major attention in this project both because of their importance in developing effective air cathodes and because of the fundamental interest in uncovering correlations of the kinetics with chemical and physical properties of the catalysts. A large part of the effort has been concentrated on developing methods for measuring the decomposition rate constants. Four of these methods will be discussed in detail. The remainder of the effort has been devoted to examining the magnetic properties, principally the magnetic susceptibilities and their correlations with the peroxide decomposition rate constants. Thus far, 21 different perovskites have been prepared of the general type $La_xSr_{1-x}MO_3$, in which m stands for a transition metal or combination of transiton metals, including Mn, Fe, Co, Ni and Ru (TableIV). The preparation methods used at Case have included the following: solid state reaction (SSR), nitrate decomposition (ND), hydroxide precipitation (HP) and inorganic complex precipitation (ICP). The ICP method involves the precipitation of an inorganic

TABLE IV

PEROVSKITES EXAMINED AT CWRU

COMPOUNDS	PREPARATION METHOD	SURFACE AREA $M^2\ G^{-1}$
$BaRuO_3$	ND[A]	-
$LaCoO_3$	ND	2.7
$La_{0.5}Sr_{0.5}CoO_3$	ND	1.2
$LaCo_{0.5}Ni_{0.5}O_3$	ND	3.0
$La_{0.8}Sr_{0.2}Co_{0.9}Ru_{0.1}O_3$	ND	1.7
$La_{0.5}Sr_{0.5}Co_{0.8}Ru_{0.2}O_3$	ND	-
$LaFeO_3$	ICP	13.7
$SrFeO_3$	ND	2.3
$LaFe_{0.5}Co_{0.5}O_3$	ND	2.9
$LaFe_{0.33}Co_{0.33}Ni_{0.33}O_3$	ND	2.4
$LaFe_{0.1}Ni_{0.9}O_3$	ND	1.4
$LaFe_{0.25}Ni_{0.75}O_3$	ND	1.4
$LaFe_{0.5}Ni_{0.5}O_3$	ND	-
$LaFe_{0.75}Ni_{0.25}O_3$	ND	-
$LaFe_{0.9}Ni_{0.1}O_3$	ND	-
$LaMnO_3$	SSR	0.9
$LaMnO_3$	OD	1.3
$La_{0.5}Pb_{0.5}MnO_3$	HP	$14.1 \rightarrow 17.8$[B]
$La_{0.5}Sr_{0.5}MnO_3$	ND	10.5
$La_{0.5}Sr_{0.5}Co_{0.5}Mn_{0.5}$	ND	-
$LaNiO_3$	ND	-
$LaNi_{0.5}Ru_{0.5}O_3$	ND	1.3

[A] ND = NITRATE DECOMPOSITION, ICP = INORGANIC COMPLEX PRECIPITATION, SSR = SOLID STATE REACTION, OD = OXALATE DECOMPOSITION, HP = HYDROXIDE PRECIPITATION.

[B] LATTER VALUE WAS OBTAINED AFTER EXTRACTION WITH ACETIC ACID.

precursor which contains the requisite A and B cations needed for the perovskite in the correct stoichiometric ratio. In effect the cations are at a molecular level of mixing, and relatively low temperatures ($\geq$450°C) are therefore needed, which helps to avoid sintering. The SSR and ND methods produce materials with relatively low areas ($\geq$ 2 m^2 g^{-1}). The HP and ICP methods produce materials of higher surface area ($\geq$ 10 m^2 g^{-1}) and thus are more attractive for preparing catalysts. The compounds were characterized using X-ray diffraction, BET surface area measurement, elemental analysis as well as magnetic susceptibility.

1. Methodology in Peroxide Decomposition Kinetics

One focus of this work has been on the development of methods which can be used in-situ in operating air electrodes and the correlation of the results with those obtained using the more traditional methods. The four methods which have been examined at Case include two methods which involve stirred suspensions of the catalysts in contact with peroxide-containing aqueous alkaline solutions. The peroxide concentration is then monitored. The first is the gasometric method, in which the volume of O_2 generation is monitored and the peroxide concentration calculated therefrom. The second method involves the monitoring of the peroxide concentration via the measurement of the limiting current for peroxide oxidation at a gold rotating disk electrode.

The other two methods involve measurements on gas-fed electrodes. The first of these involves the monitoring of the peroxide concentration via the open circuit potential after the interruption of cathodic current. The second method, the steady-state polarization method, is limited to catalyst systems in which peroxide decomposition is clearly the rate-determining step in the O_2 reduction. It involves the measurement of the steady-state cathodic current at a given potential in the Tafel-linear region of the polarization curve. One

additional method which can be used with porous electrodes has not yet received detailed attenion. In a cyclic voltammetric experiment, peroxide is first produced in a negative potential sweep and then re-oxidized in the positive sweep. The magnitude of the oxidation peak is a measure of the peroxide concentration. The first four methods are described briefly below.

a. Gasometric Method

Small amounts (15-300 mg) of the catalysts were dispersed in KOH solution and thoroughly wetted. Then an aliquot of peroxide solution was added to the suspension, and the volume of generated O_2 was monitored. The initial concentrations were 0.078 M for peroxide and 4.0 M for KOH. The peroxide concentration was calculated from the gas volume according to Eq. 3 in Reference 62.

As shown in (Fig. 42), the log of peroxide concentration vs. time is usually quite linear, indicating that the kinetics are probably first order in peroxide concentration. This method is not a stringent test of the reaction order, however because of the limited concentration range covered (less than two decades). The linearity also indicates that there is negligible potential dependence of the peroxide decomposition rate constant, at least for this particular catalyst under these particular experimental conditions. The decomposition rates are clearly dependent upon the amount of catalyst but can be normalized either to the weight of catalyst or to the total catalyst surface area. The area-normalized rate or areal rate in mol cm^{-2} s^{-1} is calculated according to (63):

$$\text{areal rate} = -(V_{liq}/A_{Cat})\ (dC_{HO_2^-}/dt) \qquad [1]$$

where V_{liq} is the volume of liquid solution (cm^3), A_{cat} is the surface area of catalyst (cm^2), $C_{HO_2^-}$ is the peroxide concentration (mol cm^{-3}) and t is the time (s). For first order dependence on peroxide, this rate is equal to

$k_{het}\ C_{HO_2^-}$, where k_{het} values calculated from the data in (Fig. 43) are constant to within < 5%. This result indicates that the catalysis is taking place on the catalyst surface and not in the solution due to possible dissolved species. This was also confirmed in an independent measurement in which KOH solution which had been in contact with the catalyst was found to have negligible activity. Several perovskites have been tested using this method. The log c vs. t plots have all been reasonably linear and the k_{het} values relatively constant. A substantial number of perovskites have now been subjected to gasometric measurements. The mass-normalized rate constants k_m for these compounds are listed in Table V together with the specific surface areas and area-normalized rate constants k_{het} for some of the compounds. The k_{het} values can be compared directly with values obtained using the other methods. Such comparisons are in progress.

b. RDE Method

This method (64-66) is similar to the gasometric method in using a stirred catalyst suspension, with the amounts and concentration as given above. The peroxide concentration is monitored amperometrically by measuring the peroxide oxidation limiting current at a rotating gold disk electrode (area = 0.196 cm^2; rotation rate = 3600 rpm; potential = +0.250 V vs. Hg/Hgo, OH^-). The peroxide concentration was calculated using the Levich equation.

As with the gasometric method, the log c vs. t plots (Fig. 44) are quite linear, again probably indicating first order kinetics. The RDE method is capable of covering a wider range of concentration and this provides a more stringent test of first order than does the gasometric method. The linearity also indicates a lack of potential dependence under these conditions.

c. Open Circuit Potential Decay (OCPD) Method

Porous gas-fed electrodes in a "floating" arrrangement (67) were used for these experiments. The apparent electrode area was 0.5 cm^2 and contained 15 mg

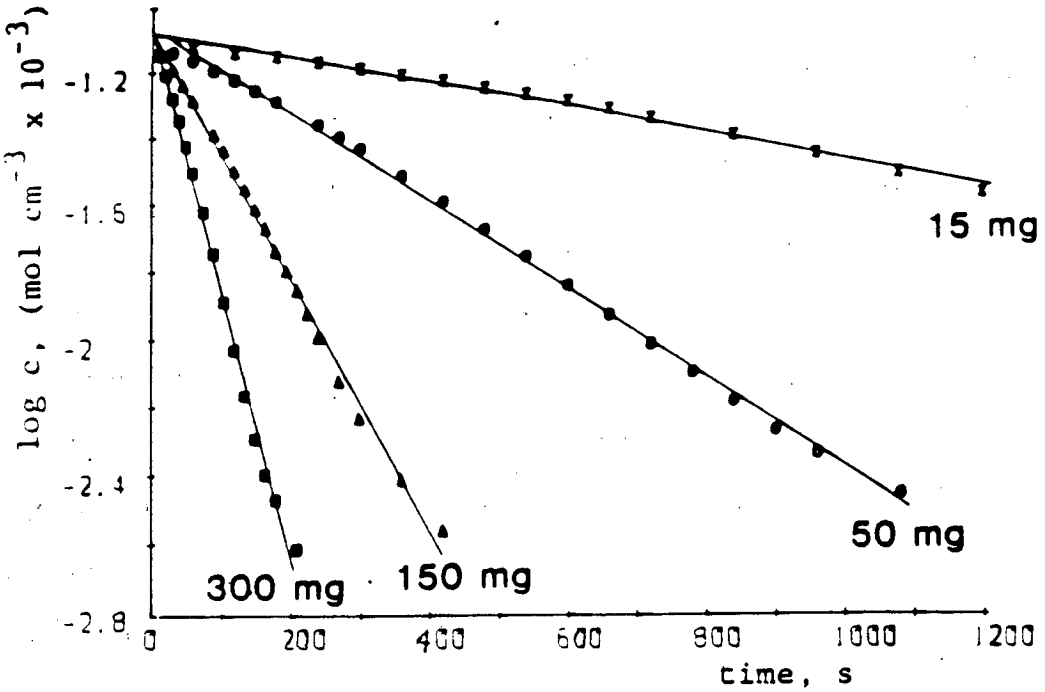

Fig. 42. Logarithm of peroxide concentration as a function of time for gasometric experiments using various amounts of the catalyst (indicated in the figure). The initial peroxide concentration was 0.0782 M in 50 cm^3 of 4 M KOH at T=22 °C.
Catalyst: $La_{0.5}Sr_{0.5}Fe_{0.33}Co_{0.33}Ni_{0.33}O_3$.

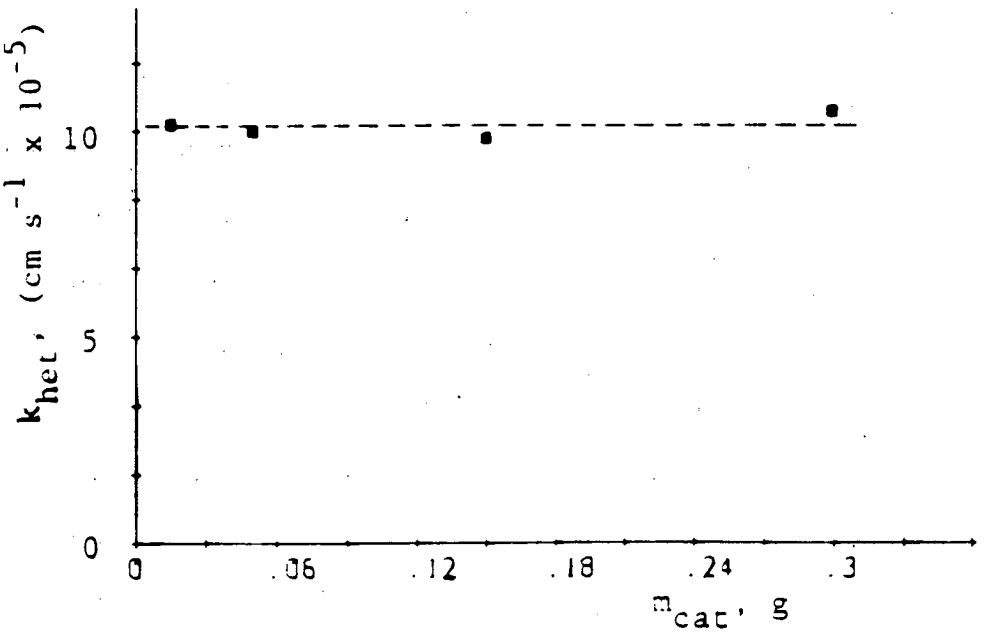

Fig. 43. Heterogeneous peroxide decomposition rate constants k_{het} as a function of the amount of catalyst. The initial peroxide concentration was 0.0782 M in 50 cm^3 of 4 M KOH at 22 °C. Catalyst: $La_{0.5}Sr_{0.5}Fe_{0.33}Co_{0.33}Ni_{0.33}O_3$.

TABLE V

PEROXIDE DECOMPOSITION RATE CONSTANTS USING PEROVSKITE CATALYSTS ON A WEIGHT BASIS (K_M) AND A SURFACE AREA BASIS (K_{HET}) IN 4 M KOH WITH 0.2 M HO_2^- AT ROOM TEMPERATURE.

Compound	$k_m/cm^3\ g^{-1}\ s^{-1}$	$(k_{het}/cm\ s^{-1})10^5$	$A/m^2\ g^{-1}$
$La_{0.5}Pb_{0.5}MnO_3$	11 ± 6	8 ± 4	14.1
$La_{0.5}Sr_{0.5}MnO_3$	8 ± 3	8 ± 2	10.5
$LaMnO_3$	0.7	6.4	1.1
$LaFe_{0.33}Co_{0.33}Ni_{0.33}O_3$	1.4 ± 0.7	6 ± 3	2.4
$LaCoO_3$	1.5 ± 0.5	6 ± 2	2.7
$LaFe_{0.25}Ni_{0.75}O_3$	3.8	27	1.4
$LaFe_{0.10}Ni_{0.90}O_3$	6.6		
$LaNiO_3$	0.06		
$LaCo_{0.5}Ni_{0.5}O_3$	2.4	8.0	3.0
$La_{0.8}Sr_{0.2}Co_{0.9}Ru_{0.1}O_3$	1.2	7.1	1.7
$LaCo_{0.5}Fe_{0.5}O_3$	0.54	1.8	2.9
$LaCrO_3$	0.28		

cm^{-2} Shawinigan acetylene black and 15 mg cm^{-2} catalyst, with 7.5 mg cm^{-2} Teflon T30B. Conductive hydrophobic backing material (Electromedia Corp.) was used. Cathodic currents in the range of 0.01 to 2.0 mA were applied and then interrupted. The open circuit potential of the electrode was used to monitor the peroxide concentration, assuming the O_2/HO_2^- couple to be nearly reversible on the high area carbon electrode:

$$O_2 + H_2O + 2e^- = HO_2^- + OH^- \quad [2]$$

The concentration was calculated using a re-arranged form of the Nernst equation:

$$c = \exp[-(2F/RT)(E-E')] \quad [3]$$

where

$$E' = E^o(O_2/HO_2^-) - E^o(HgO/Hg) + (RT/2F)\ln(p_{O_2} c_{HO^-}) \quad [4]$$

This value was determined to be -0.145V vs. Hg/HgO, 4 M KOH at 25°C (68).

When this method was first developed at Case by Ohzuku et al. (68, 69), it was found that nearly all catalysts exhibited apparent second-order behavior, even though other methods yielded first order dependence. Only recently has it come to light that a possible explanation of this apparent discrepancy was that the discharge of the double layer capacitance produces additional peroxoide, which tends to decrease dE/dt at longer times and creates the illusion of second order kinetics (62, 70). An equation was derived by Yeager and co-workers which described this behavior (71):

$$(V_{liq}/A_{cat})\ln(c/c_o) - (RTC_{tot}/4F^2A_{cat})(1/c - 1/c_o) = -k_{het}t \quad [5]$$

where V_{liq} is the volume of liquid (cm^3) within the gas-fed electrode, A_{cat} is the wetted catalyst area (cm^2), c_o is the peroxide concentration (mol cm^{-3}) at t=o, R, T and F have their usual significance, and C_{tot} is the total capacitance including double-layer capacitance and potential-dependence Faradaic surface processes (pseudo-capacitances). Methods to estimate some of these

quantities are given in Reference 62.

Two types of limiting behavior are predicted from Eq. 5 and are also observed experimentally. At short times or large initial peroxide concentrations c_o values (i.e. large currents) the first term is predominant, and first order behavior is observed (i.e. linear E vs. t). At longer times or small c_o values (i.e. smaller currents), the scond term is predominant, and apparent second order behavior is observed (i.e., linear 1/c vs. t). Examples of the latter can be seen in (Fig. 45). At higher currents, the 1/c vs. t plots begin to curve at the bottom, while the E vs. t traces begin to straighten, showing the true first order behavior. A series of ideal 1/c vs. t cures were calculated using Eq. 5 for different values of c_o (Fig. 46), showing the bonding effect for larger c_o values.

Several other perovskites have been examined using this method. Most yielded reasonably linear 1/c vs. t plots for low currents. One compound however, exhibited a leveling-off effect, which would be expected if a redox couple of the catalyst itself were perturbing the open circuit potential. Such a phenomenon would be an example of a potential-dependent pseudo-capacitance contributing to C_{tot}.

d. Steady-State Polarization Method

Under special circumstances it may be possible to determine peroxide decomposition rate constants directly from the gas-fed polarization curve if peroxide decomposition is the rate-determining step. Some of the requirements are as follows:

1. Minimal ohmic or mass transport losses
2. linear Tafel region with a slope of -2.3RT/2F V/decade (-33.0 mV/decade at 60°C)
3. separation of (RT/2F)ln(0.209) V between air and pure 0_2 curves (22.5 mV at 60°C).

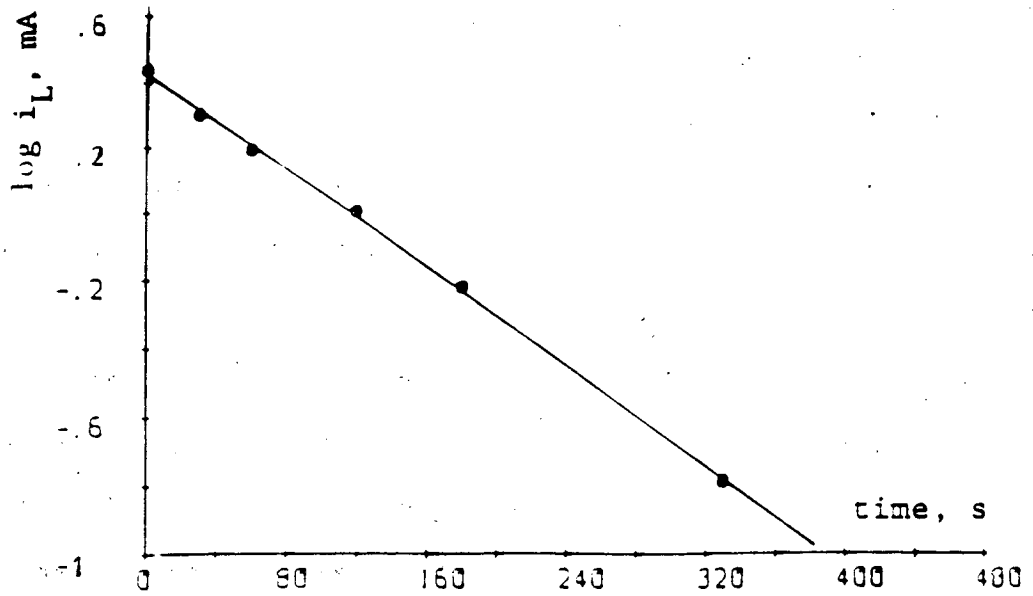

Fig. 44. Logarithm of the limiting disk current (taken at +0.250 V vs. Hg/HgO, OH^-) for HO_2^- oxidation as a function of time after the addition of 50 mg of catalyst to 50 cm^3 of 4 M KOH at 22 °C. The initial peroxide concentration was 0.0782 M. Catalyst: $La_{0.5}Sr_{0.5}Fe_{0.33}Co_{0.33}Ni_{0.33}O_3$.

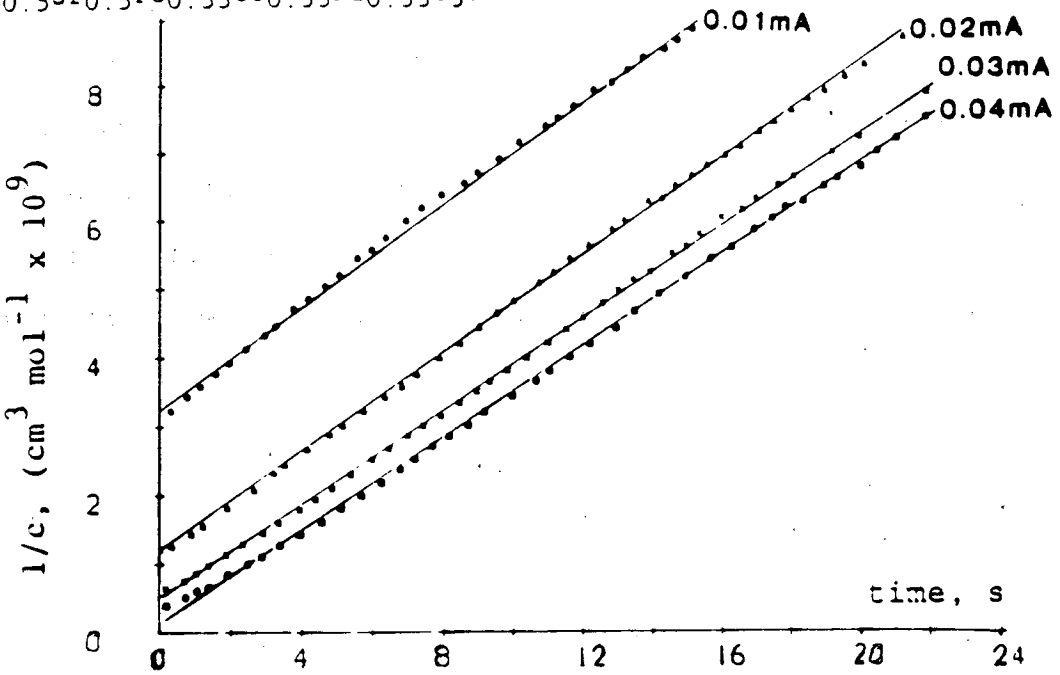

Fig. 45. Reciprocal of the peroxide concentration as a function of time after interruption of the current in a floating gas-fed electrode containing 40 wt. % catalyst, 40 wt. % Shawinigan acetylene black and 20 wt. % Teflon T30B. The electrolyte was O_2 -saturated 4 M KOH at 22 °C. The current values used are indicated. Catalyst: $La_{0.5}Sr_{0.5}Fe_{0.33}Co_{0.33}Ni_{0.33}O_3$.

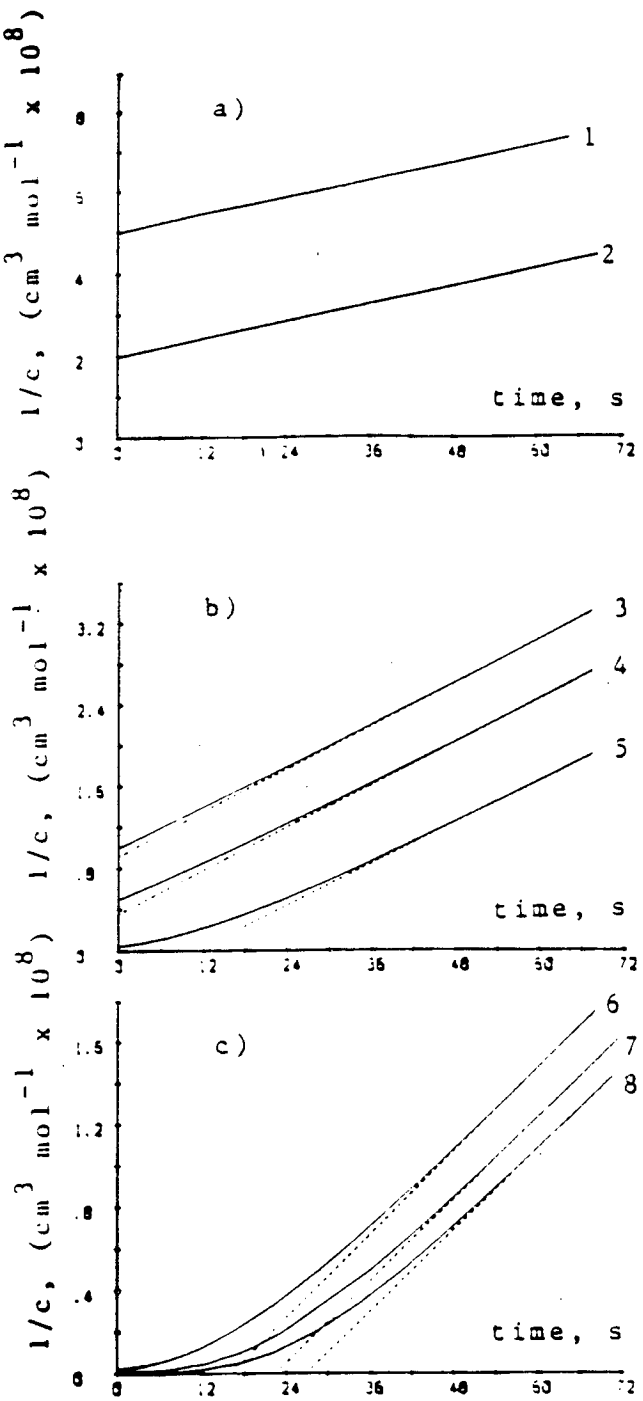

Fig. 46. Theoretical plots of reciprocal peroxide concentration vs. time after current interruption, generated using Eq. 14 for a) low, b) medium and c) high values for the initial peroxide concentration. Concentrations (mol cm^{-3}) were: 1) 2 x 10^{-9}, 2) 5 x 10^{-9}, 3) 1 x 10^{-8}, 4) 2 x 10^{-8}, 5) 2 x 10^{-7}, 6) 5 x 10^{-7}, 7) 2 x 10^{-6}, 8) 5 x 10^{-6}. Parameters used were: V_{liq} = 5 x 10^{-3} cm^3, A_{cat} = 100 cm^2, C_{tot} = 0.1 F and k_{het} = 1 x 10^{-5} cm s^{-1}.

The k_{het} value can then be calculated usisng

$$k_{het} = I/nF\ A_{cat} \qquad [6]$$

where I is the current (amperes) and n=2

The A_{cat} value can be determined voltammetrically. Such A_{cat} determinations are planned for the immediate future.

e. Comparison of k_{het} values

The k_{het} values obtained for several perovskites and one heat-treated transition metal macrocycle using the gasometric and RDE methods are summarized in Table VI. At the time of submission of this report, reliable data had only been obtained using these methods. The rate constants indicated in Table VI obtained using the two methods are in fair agreement but should agree better. A source of error could be a difference in the degree of wetting. With further development, these methods may become useful in comparing catalysts for peroxide decomposition for both fundamental and applied purposes.

2. Correlations of Peroxide Decomposition with Magnetic Properties

Definite evidence for the involvement of magnetic properties in the peroxide decomposition catalysis has now been obtained. A series of Fe, Co, and Ni-containing perovskites, all of which were paramagnetic, has shown an inverse correlation between the effective magnetic moment μ_{eff} and preliminary measurements of peroxide decomposition catalytic activity (normalized to the surface area). The greater the number of unpaired electrons, the lower was the catalytic activity. Caution must be exercised in considering such correlations, since there is no assurance that the surface properties are simply related to the bulk properties. Furthermore, exposure to the electrolyte can very substantially modify the surface properties.

Another illustration of a correlation of bulk magnetic properties with peroxide decomposition catalytic activity is provided by results obtained with the series of perovskites of the general formula La $Fe_xNi_{1-x}O_3$. As x increases,

TABLE VI

COMPARISON OF EXPERIMENTAL VALUES OF K_{HET} OBTAINED WITH THE GASOMETRIC AND RDE METHODS.

Compound	k_{het} (cm s^{-1} x 10^{-5}) gasometric	RDE
$LaFe_{0.33}Co_{0.33}Ni_{0.33}O_3$	1.7	1.0
$LaFe_{0.1}Ni_{0.9}O_3$	34.0	53.0
$La_{0.5}Pb_{0.5}MnO_3$	3.8	2.1
$La_{0.5}Sr_{0.5}Fe_{0.33}Co_{0.33}Ni_{0.33}O_3$	11.3	10.3
CoTMPP on XC-72 carbon (4.8 %, 800° C)		0.8

The k_{het} values were obtained in 4 M KOH at room temperature.

the peroxide decomposition rate constants increase, reach a sharp peak at x = 0.25 and then gradually decrease (Fig. 47). Since all of the surface areas have not been measured at this time, the rate constants are not normalized to surface area. The surface areas probably do not vary over a wide range, however, since all of the compounds were prepared using the same method.

Ex situ Mossbauer effect spectroscopy (MES) and magnetic susceptibility measurements have been used to examine the solid state properties. MES has indicated the presence of a paramagnetic-to-antiferromagnetic transition for values of x between 0.4 and 0.5, a region in which the peroxide decomposition activity changes significantly. MES has also shown that upon incorporation of Ni^{3+} into the $LaFeO_3$ structure, in which Fe is in the Fe^{3+} valence state, some of the Fe^{3+} is forced into the unusual Fe^{4+} state. The Ni^{3+} is reduced to Ni^{2+} in the process. The isomer shifts for the Fe^{4+} and Fe^{3+} species show maximal and minimal values respectively for the composition range near x = 0.25. Thus the catalytic activity can be related directly to the d-electron densities for the transition metal cations. The details are given in Reference 72..

G. Bifunctional Oxygen Electrodes

There are two possible approaches to the development of catalysts for bifunctional O_2 electrodes in alkaline electrolytes (71). The first is to develop a single material which is active in both modes and is also stable over the working potential range. The second is to develop separate catalysts for O_2 reduction and generation that are both stable over the whole working potential range. While the first approach is more elegant, the second approach has been more successful in the research at Case.

The O_2 reduction catalysts used have mostly been heat-treated transition metal macrocycles on the relatively oxidation resistant Shawinigan acetylene black. In many cases the macrocycle used was the metal-free form during the

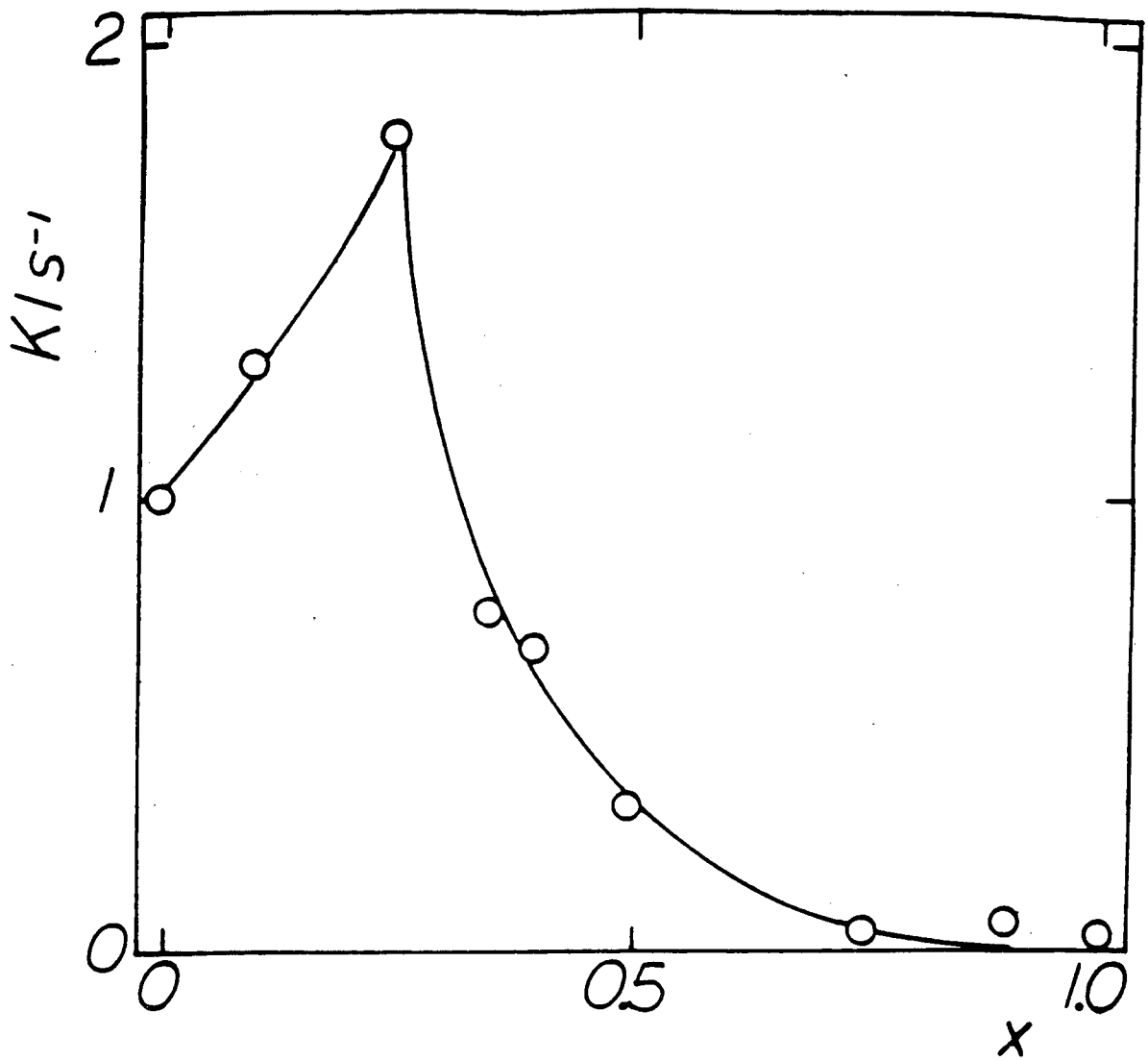

FIG. 47. HYDROGEN PEROXIDE DECOMPOSITION RATE CONSTANTS VS. X IN $LaFe_xNi_{1-x}O_3$.

THE RATE CONSTANTS WERE MEASURED BY THE GASOMETRIC METHOD IN 4 M KOH AT 22°C. THE INITIAL CONCENTRATION OF PEROXIDE WAS 0.2 M.

heat treatment, and the transition metal was supplied by oxides or hydroxides added after the heat treatment. These transition metal oxides or hydroxides are also the O_2 generation catalyst. They have included various mixtures of precipitated hydroxides, such as Mn, Fe, Co, Ni, Ag and Ru and typically have very high effective surface areas. They in fact appear to act as three-dimensional catalysts, since in some cases nearly 100% of the material is electroactive. The compounds examined have also included various transition metal-containing perovskites, which have typically had surface areas in the range of 1- 20 m^2g^{-1}.

Polarization measurements for O_2 reduction were conducted for several perovskites using gas-fed electrodes in 5.5 M KOH at 25°C (Fig. 48). The electrodes contained approximately equal weights of perovskite and Shawinigan acetylene black (SB). Oxygen reduction to peroxide takes place on the high area carbon, and peroxide decomposition takes place on the perovskite. The best performance was obtained for an electrode containing $La_{0.5}Pb_{0.5}MnO_3$, which also had the highest catalytic activity for peroxide decomposition according to gasometric measurements. Its activity is high principally because its surface area is an order of magnitude higher than for the other compounds examined (see Table IV). All of these polarization curves are rather poor, which could be due to ohmic, mass transport or kinetic problems.

The performance can be improved greatly by using heat-treated metal-free tetramethoxyphenyl porphyrin (H_2TMPP) on SB in place of unmodified SB (Fig 49). The increased activity is probably due to small amounts of transition metal ions leaching out of the perovskite, entering the solution as the oxyanions and adsorbing at nitrogen-containing surface functional groups on the heat-treated macrocycle on carbon. These adsorbed transition metal ions then act as catalytic sites for both O_2 reduction to peroxide and for peroxide decomposition.

The O_2 reduction performance of the perovskite alone with no added carbon

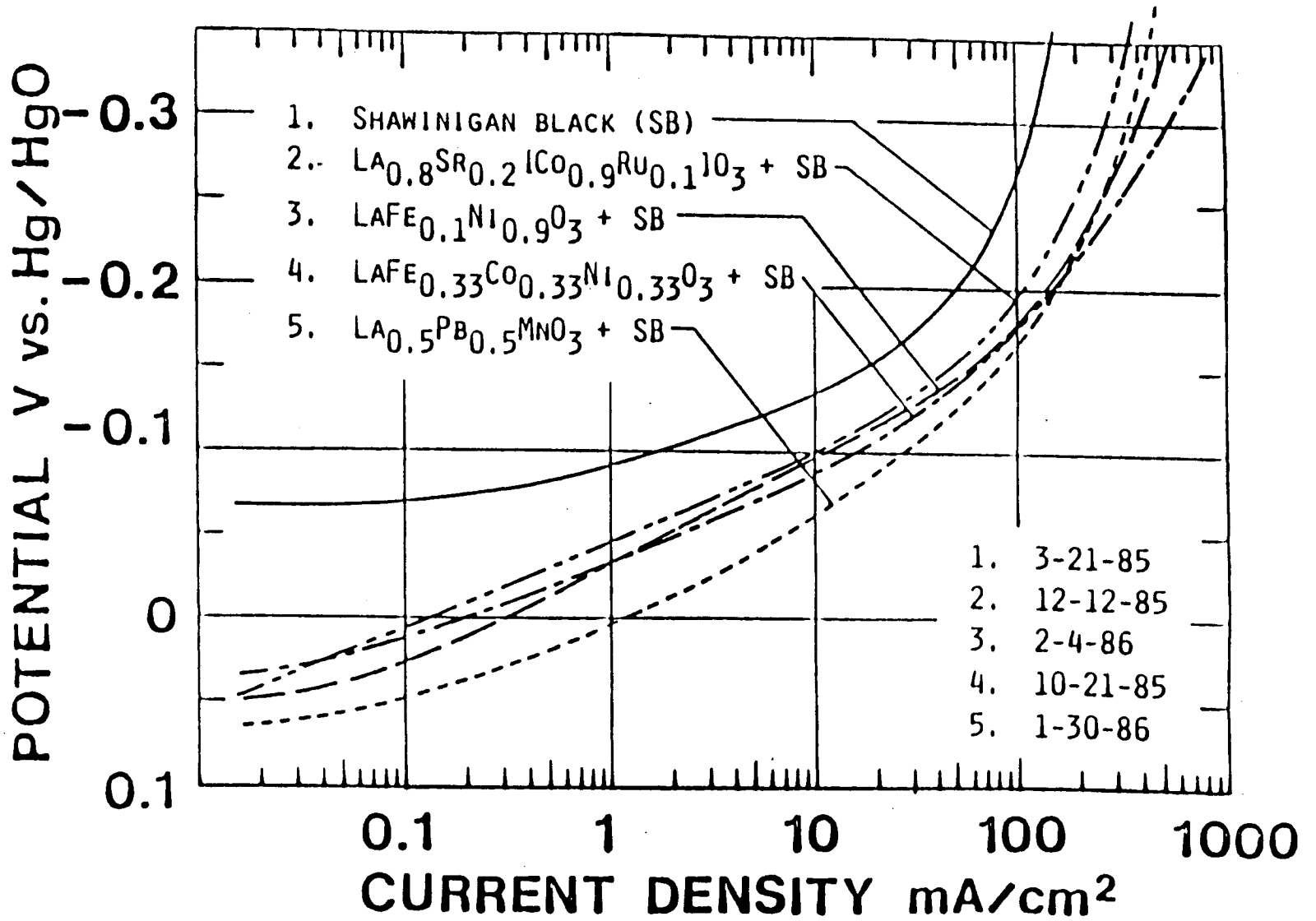

FIG. 48. POLARIZATION CURVES FOR O_2 REDUCTION WITH POROUS O_2-FED (1 ATM) ELECTRODES IN 5.5 M KOH AT 25° C. THE ELECTRODES CONTAINED APPROXIMATELY 16 MG CM^{-2} PEROVSKITE, 15 MG CM^{-2} SB AND 8 MG CM^{-2} TEFLON T30B, EXCEPT FOR ELECTRODE (1), WHICH CONTAINED 27 MG CM^{-2} SB AND 7 MG CM^{-2} TEFLON.

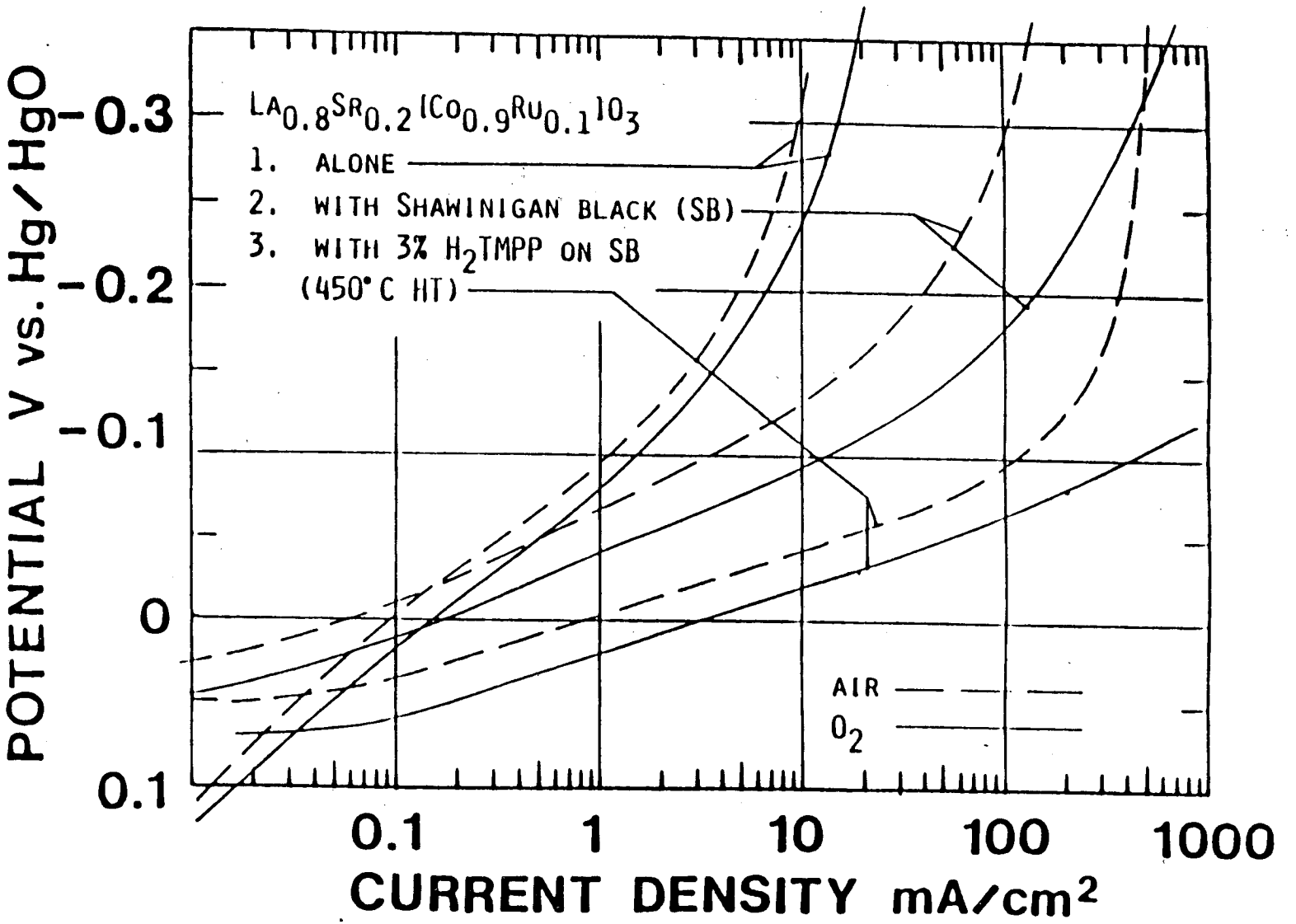

FIG. 49. POLARIZATION CURVES FOR O_2 REDUCTION WITH POROUS GAS-FED (1 ATM) ELECTRODES IN 5.5 M KOH AT 25°C. THE ELECTRODES CONTAINED 100, 15.8 AND 15.8 MG CM^{-2} PEROVSKITE; 0, 14.6 AND 14.6 MG CM^{-2} SB OR H_2TMPP/SB; AND 8.7, 8.3 AND 8.3 MG CM^{-2} TEFLON T30B FOR ELECTRODES 1, 2 AND 3, RESPECTIVELY.

is very poor (Fig. 49). This is because the activity for O_2 reduction to peroxide is low.

The process of dissolution and re-adsorption of the transition metal ions can be accelerated with the use of relatively negative potentials. It has been shown at Case that very negative potentials can convert the compound $SrFeO_3$ completely to the iron(II) hydroxide, which is then reoxidized to the oxyhydroxide FeOOH (72). This process probably involves the dissolution of an Fe(II) species. The gradual improvement of the performance of a gas-fed electrode containing heat-treated H_2TMPP and the perovskite $La_{0.8}Sr_{0.2}Co_{0.8}Ru_{0.2}O_3$ and the substantial effect of the activation procedure are consistent with the model described above.

The transition metal hydroxides have also been shown to produce highly active catalysts for O_2 reduction in conjunction with both H_2TMPP and CoTMPP, but the perovskites may offer advantages because they may produce better electrode structures and also may be more stable than the hydroxides. Thus their ultimate utility may be in providing a back-up source of the transition metal ions for the heat-trated macrocycle/carbon during long-term operation. It has been shown that one of the life-limiting processes for CoTMPP-based air cathodes in alkaline solution is the loss of the transition metal out of the catalyst.

H. O_2 Reduction Kinetics on Carbon in Aqueous and Non-Aqueous Solutions

As part of the supporting research on oxygen reduction on various carbon and graphite surfaces, the mechanism and kinetics on glassy carbon in alkaline solution have been studied intensively. Based on data obtained using the rotating ring-disk electrode technique, including the determination of the kinetic limiting currents as a function of potential, the Tafel behavior, the number of electrons (based both on disk and ring currents), the reaction orders

for O_2, HO_2^-, and OH^-, and the effect of substituting H_2O with D_2O, a tentative mechanism has been worked out. The rate-determining step in this proposed mechanism involves a redox-mediated reduction of O_2 to superoxide, possibly via reduced quinone-like surface functionalities:

$$Q^{\cdot}\ (surf) + O_2 \rightarrow Q(surf) + O_2^{\cdot} \qquad [1]$$

where the surface concentration of $Q.^-$ is potential-dependent.

The surface concentration of the quinone-like radical anion $Q.^-$ is assumed to follow a Nernstian depedence based upon the two redox reactions

$$Q(surf) + e^- \rightarrow Q^{\cdot}\ (surf) \qquad [2]$$

$$\text{and}\quad Q^{\cdot}\ (surf) + e^- \rightarrow Q^{2-}\ (surf) \qquad [3]$$

At potentials positive of the $E^{o'}$ for [2], the surface concentration $\Gamma Q.^-$ should increase one log unit for every 59.2 mV traveled in the negative direction (see Fig. 50). As the $E^{o'}$ is approached, this d log Γ/dE slope should decrease and approach zero within about 120 mV negative of $E^{o'}$. In the potential region in which $\Gamma Q.^-$ is increasing linearly, the O_2 reduction should also be increasing, with a Tafel slope of -59.2 mV per log unit of current. This assumes a linear dependence of the kinetic current density i on $\Gamma Q.^-$:

$$i_k = nFk\Gamma Q^{\cdot}\ C_{O_2} \qquad [4]$$

where n = number of electrons, assumed to be 2, F = the Faraday constant, $\Gamma Q.^-$ = surface concentration of $Q.^-$ in mol cm^{-2}, CO_2 is the bulk O_2 concentration in mol cm^{-3} and k is the rate constant for [1], with units of cm^3 $mol^{-1}s^{-1}$.

As the $E^{o'}$ for [3] is approached, $\Gamma Q.^-$ should begin to decrease and approach a negative slope of one log unit of Γ per 59.2 mV traveled in the negative direction. The i_k should then also decrease one log unit per 59.2 mV.

Theoretical Tafel plots based on this simple model fit the experimental

data fairly closely over the potential range more positive than -0.5 V vs. Hg/HgO, OH^- (Fig. 51). At potentials more negative than this, the current increases again due to O_2 reduction to peroxide via another reaction pathway.

O_2 reduction has also been examined on carbon and graphite surfaces with adsorptively attached and chemically linked quinones in alkaline solutions. For phenanthrenequinone adsorbed on highly oriented pyrolytic graphite (HOPG), the reduction behavior was very similar to that observed on GC and OPG in alkaline solution - the O_2 reduction current increased, reached a maximum and then decreased. For all of the adsorbed quinones examined, the Tafel slope has been found to be $\simeq$-60 mV/decade at low current densities. On a chemically modified surface, the slope was ~-120 mV/decade. From a detailed study of differential pulse voltammetry and rotating disk electrode for solutions of different pH, it has been demonstrated that the quinone radical anion may be responsible for O_2 reduction to peroxide. The mode of interaction of quinone species with O_2 is the subject of ongoing investigation.

Research has also been carried out on the electroreduction of O_2 in non-aqueous solutions on various electrode surfaces, inclding glassy carbon (GC), ordinary pyrolytic graphite (OPG) and highly ordered pyrolytic graphite (HOPG). The electron transfer coefficients and the standard electron transfer rate constants k^o have been determined for O_2 reduction to superoxide in dry (< 20 ppm H_2O) acetonitrile. The apparent k^o values decrease in the order: glassy carbon > ordinary pyrolytic graphite > highly ordered pyrolytic graphite. The α values for OPG and HOPG are less than 0.5, which probaly indicates that a portion of the potential drop occurs in a space-charge layer within the graphite. These results are consistent with previous double-layer capacity meaurements and redox kinetic studies on these materials at Case by Randin and Yeager and others. The results are also consistent with previous results at Case in aqueous solution, in which differing α values were obtained for GC and

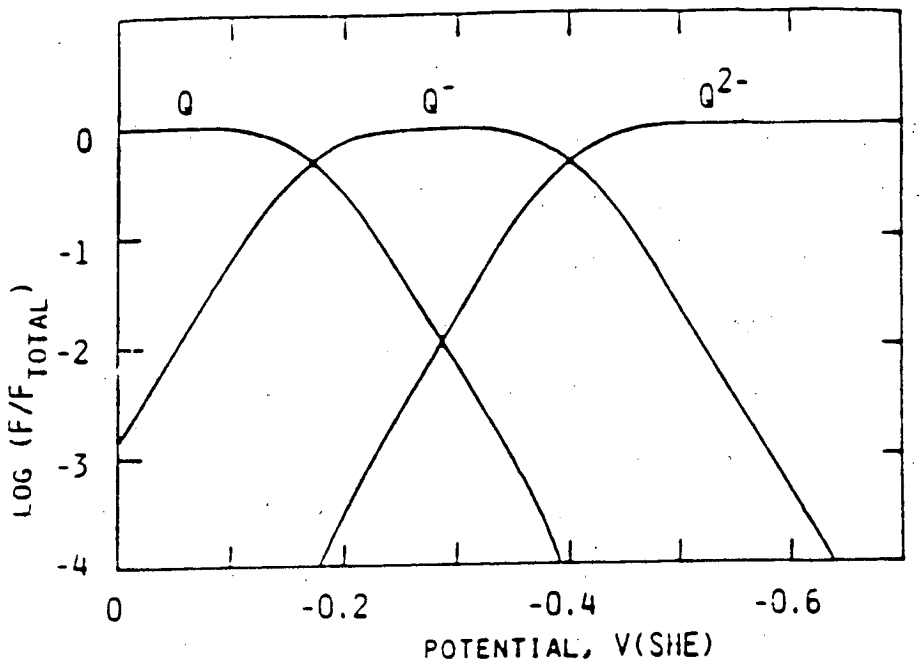

Fig. 50. Calculated potential dependence of the ratio of surface concentration of the various non-protonated redox states of quinonoid functionalities to the total in all three redox states. The Nernstian dependence was calculated using -0.17 V and -0.40 V (SHE) as the standard potentials for the Q/Q^- and Q^-/Q^{2-} couples, respectively.

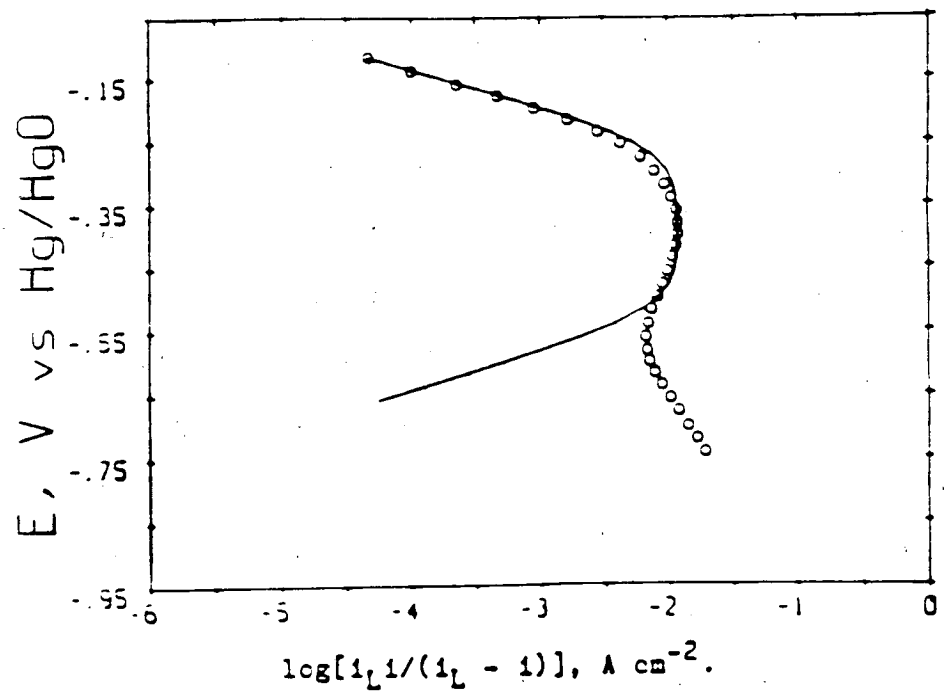

Fig. 51 Tafel plot for O_2 reduction on a polished glassy carbon rotating disk electrode in 1.0 M NaOH at 25°C. The experimental currents (o) were corrected for mass transport using a mass transport limiting current density i_L of 2.57 mA cm^{-2} for 3600 rpm. The theoretical curve was calculated using Eq. 4 with parameters given in the text.

OPG for O_2 reduction to peroxide. It is interesting to note, however, that the rate constant for oxygen reduction to superoxide in acetonitrile on HOPG, while relatively low, is orders of magnitude higher than that found in aqueous concentrated alkaline solution for the same reaction. The latter was work done at Case using electron spin resonance techniques to quantify the electrogenerated superoxide.

One of the methods used by the Case group to obtain the kinetic parameters involved the fitting of the experimental linear sweep voltammetry data with curves calculated on the basis of a simple quasi-reversible electron transfer (Fig. 52). Even though such curves have been calculated in the recent literature using digital simulation techniques based on the finite difference method, an analytical solution in the form of an integral equation was derived in 1955 by Matsuda and Ayabe (73). They also published an algorithm for solving the integral equation, and the Case group has developed a BASIC program which incorporates this (74, 75). The calculation is general for electron transfer reactions without chemical complications and allows, for example, different diffusion coefficients to be used for the oxidized and reduced species. The O_2 reduction is most reversible on GC, slightly less so on OPG and much less so on HOPG. After cycling of the potential several times, the kinetics on HOPG become faster probably because of a roughening effect, which may be due to intercalation of the tetraalkylammonium cation.

The fate of the superoxide in the presence of water intentionally added to the acetonitrile solution has also been examined on the graphite and carbon surfaces, using cyclic voltammetry, and rotating disk measurements. After its formation, superoxide reacts relatively slowly even in the presence of moderate water concentrations (~ 1 M). A second reduction process takes place at more negative potentials and the peak potential has been found to become more positive with increasing water concentration (Fig. 53). This

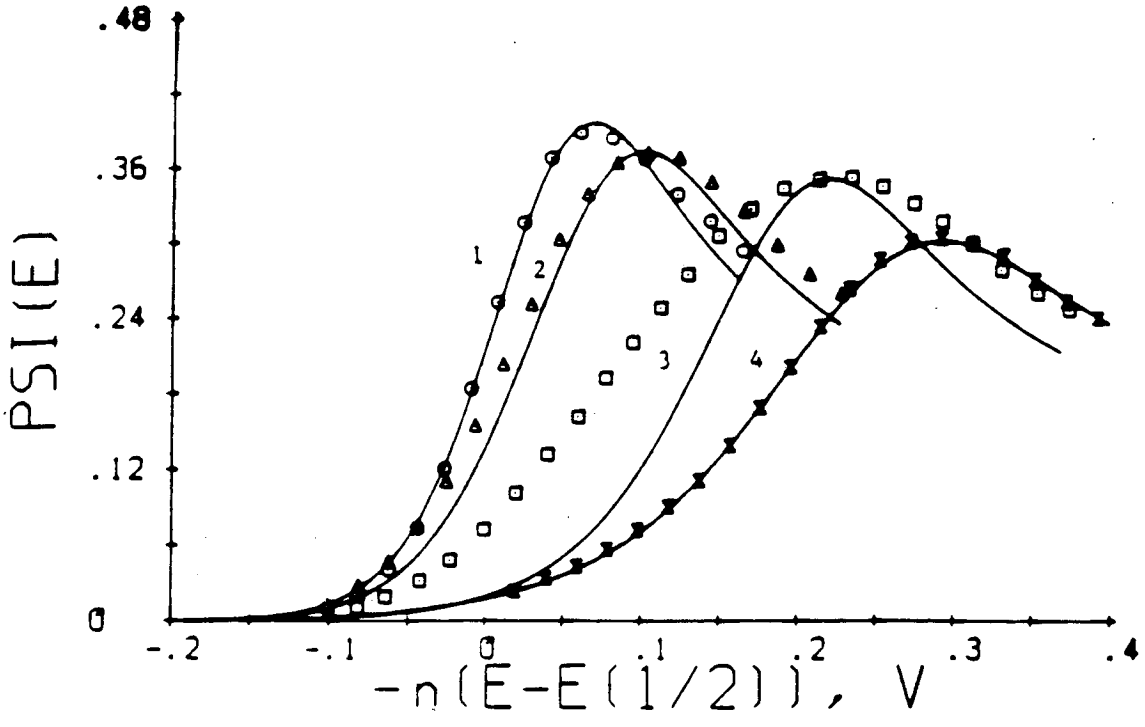

Fig. 52. Variation of current function, $\psi(E)$ with potential for GC (⊙), OPG (Δ), cycled HOPG (⊡) and uncycled HOPG (X) in O_2 - saturated CH_3CN (0.1 M TEAP). Scan rate 500 mV s^{-1}. Solid lines are theoretical curves for ideal quasi-reversible behavior. 1 - for $\alpha = 0.54$ and $k^o = 1.1 \times 10^{-2}$; 2 - for $\alpha = 0.52$ and $k^o = 5.0 \times 10^{-3}$ cm s^{-1}-; 3 - for $\alpha = 0.50$ and $k^o = 5.0 \times 10^{-4}$ cm s^{-1} and 4 - for $\alpha = 0.37$ and k^o 5.0×10^{-4} cm s^{-1}.

10. J. P. Collman, P. Denisevich, Y. Konai, M. Marrocco, C. Koval and F. C. Anson, J. Am. Chem. Soc., 102, 6027 (1980).

11. H. Y. Liu, M. J. Weaver, C. B. Wang and C. K. Chang, J. Electroanal. Chem., 145, 439 (1983).

12. S. Sarangapani, Ph.D. Dissertation, Case Western Reserve University, 1983.

13. J. Zagal, P. Bindra and E. Yeager, J. Electrochem. Soc., 127, 1506 (1980).

14. J. P. Collman and K. Kim, J. Am. Chem. Soc., 108, 7847 (1986).

15. C. Fierro, A. Tanaka, D. Scherson and E. Yeager, in "Extended Abstracts," Vol. 85-1, The Electrochemical Society, Pennington, NJ, 1985, p. 909.

16. H. Y. Liu, I. Abdelmudi, C. K. Chang and F. C. Anson, J. Phys. Chem., 89, 665 (1985).

17. T. D. Smith, J. Livorness, H. Taylor, J.R. Pilleson and G. R. Sinclair, J. Chem. Soc., Dalton Trans., 1391 (1983).

18. A. B. Anderson and R. Hoffman, J. Chem. Phys., 60, 6271 (1976).

19. C. Ercolani, M. Gardini, F. Monacelli, G. Pennesi and G. Rossi, Inorg. Chem., 22, 2584 (1983) and references therein.

20. A. A. Tanaka, C. Fierro, D. Scherson and E. Yeager, J. Phys. Chem., 91, 3799 (197).

21. E. Ercolani, M. Gardini, K. S. Murray, G. Pennesi and G. Rossi, Inorg. Chem., 25, 3972 (1986) and references therein.

22. F. Van den Brink, W. Visscher and E. Barendrecht, J. Electroanal. Chem., 172, 301; 175, 279 (1984).

23. J. E. Newton and M. B. Hall, Inorg. Chem., 23, 4627 (1984) and references therein.

24. T. Watanabe, T. Ama and Nakamoto, J. Phys. Chem., 88, 440 (1984).

25. A. J. Appleby, M. Savy and P. Caso, J. Electroanal. Chem., 111, 91 (1980) and references therein.

26. E. Ojadi, R. Selzer and H. Linschitz, J. Am. Chem. Soc., 107, 7783 (1985).

27. S. Gamburtsev, I. Iliev and A. Kaisheva, Elektrokhim., 19, 1261 (1983).

28. S. Gamburtsev, A. Kaisheva, I. Iliev, G. Gruenig, and K. Wiesener, Elektrokhim., 22, 254 (1986), Sov. Electrochem., p. 227.

29. K. Wiesener, Electrochim. Acta, 31, 1073 (1986).

30. A. Kaisheva, S. Gamburtsev and I. Iliev, Elektrokhim., 18, 139 (1982), Sov. Electrochem., p. 127.

31. G. Gruenig, K. Wiesener, A. Kaisheva, S. Gamburtsev and I. Iliev, Elektrokhim., 19, 1571 (1983), Sov. Electrochem., p. 1408.

32. S. Gupta, W. Aldred and E. Yeager, in "Extended Abstracts," Vol. 83-2, The Electrochemical Society, Pennington, NJ, 1983, p. 624.

33. R. Holze, D. Scherson, D. Tryk, S. Gupta and E. Yeager, in "Extended Abstracts," 35th Meeting of the International Society of Electrochemistry, Berkeley, CA, 1984, p. 399.

34. D. Tryk, W. Aldred, Z. Chen, C. Fierro, J. Hashiguchi, M. Hossain, Z. Zhang, F. Zhao and E. Yeager, "Bifunctional Oxygen Electrodes," Final Report, February 1983 to February 1984, Lawrence Berkeley National Laboratory - U.S. Department of Energy Subcontract No. 4521210, 1985, (Report, LBL - 19003; Order No. DE85006871, NTIS; Energy Res. Abstr., 1985, 10, Abstr. No. 21351).

35. S. Gupta, D. Tryk, R. Holze and E. Yeager, in "Extended Abstracts," Vol. 85-1, The Electrochemical Society, Pennington, NJ, 1985, p. 913.

36. D. Tryk, W. Aldred and E. Yeager, in "Extended Abstracts," Vol. 85-2, The Electrochemical Society, Pennington, NJ 1985, p. 11.

37. M. Torrens, D. Straub and L. Epstein, J. Am. Chem. Soc., 94, 4160 (1972).

38. A. Adler, F. Longo, F. Kampas and J. Kim, J. Inorg. Nucl. Chem., 32, 2443 (1970).

39. D. Scherson, S. Gupta, E. Yeager, M. Kordesch, J. Eldridge, and R. Hoffman, in "Extended Abstracts," Vol. 82-2, The Electrochemical Society, Pennington, NJ., 1982, p. 57.

40. D. Scherson, Case Western Reserve University, unpublished results.

41. D. Scherson, A. Tanaka, S. Gupta, D. Tryk, C. Fierro, R. Holze, E. Yeager and R. Lattimer, Electrochim. Acta, 31, 1247 (1986).

42. A. Tanaka, Ph.D. Dissertation, Case Western Reserve University, 1987.

43. J.A.R. VanVeen, J. F. VanBaar and K. J. Kroess, J. Chem. Soc., Faraday Trans. I, 78, 1021 (1982).

44. A. A. Bett, H. R. Kunz, S. W. Smith, Investigation of Alloy Catalysts and Redox Catalysts for Phosphoric Acid Electrochemical Systems, International Fuel Cells, Inc., South Windsor, Conn., Final Report, Los Alamos National Laboratory, 1984.

45. C. Maricondi, D. K. Straub and L. M. Epstein, J. Am. Chem. Soc., 96, 4157 (1972).

46. J. W. Niemantsverdriet, A. M. vanderkraan, W. M. Delgass and M. A. Vannice, J. Phys. Chem., 89, 67 (1985).

47. D. A. Scherson, R. W. Grimes, R. Holze, A. Tanaka, C. Fierro, E. Yeager and R. Lattimer, Extended Abstracts, Vol. 84-2, The Electrochemical Society, Pennington, NJ, 1984, p. 810.

48. D. Scherson, S. Gupta, C. Fierro, E. Yeager, M. Kordesch, J. Eldridge, R. Hoffman and J. Blue, Electrochim. Acta, 28, 1205 (1983).

49. C. Gilbert, Case Western Reserve University, unpublished results.

50. D. Gervasio, Case Western Reserve University, unpublished results.

51. R. R. Durand, Jr., C. S. Bencosme, J. P. Collman and F. C. Anson, J. Am. Chem. Soc., 105 2710 (1983).

52. F. Bedioui, J. Devynck, C. Hinnen, A. Rouseau, C. Bied-charreton and A. Gaudemer, J. Electrochem. Soc., 132, 2120 (1985).

53. R. Shigehara and F. C. Anson, J. Phys. Chem., 86, 2776 (1985).

54. M. H. Barley, K. J. Takeuchi and T. J. Mayer, J. Am. Chem. Soc., 108, 5876 (1986).

55. S. Zecevic, B. Simic-Glavaski, E. Yeager, A. B. P. Lever and P. C. Minor, J. Electroanal. Chem., 196, 339 (1985).

56. S. L. Gupta, Case Western Reserve University, unpublished results.

57. R. Holze, Case Western Reserve University, unpublished results.

58. S. Gupta, D. Tryk, M. Daroux, W. Aldred and E. Yeager, in "Proceedings of the Symposium on Load Levelling and Energy Conservation in Industrial Processes", D. Chin, Editor, The Electrochemical Society, Pennington, NJ, in press, and "Extended Abstracts", Vol. 86-1, The Electrochem. Society, Pennington, NJ 1986, p. 603.

59. H. Teoh, P. Metz and W. Wilhelm, Mol. Cryst. Liq. Cryst., 83, 297 (1983).

60. J. Hinden and J. Gauger, J. Electrochem. Soc., 133, 592 (1986).

61. S. Gupta, D. Tryk, W. Aldred, I. T. Bae and E. Yeager, in "Extended Abstracts", Vol. 87-1, The Electrochemical Society, Pennington, NJ, 1987, 455.

62. R. Carbonio, D. Tryk and E. Yeager in "Proceedings of the Symposium on Electrode Materials and Processes for Energy Conversion and Storage", S. Srinivasan et al., Editors, in press, and "Extended Abstracts", Vol. 87-1, The Eletrochemical Society, Pennington, NJ, 1987, p. 751.

63. M. Boudart and E. Djega-Mariadassou, "Kinetics of Heterogeneous Catalytic Reactions," Princeton University Press, Princeton, NJ, 1984, p. 6.

64. H. Takahashi and E. Yeager, in "Oxygen Electrodes for Energy Conversion and Storage," Annual Report No. I, October 1977 to September 1978, Diamond Shamrock Corporation - USDOE Contract No. EC-77-C-02-4146, pp. 138-163.

65. H. Takahashi, P. Bindra and E. Yeager, in "Oxygen Electrodes for Energy Conversion and Storage," Annual Report No. II, October 1978 to September 1979, Diamond Shamrock Corporation - USDOE, Contract No. EC-77-C-02-4146, Appendix E.

66. B. C. Wang and E. Yeager, in "Extended Abstracts," Vol. 81-2, The Electrochemical Society, Pennington, NJ, 1981, p. 280; "Extended Abstracts," 32nd Meeting of the International Society of Electrochemistry, Dubrovnik/Cavtat, Yugoslavia, September, 1981, p. 125, and "Oxygen Electrodes for Energy Conversion and Storage," Annual Report No. III, October 1979 to September 1980, Diamond Shamrock Corporation - USDOE Contract No. EC-77-C-02-4146, pp. 54-78.

67. A. J. Appleby and M. Savy, Electrochim. Acta, 21, 567 (1976).

68. T. Ohzuku, D. Tryk and E. Yeager, in "Extended Abstracts," Vol. 82-2, The Electrochemial Society, Pennington, NJ, 1982, p. 59.

69. D. Tryk, W. Aldred, T. Ohzuku and E. Yeager, "Bifunctional Oxygen Electrodes," Final Report, October 1980 - April 1983, LBL-USDOE Subcontract No. 1377901.

70. R. Carbonio, W. Aldred, D. Tryk and E. Yeager, in "Extended Abstracts," Vol. 86-2, The Electrochemical Society, Pennington, NJ, 1986, p. 211.

71. D. Tryk, W. Aldred and E. Yeager, in Extended Abstracts, Vol. 85-2, The Electrochemical Society, Penningtom, NJ, 1985, p. 11.

72. C. Fierro, R. E. Carbonio, D. Scherson and E. Yeager, in "Extended Abstracts", Vol. 87-1, The Electrochemical Society, Pennington, NJ, 1987, p. 347.

73. H. Matsuda and Y. Ayabe, Z. Elektrochem., 59, 494 (1955).

74. M. S. Hossain, Ph.D. Dissertation, Case Western Resevre University, 1986.

75. M. S. Hossain, D. Tryk, Z. Zhang, L. Lu and E. Yeager, manuscript in preparation.

76. Z. W. Zhang, F. L. Zhao, D. Tryk and E. Yeager, in "Extended Abstracts", Vol. 87-1, The Electrochemical Society, Pennington, NJ, 1987, p. 347.

LAWRENCE BERKELEY LABORATORY
TECHNICAL INFORMATION DEPARTMENT
UNIVERSITY OF CALIFORNIA
BERKELEY, CALIFORNIA 94720